
**Title 40 CFR Part 191
Subparts B and C
Compliance Recertification
Application
for the
Waste Isolation Pilot Plant

Appendix MgO-2009
Magnesium Oxide as an Engineered Barrier**



**United States Department of Energy
Waste Isolation Pilot Plant**

**Carlsbad Field Office
Carlsbad, New Mexico**

Appendix MgO-2009
Magnesium Oxide as an Engineered Barrier

Table of Contents

MgO-1.0 IntroductionMgO-1

MgO-2.0 Description of the Engineered Barrier System.....MgO-3

 MgO-2.1 7 Emplacement of MgOMgO-3

 MgO-2.1.1 SupersacksMgO-3

 MgO-2.1.2 Minisacks.....MgO-4

 MgO-2.1.3 Changes Since the CRA-2004 in Emplacement of MgOMgO-6

 MgO-2.2 Vendors That Provided or Are Providing MgO.....MgO-6

 MgO-2.2.1 Changes since the CRA-2004 in Vendors Proving MgO.....MgO-7

MgO-3.0 Characteristics of MgOMgO-9

 MgO-3.1 Production of National Magnesia MgOMgO-9

 MgO-3.2 Premier MgO.....MgO-9

 MgO-3.2.1 ProductionMgO-10

 MgO-3.2.2 Characterization.....MgO-10

 MgO-3.2.3 Results since the CRA-2004 in Characteristics of MgOMgO-11

 MgO-3.3 Martin Marietta MgO.....MgO-12

 MgO-3.3.1 ProductionMgO-12

 MgO-3.3.2 Characterization.....MgO-14

MgO-4.0 Hydration and Carbonation of MgOMgO-18

 MgO-4.1 Hydration of MgO.....MgO-18

 MgO-4.1.1 Hydration of Premier MgOMgO-18

 MgO-4.1.2 Results since the CRA-2004 Regarding Hydration of MgOMgO-20

 MgO-4.2 1 Carbonation of MgOMgO-21

 MgO-4.2.1 Carbonation of Premier Chemicals MgO.....MgO-21

 MgO-4.2.2 Formation of Magnesite in the WIPP.....MgO-22

 MgO-4.2.3 Possible Passivation of MgO in the WIPPMgO-26

MgO-5.0 Effects of MgO on the WIPP Disposal SystemMgO-30

 MgO-5.1 Effects of MgO on Brine Composition, f_{CO_2} , pH, and Actinide SolubilitiesMgO-30

 MgO-5.1.1 Changes Since the CRA-2004 in Effects of MgO on Brine Composition, f_{CO_2} , pH, and Actinide Solubilities.....MgO-34

 MgO-5.2 Effects of MgO on Colloidal Actinide (An) ConcentrationsMgO-36

 MgO-5.2.1 Results since the CRA-2004.....MgO-36

 MgO-5.3 Effects of MgO on Other Near-Field Processes and ConditionsMgO-36

 MgO-5.3.1 Effects of MgO on Repository H₂O Content.....MgO-37

 MgO-5.3.2 Effects of MgO on Gas Generation.....MgO-37

 MgO-5.3.3 Effects of MgO on Room Closure.....MgO-39

 MgO-5.4 Effects of MgO on Far-Field An TransportMgO-39

MgO-6.0 The MgO Excess Factor.....MgO-41

 MgO-6.1 Effects of Microbial Respiratory Pathways on the MgO Excess FactorMgO-41

MgO-6.2 History of the MgO Excess Factor.....MgO-43
 MgO-6.2.1 Establishment of the MgO Excess FactorMgO-43
 MgO-6.2.2 Reduction of the MgO Excess Factor from 1.95 to 1.67.....MgO-44
 MgO-6.2.3 Additional Developments Relevant to the MgO Excess Factor Prior to
 the CRA-2004.....MgO-46
 MgO-6.2.4 Changes since the CRA-2004 in the MgO Excess Factor.....MgO-54
 MgO-7.0 References.....MgO-81

List of Figures

Figure MgO-1. Supersacks of MgO Emplaced on Top of the Waste StackMgO-4
 Figure MgO-2. Racks Used to Emplace Additional MgO.....MgO-7
 Figure MgO-3. SEM Image of Premier Chemicals MgO after Hydration in GWB
 at 90 °C (194 °F) for 21 Days (SNL Experiment
 CC-GW-90-30-5).....MgO-19
 Figure MgO-4. SEM Image of Premier Chemicals MgO after Hydration in
 ERDA-6 Brine at 70 °C (158 °F) after 21 days (SNL Experiment
 CC-ER-70-30-5)MgO-20

List of Tables

Table MgO-1. Particle-Size Distribution of Two Batches of Premier MgO
 (Bryan and Snider [2001a])MgO-11
 Table MgO-2. Effects of LOI Analysis Temperature on the Extent of Hydration
 under Accelerated Conditions on Fisher and Premier Chemicals
 MgO.....MgO-12
 Table MgO-3. Effects of Temperature Used for LOI Analyses of MgO
 Hydration Products on the Brucite + Portlandite Concentrations
 of the Hydrated Samples.....MgO-15
 Table MgO-4. Particle-Size Distribution of 10 Samples from One Lot of Martin
 Marietta MgO.....MgO-16
 Table MgO-5. Results of LOI Analysis and TGA on WTS-60.....MgO-17
 Table MgO-6. Compositions of GWB and ERDA-6 Brine Predicted by FMT for
 the An-Solubility Calculations for the CRA-2004 PABC (Brush
 and Xiong 2005a; 2005b; Brush 2005) (M, unless Otherwise
 Noted) before and after Equilibration with Brucite,
 Hydromagnesite, Halite, Anhydrite, and Other SolidsMgO-31
 Table MgO-7. Effect of the Mg-Carbonate Solid on the f_{CO_2} (atm), TIC
 Concentration (M), pH (Standard Units), and An Solubilities (M)
 in GWB after Equilibration with Brucite, Halite, Anhydrite, and
 Other SolidsMgO-32
 Table MgO-8. Effect of the Mg-Carbonate Solid on the f_{CO_2} (atm), TIC
 Concentration (M), pH (Standard Units), and An Solubilities (M)
 in ERDA-6 Brine after Equilibration with Brucite, Halite,
 Anhydrite, and Other SolidsMgO-32

Table MgO-9. Effects of Panel Loading and the Source of SO_4^{2-} on Microbial Respiratory Pathways and the MgO Excess Factor—Base Case.....MgO-49

Table MgO-10. Effects of Panel Loading and the Source of SO_4^{2-} on Microbial Methanogenesis and the MgO Excess Factor—Effects of Having no Castile Brine Intrude Panel XMgO-50

Table MgO-11. Effects of Panel Loading and the Source of SO_4^{2-} on Microbial Respiratory Pathways and the MgO Excess Factor—Effects of Doubling the Time Required for Consumption of All CPR MaterialsMgO-51

Table MgO-12. Effects of Panel Loading and the Source of SO_4^{2-} on Microbial Respiratory Pathways and the MgO Excess Factor—Effects of Doubling the Effective Diffusion Coefficient for SO_4^{2-} MgO-52

This page intentionally left blank.

Acronyms and Abbreviations

%	percent
µm	micrometer
AlSinR	a synthetic brine representative of fluids sampled from the Culebra Member of the Rustler Formation in the WIPP air intake shaft
ALARA	as low as reasonably achievable
am	amorphous
AMWTP	Advanced Mixed Waste Treatment Program
An(III)	actinide element(s) in the III oxidation state
An(IV)	actinide(s) in the IV oxidation state
An(V)	actinide(s) in the V oxidation state
aq	aqueous
ASTM	American Society for Testing and Materials
atm	atmosphere(s)
BNL	Brookhaven National Laboratory
BRAGFLO	Brine and Gas Flow
Brine A	a synthetic brine representative of intergranular Salado brines
C	Celsius
CCA	Compliance Certification Application
CCDF	complementary cumulative distribution function
CH-TRU	contact-handled transuranic
CPR	cellulosic, plastic, and rubber
CRA	Compliance Recertification Application
DI	deionized
DOE	U.S. Department of Energy
DRZ	disturbed rock zone
<i>E. coli</i>	<i>Escherichia coli</i>
EPA	U.S. Environmental Protection Agency
EQ3/6	a geochemical software package for speciation and solubility calculations (EQ3NR) and reaction-path calculations (EQ6)
ERDA-6	Energy Research and Development Administration (WIPP Well) 6
FMT	Fracture-Matrix Transport
ft	foot

g	gaseous or gram
gal	gallon
g/mol	grams per mole
GWB	Generic Weep Brine
HDPE	high-density polyethylene
ICP-AES	inductively coupled plasma-atomic emission spectroscopy
INEEL	Idaho National Engineering and Environmental Laboratory
K_d	matrix distribution coefficient
kg	kilogram
kg/g	kilograms per gram
kg/lb	kilograms per pound
L	liter
lb	pound
LOI	loss-on-ignition
m	meter or molal
M	molar
m/s	meters per second
m^2/s	meters squared per second
m^3	cubic meters
mL	milliliter
mm	millimeter
mM	millimolar
mol	mole
mol %	mole percent
ND	not determined
nm	nanometer
NRC	National Research Council
OECD	Organisation for Economic Cooperation and Development
PA	performance assessment
PABC	Performance Assessment Baseline Calculations
PAVT	Performance Assessment Verification Test
PCR	Planned Change Request
pH	the negative, common logarithm of the activity of H^+

RCRA	Resource Conservation and Recovery Act
RH	relative humidity
RSI	Institute for Regulatory Science
RTR	real-time radiography
s	second(s) or solid
SCA	S. Cohen and Associates
SEM	scanning electron microscopy
SNL	Sandia National Laboratories
SPC	Salado Primary Constituents, a synthetic brine similar to Brine A
STTP	Source Term Test Program
SWB	standard waste box
TDOP	ten-drum overpack
TEA	Trinity Engineering Associates
TGA	thermal gravimetric analysis
TIC	total inorganic carbon
TRU	transuranic
VE	visual examination
vol %	volume percent
WIPP	Waste Isolation Pilot Plant
wt %	weight percent
WTS	Washington TRU Solutions, LLC
XRD	X-ray diffraction

Elements and Chemical Compounds

Al ₂ O ₃	aluminum oxide or alumina
Am	americium
An	actinide
Br	bromine
C	carbon
Ca	calcium
CaCl ₂	calcium chloride
Ca ²⁺	calcium ion

CaCO ₃	calcite
CaMg(CO ₃) ₂	dolomite
CaMg ₃ (CO ₃) ₄	huntite
CaMgSiO ₄	monticellite
CaO	calcium oxide or lime
CaO·MgO	dolime
CaSO ₄	anhydrite
CH ₄	methane
Cl ⁻	chloride ion
Cl	chlorine
CO ₂	carbon dioxide
CO ₃ ²⁻	carbonate ion
f _{co₂}	fugacity of CO ₂
Fe	iron
Fe ₂ O ₃	Fe(III) oxide, ferric oxide, or hematite
FeAl ₂ O ₄	hercynite
FeCr ₂ O ₄	chromite
H ⁺	hydrogen ion
H ₂ O	water (aq or g)
H ₂ S	hydrogen sulfide
K ⁺	potassium ion
Mg	magnesium
Mg(OH) ₂	brucite
Mg ²⁺	magnesium ion
Mg ₂ SiO ₄	forsterite
Mg ₄ (CO ₃) ₃ (OH) ₂ ·3H ₂ O	hydromagnesite (4323)
Mg ₅ (CO ₃) ₄ (OH) ₂ ·4H ₂ O	hydromagnesite (5424)
MgAl ₂ O ₄	spinel
MgCO ₃	magnesite
MgCO ₃ ·3H ₂ O	nesquehonite
MgCr ₂ O ₄	magnesiochromite
MgO	magnesium oxide

Mn	manganese
N ₂	nitrogen
Na	sodium
Na ⁺	sodium ion
Na ₂ Ca(SO ₄) ₂	glauberite
NaCl	sodium chloride or halite
NO ₃ ⁻	nitrate ion
Np	neptunium
O ₂	oxygen
O ₂ ⁻	anionic dioxygenyl radical
OH ⁻	hydroxide ion
OH [•]	hydroxyl radical(s)
Pb	lead
periclase	pure, crystalline MgO, the primary constituent of the WIPP engineered barrier
Pu	plutonium
SiO ₂	silicon dioxide or silica
SO ₄	sulfate
SO ₄ ²⁻	sulfate ion
Ti(Fe,Mg) ₂ O ₄	ulvöspinel
Th	thorium
U	uranium

This page intentionally left blank.

1 **MgO-1.0 Introduction**

2 The U.S. Department of Energy (DOE) is emplacing magnesium oxide (MgO) in the Waste
3 Isolation Pilot Plant (WIPP) repository to provide an engineered barrier that decreases the
4 solubilities of the actinide (An) elements in transuranic (TRU) waste in any brine present in the
5 postclosure repository (U.S. Department of Energy 1996a, Appendix BACK; Appendix
6 SOTERM; U.S. Department of Energy 2004, Appendix BARRIERS; Appendix PA, Attachment
7 SOTERM). Because it will decrease An solubilities, MgO helps meet the U.S. Environmental
8 Protection Agency's (EPA's) requirement for multiple natural and engineered barriers, one of the
9 assurance requirements in its regulations for radioactive waste repositories at 40 CFR §
10 191.14(d) (U.S. Environmental Protection Agency 1993).

11 In 40 CFR § 191.12 (U.S. Environmental Protection Agency 1993), the EPA defined barriers as
12 "any material or structure that prevents or substantially delays movement of water or
13 radionuclides toward the accessible environment. For example, a barrier may be a geologic
14 structure, a canister, a waste form...or a material placed over and around waste provided that the
15 material or structure substantially delays movement of water or radionuclides."

16 The DOE proposed four engineered barriers in its Compliance Certification Application (CCA)
17 for the WIPP, submitted to the EPA in October 1996 (U.S. Department of Energy 1996a). The
18 four engineered barriers proposed by the DOE were MgO, panel closures, shaft seals, and
19 borehole plugs. The EPA, however, specified MgO as the only engineered barrier in the WIPP
20 disposal system that meets the assurance requirement in its May 1998 certification rulemaking
21 (U.S. Environmental Protection Agency 1998a; 1998b). The EPA specified MgO as the only
22 engineered barrier because it considered panel closures, shaft seals, and borehole plugs to be part
23 of the disposal-system design.

24 MgO as used in the WIPP will decrease An solubilities by consuming essentially all of the
25 carbon dioxide (CO₂) that would be produced should microbial activity consume all of the
26 cellulosic, plastic, and rubber (CPR) materials in the TRU waste, waste containers, and waste-
27 emplacement materials in the repository. Although MgO will consume essentially all the CO₂,
28 minute quantities (relative to the quantity that would be produced by microbial consumption of
29 all of the CPR materials) will persist in the aqueous and gaseous phases. The residual quantities
30 would be so small relative to the initial quantity that the adverb "essentially" is hereafter omitted
31 in this appendix.

32 Consumption of CO₂ will decrease An solubilities by (1) buffering the fugacity of CO₂ (f_{CO_2}) at a
33 value or within a range of values favorable from the standpoint of the speciation and solubilities
34 of the An elements (the fugacity of a gaseous species, f_i , is similar to the partial pressure of that
35 species, p_i); (2) controlling the pH at a value favorable from the standpoint of An solubilities;
36 and (3) preventing the production of carbonate ion (CO₃²⁻) in significant quantities. The effect of
37 this residual CO₃²⁻ on the solubilities of An elements is described in Appendix SOTERM-2009,
38 Section SOTERM-3.2.1 and Section SOTERM-3.3.1.3.

39 The effects of MgO carbonation (consumption of CO₂) have been included in WIPP performance
40 assessment (PA) calculations by assuming that there will be no CO₂ in the repository. This
41 assumption has been implemented in PA by (1) removing CO₂ from the gaseous phase in the

1 Brine and Gas Flow (BRAGFLO) calculations, thereby somewhat reducing the predicted
2 pressurization of the repository; and (2) using the values of f_{CO_2} and pH predicted for reactions
3 among MgO, brine, and aqueous or gaseous CO_2 to calculate An solubilities. The assumption
4 that there will be no CO_2 has been implemented in all compliance-related WIPP PA calculations.
5 These include (1) the CCA PA calculations (Novak et al. 1996; the CCA, Appendix SOTERM),
6 (2) the CCA Performance Assessment Verification Test (PAVT) (Novak 1997; U.S.
7 Environmental Protection Agency 1998c, 1998d, and 1998e), (3) the PA calculations for the
8 2004 WIPP Compliance Recertification Application (CRA-2004) (U.S. Department of Energy
9 2004; the CRA-2004, Appendix PA, Attachment SOTERM), (4) the CRA-2004 Performance
10 Assessment Baseline Calculations (PABC) (Brush and Xiong 2005a and 2005b, Brush 2005,
11 Leigh et al. 2005), and (5) the CRA-2009 PA.

12 In this appendix, “MgO” refers to the bulk, granular material being emplaced in the WIPP to
13 serve as the engineered barrier. MgO comprises periclase (pure, crystalline MgO—the main,
14 reactive constituent of the WIPP engineered barrier) and various impurities described in Section
15 MgO-3.0. Pure, crystalline MgO is always referred to as “periclase” in this Appendix. The term
16 “periclase” and other mineral names used herein are, strictly speaking, restricted to naturally
17 occurring forms of the materials that meet all the other requirements of the definition of a
18 mineral (see, for example, Bates and Jackson 1984). However, mineral names are used in this
19 report for convenience.

1 **MgO-2.0 Description of the Engineered Barrier System**

2 This section describes the emplacement of MgO in WIPP disposal rooms (Section MgO-2.2) and
3 the vendors that provided or are providing MgO to the WIPP (Section MgO-2.2).

4 Washington TRU Solutions, LLC (WTS) (2005) provides the current specifications for the
5 prepackaged MgO emplaced in the WIPP.

6 **MgO-2.1 Emplacement of MgO**

7 The DOE emplaced MgO in both supersacks and minisacks from the opening of the WIPP in
8 March 1999 until January 2001. During this period, the MgO emplaced in supersacks and that
9 emplaced in minisacks constituted about 85% and 15%, respectively, of the total quantity of
10 MgO emplaced in the repository.

11 In 2000, however, the DOE requested EPA approval to eliminate the minisacks (Triay 2000,
12 U.S. Department of Energy 2000); the EPA approved this request in 2001 (Marcinowski 2001,
13 U.S. Environmental Protection Agency 2001). Section MgO-2.1.1 describes the supersacks;
14 Section MgO-2.0 describes the minisacks and the reasons for their elimination; and Section
15 MgO-2.1.2 describes changes since the CRA-2004.

16 **MgO-2.1.1 Supersacks**

17 The DOE is emplacing MgO in polypropylene supersacks atop each stack of 3 7-packs of 55-
18 gallon (gal) (208-liter [L]) drums, 3 standard waste boxes (SWBs), or various combinations of
19 these and other waste containers. Other such containers include ten-drum overpacks (TDOPs),
20 4-packs of 85-gal (321-L) drums, and 3-packs of 100-gal (379-L) drums. According to WTS
21 specifications, each supersack must contain 4200 ± 50 pounds (lb) (1905 ± 23 kilograms [kg]) of
22 MgO (WTS 2005). Forklifts are used to place the supersacks on top of the waste stacks. Figure
23 MgO-1 shows supersacks of MgO emplaced on top of the waste stack.

24 Emplacement of MgO in supersacks (1) facilitates handling and emplacement of MgO, (2)
25 minimizes potential worker exposure to dust, and (3) minimizes the exposure of periclase (the
26 main reactive constituent of MgO) to atmospheric CO₂ and H₂O during handling and
27 emplacement, and prior to panel closure. Washington TRU Solutions (2005) provides detailed
28 specifications for the supersacks. In particular, Washington TRU Solutions (2005) specifies that
29 the supersacks “shall provide a barrier to atmospheric moisture and carbon dioxide (CO₂) ...
30 equivalent to or better than that provided by a standard commercial cement bag” and “must be
31 able to retain [their] contents for a period of two years after emplacement without rupturing from
32 [their] own weight.” The specifications also require a certificate of compliance with all
33 requirements of Washington TRU Solutions (2005) for every shipment of MgO (see below), and
34 a certified chemical analysis for each new lot of MgO. The supersacks are subject to random
35 receipt inspection at the WIPP to ensure compliance with the dimensions and labeling specified
36 by Washington TRU Solutions (2005), and to identify any damage incurred during shipping.



1

2

Figure MgO-1. Supersacks of MgO Emplaced on Top of the Waste Stack

3

4

5

6

7

8

9

The supersacks contain dry, granular MgO, of which less than 0.5% can exceed 3/8 inches (9.5 millimeters [mm]) in diameter (Washington TRU Solutions 2005). Emplacement of granular MgO instead of powder (1) results in a bulk density high enough that sufficient MgO can be emplaced without causing major operational difficulties, (2) reduces the likelihood of dust formation and release in the event of premature supersack rupture, and (3) ensures that the permeability of the material is high enough to promote complete reaction with aqueous or gaseous CO₂.

10

11

12

13

Creep closure of WIPP disposal rooms will rupture the supersacks and disperse the MgO among and within the ruptured waste containers. This will, in turn, expose the MgO to the room's atmosphere, to any CO₂ produced by the microbial consumption of CPR materials, and to H₂O vapor and any brine present.

14

MgO-2.1.2 Minisacks

15

16

17

Initially, the DOE emplaced MgO in both supersacks and 25-lb (11-kg) minisacks. The minisacks were emplaced among the waste containers and between the waste containers and the ribs (sides) of the disposal rooms.

18

19

20

21

In its request for EPA approval to eliminate the minisacks (Triay 2000 and U.S. Department of Energy 2000), the DOE emphasized the need to reduce the industrial and radiological hazards associated with the manual emplacement of the minisacks. The DOE (U.S. Department of Energy 2000, p. 2) stated

22

23

Elimination of the mini-sacks will reduce the industrial hazards associated with the lifting and handling of the mini-sacks. While the bulk of the MgO backfill (85%) is contained in the

1 supersacks which are emplaced using a forklift, each mini-sack of MgO must be emplaced
2 manually. This requires that personnel emplace eighteen twenty-five pound mini-sacks around the
3 drums for each waste stack, and 11 mini-sacks against the rib at the end of each row, a process
4 which will be repeated for the more than 108,000 estimated waste stacks (about 2,142,000 mini-
5 sacks) to be emplaced during the life of the facility. Handling and emplacing the mini-sacks
6 requires excessive bending and lifting, as well as climbing ladders on an uneven surface to
7 emplace mini-sacks in the upper tiers. Each of these actions [has] a risk of physical injury.

8 Also, elimination of the mini-sacks will reduce the potential radiation exposure to workers. This
9 exposure has been evaluated by timing the steps associated with emplacement and estimating the
10 radiological exposure over this time period (WID [Westinghouse Waste Isolation Division] 1997).
11 Although the total potential dose is not excessive, particularly when spread over the life of the
12 facility, any potential reduction of dose supports the ALARA (As Low As Reasonably
13 Achievable) concept, which defines [the] DOE's basic operating philosophy regarding radiation
14 exposure. It is the installation of the mini-sacks that is responsible for most of the radiological
15 dose associated with backfill emplacement. Elimination of the mini-sacks from the backfill
16 system will result in the elimination of associated radiological exposure.

17 The DOE also demonstrated that eliminating the minisacks would (1) not affect the ability of
18 MgO to function as an effective engineered barrier, thus meeting the EPA's assurance
19 requirement for multiple natural and engineered barriers; and (2) "[r]etain an acceptable safety
20 factor ..." (U.S. Department of Energy 2000, p. 3). Section MgO-6.0 defines the MgO excess
21 factor; Section MgO-6.2.2 describes the effect of eliminating the minisacks on the MgO excess
22 factor.

23 Wang (2000a and 2000b) supported the DOE's request to eliminate the minisacks by justifying
24 the DOE assertion that doing so would not affect the ability of MgO to function as an effective
25 engineered barrier and would not reduce the MgO excess factor to an unacceptable extent. Wang
26 (2000a) (1) described new evidence from laboratory studies of microbial gas generation, which
27 demonstrated that microbial methanogenesis could be an important process in the WIPP; and
28 (2) showed that, if methanogenesis were the dominant microbial respiratory pathway, a smaller
29 amount of CO₂ would be generated and the MgO excess factor would increase from values of
30 1.95 prior to and 1.67 after the proposed elimination of the minisacks to values of 3.73 prior to
31 and 3.23 after minisack elimination. Section MgO-6.1 describes the effects of microbial
32 respiratory pathways on the MgO excess factor; Section MgO-6.2.2 discusses the effects of
33 eliminating the minisacks on the MgO excess factor and the laboratory results demonstrating that
34 methanogenesis could be an important respiratory pathway.

35 In addition, Wang (2000b) used a bounding calculation to demonstrate that, even in the absence
36 of the minisacks, molecular diffusion in WIPP brines would be fast enough for MgO to control
37 chemical conditions in the repository.

38 In its 2001 approval of the DOE's request to eliminate the minisacks, the EPA stated, "... this
39 change, ... proposed to improve operational safety, will not significantly impact the WIPP's
40 long-term performance" (Marcinowski 2001). After inspecting the waste emplaced in Panel 1,
41 the EPA also "found that DOE accurately represented the steps required to attach minisacks to
42 the waste containers and the worker safety considerations involved in this activity" (U.S.
43 Environmental Protection Agency 2001). Furthermore, the EPA (U.S. Environmental Protection
44 Agency 2001) noted that "DOE's conceptualization of MgO performance in the repository was
45 very conservative," and cited the following as examples:

- 1 • The DOE did not take credit for the beneficial effects of MgO hydration on the long-term
2 performance of the repository.
- 3 • The “DOE proposes to reduce only excess MgO, which was not used in the [PA]
4 calculations” and “there would still be a large excess of MgO relative to any potential
5 evolved carbon [C].”
- 6 • “Attachment 4 [Wang (2000b)] concludes that molecular diffusion alone can effectively
7 mix brine with MgO from degraded super-sacks in a repository that has experience[d]
8 salt creep closure.... We reviewed DOE’s calculations and agree these processes will
9 function as expected and sufficient MgO will be available to react.”

10 **MgO-2.1.3 Changes Since the CRA-2004 in Emplacement of MgO**

11 In March 2004, the EPA approved the emplacement in the WIPP of compressed
12 (supercompacted) waste from the Advanced Mixed Waste Treatment Project (AMWTP) at the
13 Idaho National Engineering and Environmental Laboratory (INEEL) (Marcinowski 2004, Trinity
14 Engineering Associates 2004, and U.S. Environmental Protection Agency 2004). However, the
15 EPA required that the DOE maintain an MgO excess factor (Section MgO-6.0) of 1.67 on a
16 room-by-room basis. Some of the AMWTP waste contains concentrations of CPR materials that
17 are high relative to the average concentration of CPR materials in TRU waste, thereby
18 necessitating the emplacement of additional MgO in the repository. To account for this, the
19 DOE has emplaced additional MgO supersacks on racks among the waste containers. Each rack
20 contains 5 supersacks identical to those placed on top of the waste containers, and spans the
21 same vertical distance normally occupied by the waste stack (3 7-packs of 55-gal [208-L] drums,
22 3 SWBs, or various combinations of these and other waste containers) and the supersack
23 emplaced atop the waste stack. Thus, emplacing additional MgO in the repository uses space
24 normally occupied by contact-handled (CH) transuranic (TRU) (CH-TRU) waste. Figure MgO-2
25 shows a rack used to emplace additional MgO in the WIPP.

26 As of June 12, 2008, a total of 80 racks had been emplaced in the WIPP, comprising 30 racks in
27 Panel 2, Room 1; 21 racks in Panel 3, Room 5; 3 racks in Panel 3, Room 4; 3 racks in Panel 4,
28 Room 6; and 23 racks in Panel 4, Room 4.

29 **MgO-2.2 Vendors That Provided or Are Providing MgO**

30 National Magnesia Chemicals in Moss Landing, CA, was the first vendor to provide MgO for the
31 WIPP. National Magnesia supplied MgO from the opening of the WIPP in March 1999 through
32 mid-April 2000; during this period, waste was emplaced only in Panel 1, Room 7. This vendor
33 was sometimes referred to as National Refractory Materials (e.g., Papenguth 1999). Note that in
34 every seven-room WIPP panel, waste is emplaced in Room 7, at the back of the panel first and in
35 Room 1 last.

36 After National Magnesia stopped producing MgO, WTS considered Martin Marietta Magnesia
37 Specialties LLC, currently headquartered in Baltimore, MD, and Premier Chemicals of Gabbs,
38 NV, as potential vendors. At the request of the DOE’s Carlsbad Area Office, Papenguth (1999)



1
2

Figure MgO-2. Racks Used to Emplace Additional MgO

3 carried out a technical evaluation of MgO from both Martin Marietta and Premier to support
4 WTS's selection of a new vendor. The criteria used for this evaluation included density; particle
5 size; purity; and reactivity, quantified using a test developed by Krumhansl et al. (1997).
6 Based on cost and the results of the technical evaluation, WTS selected Premier Chemicals.
7 This vendor supplied MgO from mid-April 2000 (Panel 1, Room 7) through January 2005 (Panel
8 2, Room 2).

9 Section MgO-3.2 presents the results of the Premier MgO characterization.

10 **MgO-2.2.1 Changes since the CRA-2004 in Vendors Proving MgO**

11 Premier Chemicals informed WTS in 2004 that it would soon be unable to provide MgO that met
12 the requirement for the minimum concentration of MgO specified by Washington TRU Solutions
13 (2003): "The sum of MgO plus calcium oxide (CaO) shall be a minimum of 95%, with MgO
14 being no less than 90%."

15 Martin Marietta Magnesia Specialties, LLC, was selected and has supplied the MgO emplaced
16 since January 2005 (Panel 2, Room 2). Martin Marietta MgO was selected based on cost and a

1 technical evaluation of its suitability by Wall (2005). The results of this study and additional
2 characterization of Martin Marietta MgO are described in more detail in Section MgO-3.3.2.

3 Because Martin Marietta did not begin supplying MgO until January 2005, all results reported
4 for Martin Marietta MgO have been obtained since the CRA-2004 (Section MgO-3.3 and Section
5 MgO-4.1.2).

1 **MgO-3.0 Characteristics of MgO**

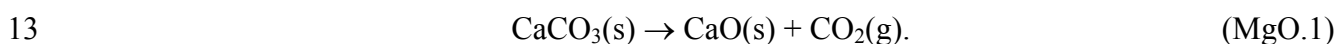
2 This section describes the characteristics of the MgO provided to the WIPP by National
3 Magnesia Chemicals (Section MgO-3.1), Premier Chemicals (Section MgO-3.2), and Martin
4 Marietta Magnesia Specialties, LLC (Section MgO-3.3).

5 **MgO-3.1 Production of National Magnesia MgO**

6 This section is based on a brief description provided by Papenguth (1999).

7 National Magnesia produced MgO for the WIPP by mixing seawater (the source of Mg(OH)₂)
8 with calcined limestone at their plant in Moss Landing, CA. Limestone is a rock that mainly
9 comprises the mineral calcite (CaCO₃) or other polymorphs of CaCO₃. In some cases, this rock
10 can comprise nearly pure calcite. Clay minerals and quartz commonly occur as impurities in
11 limestone.

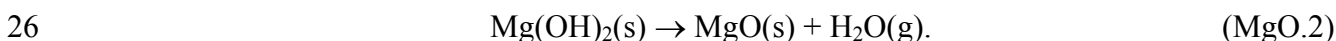
12 The calcination reaction for limestone is



14 The formula for limestone on the left-hand side of Reaction (MgO.1) does not include impurities
15 such as clay minerals and quartz, which presumably occur in small quantities in the material
16 quarried to produce National Magnesia MgO.

17 National Magnesia then mixed seawater with the lime (CaO) obtained from Reaction (MgO.1).
18 Although Papenguth (1999) did not describe the reaction(s) that occurred upon mixing, brucite
19 (Mg(OH)₂) presumably precipitated via a reaction similar to that discussed in Section MgO-
20 3.3.1, except that National Magnesia used seawater instead of brine, and lime instead of dolime
21 (CaO·MgO(solid[s])). Seawater solutes, such as sodium (Na⁺), calcium (Ca²⁺), chlorine (Cl⁻),
22 and SO₄²⁻, presumably remained mainly in solution.

23 After filtering and washing the precipitate to remove all the seawater, National Magnesia hard-
24 burned (calcined at 1000-1500 °C [1832-2732 °F]) the brucite to convert it to periclase via the
25 reaction



27 Hard burning produces MgO that is more reactive than dead-burned MgO (calcined at 1500-
28 2000 °C [2732-3632 °F]), but less reactive than light-burned MgO (calcined at 700-1000 °C
29 [1292-1832 °F]).

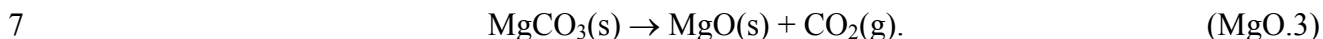
30 **MgO-3.2 Premier MgO**

31 This section describes the process that Premier Chemicals used to manufacture MgO for the
32 WIPP (Section MgO-3.2.1), the DOE's characterization of this product (Section MgO-3.2.2),
33 and changes in the WIPP project's understanding of its characteristics since the CRA-2004
34 (Section MgO-3.2.3).

1 **MgO-3.2.1 Production**

2 This section is based on a brief description provided by the DOE (the CRA-2004, Appendix
3 BARRIERS, Section BARRIERS-2.3.1).

4 Premier Chemicals produced MgO for the WIPP by mining ore from a sedimentary magnesite
5 (MgCO_3) deposit and calcining it to expel all CO_2 , thereby producing periclase directly instead
6 of from calcined brucite:



8 Calcination of accessory CaCO_3 produced small quantities of lime. Calcination of other
9 accessory minerals in the ore, such as clay minerals and quartz, created minor quantities of oxide
10 and silicate minerals, such as spinel (MgAl_2O_4), ulvöspinel ($\text{Ti}(\text{Fe,Mg})_2\text{O}_4$), forsterite
11 (Mg_2SiO_4), and monticellite (CaMgSiO_4). Calcination also drove off any H_2O in the ore.

12 **MgO-3.2.2 Characterization**

13 This section is based on the summary of the DOE's characterization of Premier Chemicals MgO
14 provided in the CRA-2004, Appendix BARRIERS, Section BARRIERS-2.3.1 and Section
15 BARRIERS-2.3.2.1.

16 This section emphasizes the DOE's identification and quantification of the reactive constituents
17 periclase and lime, and the nonreactive constituents of Premier Chemicals MgO. In this
18 appendix, *reactive constituents* refers to those solids that hydrate and carbonate to a significant
19 extent on the time scales of the accelerated or WIPP-relevant laboratory experiments described
20 below (Section MgO-4.1 and Section MgO-4.2). It is possible that the nonreactive constituents
21 of Premier MgO (or the MgO provided by other vendors) could significantly hydrate and
22 carbonate during the 10,000-year WIPP regulatory period. However, these experiments were
23 designed to investigate the hydration and carbonation of the reactive constituents of MgO, not
24 the relatively minor nonreactive constituents. Therefore, credit is not taken for possible CO_2
25 uptake by the nonreactive constituents.

26 Bryan and Snider (2001a) reported that a typical chemical analysis of Premier Chemicals MgO
27 yielded about 91 weight percent (wt %) MgO, 1 wt % alumina (Al_2O_3), 3 wt % silica (SiO_2),
28 4 wt % CaO, and 1 wt % iron(III) ($\text{Fe}(\text{III})$) oxide (Fe_2O_3). These chemical analyses did not
29 differentiate between the MgO contained in the reactive constituent periclase and that contained
30 in the nonreactive constituents spinel, ulvöspinel, forsterite, and monticellite; or between the
31 CaO contained in the reactive constituent lime and that contained in the nonreactive constituent
32 monticellite. However, most of the MgO and CaO occurred as periclase and lime, respectively,
33 in Premier Chemicals MgO. On the other hand, some of the MgO and CaO, and most, if not all,
34 of the Al_2O_3 , SiO_2 , and Fe_2O_3 were present in the accessory oxide and silicate minerals described
35 above.

36 Snider (2002, Figure 1, Figure 2, Figure 6, and Figure 7) observed that the hydration of Premier
37 Chemicals MgO reached completion after formation of about 85 mole % (mol %) brucite in
38 accelerated experiments. Snider (2003a) calculated that the average brucite concentration in this
39 lot of Premier Chemicals MgO was 84.6 mol % after complete hydration, based on the last 8 data

1 points of the inundated hydration experiment with deionized (DI) H₂O at 90 °C (194 °F) (Snider
2 2002, Figure 1 and Figure 2) and the last 16 data points of the humid hydration run at 95%
3 relative humidity (RH) and 80 °C (176 °F) (Snider 2002, Figure 6 and Figure 7). Therefore, it
4 was assumed in the CRA-2004 that this lot of Premier Chemicals MgO contained 84.6 mol %
5 periclase prior to hydration.

6 It is important to note that Snider (2002) determined the brucite concentration of the MgO
7 hydration products by loss-on-ignition (LOI) analysis, which quantified the mass of H₂O
8 released by brucite upon heating to 500 °C (932 °F). However, based on the results of Deng et al.
9 (2006) and Deng, Xiong, and Nemer (2007) (Section MgO-3.3.2), it is now clear that LOI or
10 thermal gravimetric analysis (TGA) cannot readily differentiate between the H₂O lost by brucite
11 and portlandite. Therefore, Deng et al. (2006) and Deng, Xiong, and Nemer (2007) reported
12 their results as mole percent brucite and portlandite or weight percent brucite and portlandite.
13 Thus, the results of Snider (2002) are described as mole percent brucite and portlandite in this
14 appendix, which correspond to the concentration in mole percent of periclase and lime prior to
15 hydration.

16 Snider (2003b) used inductively coupled plasma-optical atomic spectroscopy (ICP-AES) and
17 gravimetric analysis to quantify the mineralogical composition of one of the lots of Premier
18 Chemicals MgO used for the hydration and carbonation experiments (Section MgO-6.0). Based
19 on the assumption that the silicate in this MgO was forsterite, this lot of MgO contained
20 86.9 wt % periclase, 2.39 wt % lime, 2.07 wt % spinel, and 5.02 wt % forsterite. If the silicate
21 was monticellite, this lot contained 88.7 wt % periclase, 1.27 wt % lime, 2.07 wt % spinel, and
22 5.76 wt % monticellite. Given the uncertainties inherent in quantifying the mineralogical
23 composition of materials such as Premier Chemicals MgO, it is reasonable to conclude that this
24 material contained about 90 wt % reactive constituents (periclase and lime) and 10 wt %
25 nonreactive constituents (oxides and silicates).

26 Bryan and Snider (2001a) carried out particle-size analyses of two batches of MgO used for their
27 experiments. Table MgO-1 provides the results of these analyses.

28 **MgO-3.2.3 Results since the CRA-2004 in Characteristics of MgO**

29 Snider and Xiong (2004) reported the results of experiments on the inundated hydration and the
30 inundated carbonation of Premier Chemicals MgO. The objectives of this study were to
31 determine why Snider (2002, 2003a) had observed that the hydration of Premier Chemicals MgO
32 reached completion after formation of about 85 mol % brucite in three sets of experiments
33 (Experiments 1, 2, and 3) and why the extent of Premier Chemicals MgO hydration in
34 accelerated tests was less than expected (Snider 2002, 2003a, 2003b).

35 Snider and Xiong (2004, Section 3.1.2.1 and Section 3.3.2.1) conducted Experiment 1 to
36 examine the effects of particle size on the extent of hydration and it yielded no useful data. The
37 cause of the unexpectedly low extent of hydration was identified by Experiments 2 and 3
38 (below).

Table MgO-1. Particle-Size Distribution of Two Batches of Premier MgO (from Bryan and Snider [2001a])

Size Range (mm)	Batch 1	Batch 2
< 0.15	31.0%	9.89%
0.15 to 0.30	8.36%	29.4%
0.30 to 0.50	4.59%	29.7%
0.50 to 0.71	3.50%	15.0%
0.71 to 2.00	14.2%	14.5%
> 2.00	37.4%	1.53%

Snider and Xiong (2004, Section 3.1.2.2 and Section 3.3.2.2) conducted Experiment 2 to test the validity of LOI analysis at 500 °C (932 °F). For this experiment, 22 separate runs were conducted with 5 grams (g) of reagent grade Fisher MgO and 100 milliliters (mL) of DI water in 125-mL polypropylene bottles at 90 °C (194 °F) for 1 to 15 days, followed by LOI analysis at 500 °C (932 °F). These runs yielded results from 87 to 99 mol % brucite, with no apparent increase in the extent of hydration from 1 to 15 days (Snider and Xiong 2004, Figure 8). Snider and Xiong (2004, p. 16) concluded, “The most likely reason for why hydration of Fisher MgO did not produce 100 mol % brucite in this experiment is that LOI analysis at 500 °C (932 °F) did not drive off all bound H₂O (see Experiment 3 below).”

Snider and Xiong (2004, Section 3.1.2.3 and Section 3.3.2.3) performed Experiment 3 to further test the validity of LOI at 500 °C (932 °F) by conducting 8 runs with either 5 g of Fisher or Premier Chemicals MgO and 100 mL of DI water in 125 mL polypropylene bottles at 90 °C (194 °F) for 29 days, followed by LOI analysis at 500 or 750 °C (932 or 1382 °F). Table MgO-2 provides the results of Experiment 3. These results imply that (1) not all of the bound H₂O is released during LOI analysis at 500 °C (932 °F), and (2) the concentration of brucite and portlandite in their hydration products and the concentration of periclase and lime for Premier Chemicals MgO prior to reaction were about 89 mol % and 92 wt % for the LOI analysis at 750 °C (1382 °F), thus confirming the impact of higher temperature on the LOI analysis.

MgO-3.3 Martin Marietta MgO

This section discusses the process that Martin Marietta Magnesia Specialties LLC uses to produce MgO for the WIPP (Section MgO-3.3.1) and the DOE’s characterization of this product (Section MgO-3.3.2). Because Premier Chemicals was replaced by Martin Marietta in January 2005 (Section MgO-2.2.1), all the information described in this section has been obtained since the CRA-2004.

MgO-3.3.1 Production

This section summarizes the process Martin Marietta Magnesia Specialties, LLC, uses to produce its MgO. This summary is based on information provided by Martin Marietta (Martin Marietta Magnesia Specialties 2006) and the text in Brush and Roselle (2006, Section 2.3.1).

1 **Table MgO-2. Effects of LOI Analysis Temperature on the Extent of Hydration under**
 2 **Accelerated Conditions on Fisher and Premier Chemicals MgO**

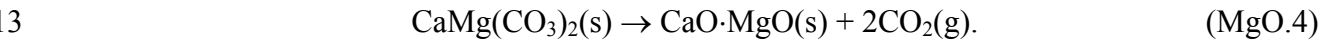
Type of MgO	Brucite, 500 °C (932 °F) (mol %)	Brucite, 500 °C (932 °F) (wt %)	Brucite, 750 °C (1382 °F) (mol %)	Brucite, 750 °C (1382 °F) (wt %)
Fisher	90.5	93.2	NA ^a	NA
Fisher	90.2	93.0	NA	NA
Fisher	NA	NA	97.3	98.2
Fisher	NA	NA	98.5	99.0
Premier	84.2	88.5	NA	NA
Premier	83.0	87.6	NA	NA
Premier	NA	NA	88.7	91.9
Premier	NA	NA	89.4	92.4

^a NA = not analyzed.

3
 4 Martin Marietta pumps brine from a depth of about 762 m (2,500 feet (ft)) in the Michigan
 5 Basin. According to their website, this brine consists of CaCl₂ + MgCl₂ + H₂O. This simplified
 6 composition of the brine does not include solutes such as Na⁺, K⁺, and SO₄²⁻, which are
 7 important constituents of WIPP brines and which presumably are present at least to some extent
 8 in brines from the Michigan Basin.

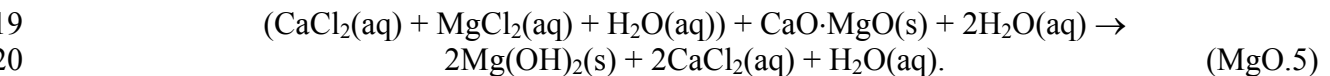
9 Martin Marietta produces dolime by calcining dolomite (CaMg(CO₃)₂) quarried in Ohio.
 10 Dolomite, which is also commonly referred to as “dolomitic limestone,” is a rock that mainly
 11 comprises the mineral dolomite. In some cases, this rock can comprise nearly pure dolomite.

12 The calcination reaction for dolomite is



14 The formula for dolomite on the left-hand side of Reaction (MgO.4) does not include impurities
 15 such as clay minerals and quartz, which presumably occur in small quantities in the rock quarried
 16 to produce Martin Marietta MgO.

17 Martin Marietta then mixes the brine, dolime, and water to produce a slurry containing dissolved
 18 CaCl₂ and particulate Mg(OH)₂ produced via the following reaction:



21 Note that CaCl₂ and MgCl₂ are written as neutral complex species instead of ionic species in
 22 Reaction (MgO.5), and that H₂O is included on both sides of Reaction (MgO.5) to be consistent
 23 with the information on the Martin Marietta website.

24 Next, Martin Marietta allows the brucite to settle. They filter and wash it to remove all of the
 25 brine and the CaCl₂ dissolved in this brine.

1 Finally, Martin Marietta hard-burns (calcines at 1000-1500 °C [1832-2732 °F]) the brucite to
2 convert it to periclase via Reaction (MgO.2) (Section MgO-3.1).

3 **MgO-3.3.2 Characterization**

4 This subsection reviews the DOE's characterization of Martin Marietta Magnesia Specialties
5 MgO, hereafter called Martin Marietta MgO. It is based on the text in Brush and Roselle (2006,
6 Section 2.3).

7 This section emphasizes the DOE's identification and quantification of the reactive and
8 nonreactive constituents of Martin Marietta MgO. The meanings of *reactive* and *nonreactive*
9 *constituents* are explained in Section MgO-3.2.

10 Wall (2005) carried out a technical evaluation on the suitability of Martin Marietta MgO. This
11 evaluation, which supported the 2004 selection of Martin Marietta as the vendor of MgO for the
12 WIPP (Section MgO-2.2.1), emphasized quantifying the concentration of the reactive phases
13 periclase and lime, but also considered the rate at which these phases hydrate in accelerated tests.

14 Wall (2005) conducted accelerated hydration experiments (hydration of MgO in DI water at
15 90 °C [194 °F]) to (1) measure the concentrations of periclase and lime in these materials and
16 compare them to those of Premier Chemicals MgO (Snider and Xiong 2004); (2) measure the
17 accelerated hydration rates of the Martin Marietta products and compare them to those of
18 Premier Chemicals MgO; (3) improve, if possible, the LOI technique used to measure the brucite
19 and portlandite contents of MgO hydration products. Wall (2005) evaluated three materials from
20 Martin Marietta: MagChem 10 WTS-20, MagChem 10 WTS-30, and MagChem 10 WTS-60.
21 ("MagChem 10" is omitted hereafter.) All of these products are hard-burned MgO (calcined at
22 1000-1500 °C [1832-2732 °F]) with a specified MgO content of 95 wt % and a bulk density of
23 87 lb/cubic foot (ft³) (1,400 kg/cubic meter (m³)). Assay results are typically 97 wt % MgO.
24 However, these results include MgO in phases other than periclase, such as other oxides or
25 silicates (Section MgO-3.2.2).

26 Table MgO-3 compares Wall's (2005) results for sample products WTS-20, WTS-30, and
27 WTS-60 with those obtained by Snider and Xiong (2004) for Premier Chemicals MgO. Snider
28 and Xiong (2004) and Wall (2005) reported the results of their MgO hydration product LOI
29 analysis as mole percent brucite or weight percent brucite. However, based on the results of
30 Deng et al. (2006) and Deng, Xiong, and Nemer (2007) (see below), it is now clear that LOI or
31 TGA cannot readily differentiate between the H₂O lost by brucite and portlandite. Therefore,
32 Deng et al. (2006) and Deng, Xiong, and Nemer (2007) reported their results as mole percent
33 brucite and portlandite or weight percent brucite and portlandite. Thus, the results of Snider and
34 Xiong (2004) and Wall (2005) are described as mole percent brucite and portlandite or weight
35 percent brucite and portlandite in this appendix, which corresponds to the mole percent or weight
36 percent concentration of periclase and lime prior to hydration.

37 Table MgO-3 illustrates the effects of the materials used for the accelerated hydration
38 experiments and the temperature used for LOI on the brucite and portlandite contents of the
39 hydration products and—by assumption—the periclase and lime contents of these materials.
40 Two important conclusions can be drawn from these results:

1 **Table MgO-3. Effects of Temperature Used for LOI Analyses of MgO Hydration Products**
 2 **on the Brucite + Portlandite Concentrations of the Hydrated Samples.**
 3 **From Wall (2005, Table 1), Unless Otherwise Noted.**

Material	Temperature Used for LOI			
	500 °C ^a		750 °C ^a	
	Mol %	Wt %	Mol %	Wt %
WTS-20	87 ± 5 ^b	91 ± 4 ^b	ND ^c	ND ^c
WTS-30	87 ± 5 ^b	91 ± 4 ^b	96 ± 5 ^b	97 ± 3 ^b
WTS-60	90 ± 3 ^b	93 ± 2 ^b	ND ^c	ND ^c
Premier	85 ^d	89 ^d	89 ^d	92 ^d

^a Snider and Xiong (2004) and Wall (2005) reported their results of LOI analysis of MgO hydration products as mole percent brucite or weight percent brucite. However, Deng et al. (2006a) and Deng, Xiong, and Nemer (2007) report their results as mole percent brucite + portlandite or weight percent brucite + portlandite (see text). In this appendix, all of these results are reported as mole percent brucite + portlandite or weight percent brucite + portlandite.

^b Reported uncertainties represent two standard deviations (2σ).

^c ND = not determined.

^d Snider and Xiong (2004).

- 4
- 5 1. All three materials from Martin Marietta have the same or higher contents of reactive
 6 constituents (periclase and lime) than Premier Chemicals MgO.
- 7 2. LOI at 750 °C (1382 °F) yields higher brucite and portlandite contents (and, by assumption,
 8 higher initial periclase and lime contents) than LOI at 500 °C (932 °F). The results obtained
 9 for Premier MgO since the CRA-2004 (Section MgO-3.2.3) imply that the 750 °C (1382 °F)
 10 results are more accurate than the 500 °C (932 °F) results.

11 Wall (2005) reported that LOI at 750 °C (1382 °F) was unsuccessful for WTS-20 and WTS-60
 12 due to decrepitation of these samples at this temperature. Wall (2005) was unable to develop a
 13 procedure for LOI at 750 °C (1382 °F) that prevented decrepitation of these samples. However,
 14 the fact that LOI for WTS-60 at 500 °C (932 °F) yielded a higher brucite and portlandite content
 15 than LOI with WTS-30 at this temperature strongly suggested that the sample of WTS-60 tested
 16 by Wall (2005) had a periclase and lime content greater than or equal to that of WTS-30, and that
 17 the brucite and portlandite content of WTS-60 from LOI at 750 °C (1382 °F) would equal or
 18 exceed 96 ± 5 mol %, or 97 ± 3 wt % (see Table MgO-3). Therefore, it is reasonable to conclude
 19 based on these results that WTS-60, the MgO currently being emplaced in the WIPP, contains 96
 20 ± 5 mol % (97 ± 3 wt %) periclase and lime.

21 Another important result of Wall's (2005) work is that Martin Marietta MgO hydrated
 22 significantly faster in accelerated hydration experiments than Premier Chemicals MgO at the
 23 same temperature (90 °C [194 °F]). Although the DOE does not have any 25 °C (77 °F)
 24 hydration data for Martin Marietta MgO, comparison of the 90 °C (194 °F) data suggests that
 25 Martin Marietta MgO will hydrate faster—and carbonate faster—than Premier MgO at 28 °C
 26 (82 °F), the temperature in the undisturbed Salado Formation at the repository horizon and hence
 27 the temperature expected in the repository after it is filled and sealed (Munson et al. 1987).

1 Deng et al. (2006) and Deng, Xiong, and Nemer (2007) carried out additional characterization of
 2 Martin Marietta WTS-60 MgO, the MgO currently being emplaced in the WIPP. Their
 3 characterization included the following analyses, all of which were conducted on Lot SL2980076
 4 of this material:

- 5 1. Particle-size analysis
- 6 2. Analysis of the chemical composition
- 7 3. Preliminary identification of the nonreactive constituents
- 8 4. LOI analysis and TGA of the reactive constituents in Martin Marietta WTS-60

9 This work was part of an ongoing laboratory study on the efficacy of Martin Marietta MgO
 10 (Deng, Nemer, and Xiong [2006] and Deng, Xiong, and Nemer [2007]).

11 Deng, Xiong, and Nemer (2007, Section 3.1) carried out particle-size analysis of Martin Marietta
 12 WTS-60 MgO by sieving. Table MgO-4 provides the results of their analysis.

13 **Table MgO-4. Particle-Size Distribution of 10 Samples from One Lot of Martin Marietta**
 14 **MgO. Adapted from Deng, Xiong, and Nemer (2007, Table 3).**

Size Range (mm)	Average (wt %)	Standard Deviation (wt %)
> 2.0 mm	7.02	0.91
1.0 to 2.0 mm	32.5	1.76
600 micrometer (µm) to 1.0 mm	20.2	1.28
300 µm to 600 µm	12.7	2.19
150 µm to 300 µm	5.4	0.70
75 µm to 150 µm	3.4	0.35
< 75 µm	17.9	1.88

15
 16 Deng et al. (2006, Section 3.1 and Appendix B, Section B.1) and Deng, Xiong, and Nemer
 17 (2007, Section 3.2 and Appendix B, Section B.1) determined the overall chemical composition
 18 of Martin Marietta WTS-60 MgO by dissolving it in nitric acid, analyzing the liquid by ICP-
 19 AES, and weighing the remaining solids. They reported the following concentrations of oxides
 20 (average concentrations and standard deviations) based on 12 analyses of Lot SL2980076:

- 21 1. MgO: 98.5 ± 2.5 wt %
- 22 2. Al₂O₃: 0.13 ± 0.02 wt %
- 23 3. SiO₂: 0.31 ± 0.01 wt %
- 24 4. CaO: 0.87 ± 0.03 wt %
- 25 5. Fe₂O₃: 0.12 ± 0.01 wt %

1 6. Total: 99.9 ± 2.5 wt %

2 These chemical analyses did not differentiate between the MgO and CaO contained in
 3 the reactive constituents periclase and lime and those contained in the nonreactive constituents.
 4 Preliminary characterization of the nonreactive constituents in WTS-60 suggests that they
 5 comprise (1) a spinel-group mineral that appears to be a solid solution of the four end members
 6 chromite (FeCr_2O_4), hercynite (FeAl_2O_4), magnesiochromite (MgCr_2O_4), and spinel; (2) hematite
 7 (Fe_2O_3); and (3) SiO_2 (polymorph was not determined). The relative proportions of these phases
 8 also have not been determined. It is possible that one or more of these nonreactive constituents
 9 could also consume significant quantities of CO_2 and H_2O in the WIPP, albeit at lower rates than
 10 periclase and lime.

11 Deng et al. (2006, Section 3.2; Section 4; and Appendix B, Section B.2) and Deng, Xiong, and
 12 Nemer (2007, Section 3.3; Section 4; and Appendix B, Subsection B.2) established the
 13 concentration of reactive constituents in Martin Marietta WTS-60 MgO by (1) hydrating samples
 14 of this material in DI H_2O at 90°C (194°F) for at least 3 days; (2) using LOI analysis and TGA
 15 to determine the quantity of H_2O released by hydrated MgO from $150\text{-}800^\circ\text{C}$ ($302\text{-}1472^\circ\text{F}$); and
 16 (3) assuming that nonreactive components did not hydrate to a significant extent, and that any
 17 unbound water was lost at temperatures below 150°C (302°F). In addition, they conducted a
 18 total carbon (C) analysis on samples of WTS-60 by C coulometry before and after hydration to
 19 ensure that precipitation of CaCO_3 , which might have occurred during hydration, did not affect
 20 the results of the LOI analyses and TGA. Based on eight LOI analyses and TGA, they reported
 21 that WTS-60 contains 96.0 ± 1.9 mol % (95.6 ± 1.7 wt %) periclase and lime (see Table MgO-5).

22 **Table MgO-5. Results of LOI Analysis and TGA on WTS-60. From Deng et al. (2006),**
 23 **Table 7 and Table 8, and Deng, Xiong, and Nemer (2007), Table 8 and**
 24 **Table 9.**

Reactive Constituent	Average (mol %)	Standard Deviation (mol %)	Average (wt %)	Standard Deviation (mol %)
Periclase	95.2 ^a	1.82 ^a	94.8 ^b	1.72 ^b
Lime	0.6 ^a	0.04 ^a	0.9 ^b	0.02 ^b
Periclase + lime	95.8 ^a	1.86 ^a	95.7 ^c	1.74 ^b

^a From Deng et al. (2006a, Table 7).

^b From Deng et al. (2006a, Table 8).

^c Value corrected from the value of 95.6 provided by Deng et al. (2006a, Table 8).

25

1 **MgO-4.0 Hydration and Carbonation of MgO**

2 This section reviews the results of the DOE's studies on the hydration and carbonation of MgO
3 (Section MgO-4.1 and Section MgO-4.2, respectively).

4 **MgO-4.1 Hydration of MgO**

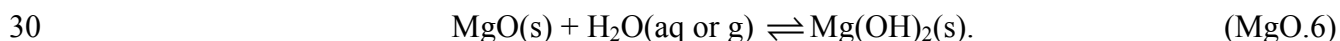
5 The DOE carried out extensive studies on the hydration of Premier Chemicals MgO under four
6 versions of Test Plan 00-07 (Wang and Bryan 2000; Wang, Bryan, and Wall 2001; Snider and
7 Xiong 2002b; Snider, Xiong, and Wall 2004); Section MgO-4.1.1 describes the results of these
8 studies obtained prior to the CRA-2004. Since then, the DOE completed its studies on the
9 hydration of Premier Chemicals MgO and initiated new studies with MgO from Martin Marietta
10 Magnesia Specialties LLC (Deng, Nemer, and Xiong 2006; Deng, Nemer, and Xiong 2007);
11 Section MgO-4.1.2 discusses the results of these studies.

12 **MgO-4.1.1 Hydration of Premier MgO**

13 This section, which reviews the results of studies on the hydration of Premier Chemicals MgO
14 completed prior to the CRA-2004, is based on the text in the CRA-2004, Appendix BARRIERS,
15 Section BARRIERS-2.3.2.1.

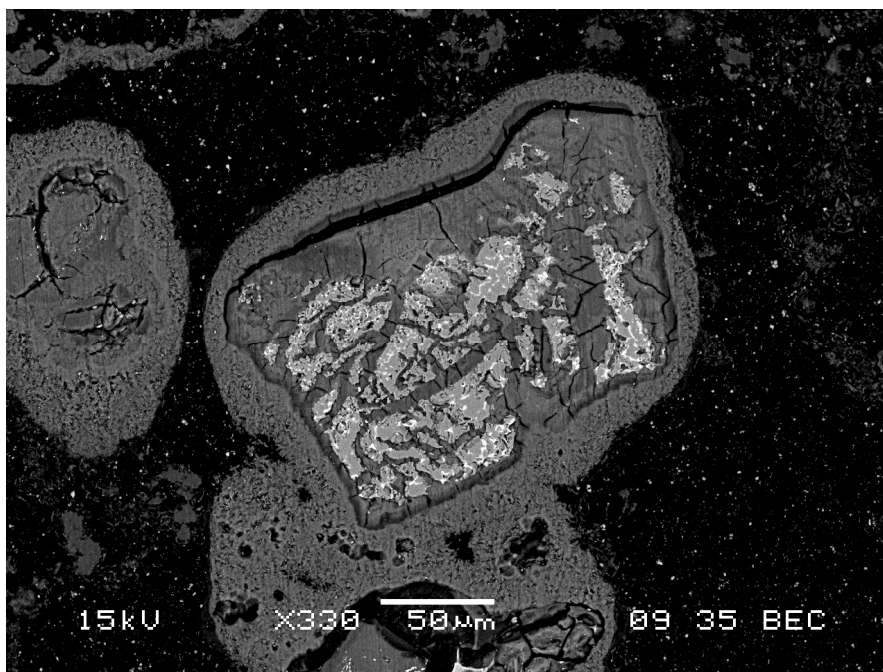
16 Bryan and Snider (2001a and 2001b), Snider (2002 and 2003b), and Xiong and Lord (2008)
17 studied the hydration of Premier Chemicals MgO under humid and inundated conditions. They
18 carried out humid experiments with 3 g of uncrushed Premier Chemicals MgO at an RH of 35,
19 50, 75, or 95% and temperatures of 25, 40, 60, or 80 °C (77, 104, 140, or 176 °F) for up to 460
20 days (Snider 2003b). Inundated experiments were conducted with 5 g of uncrushed Premier
21 Chemicals MgO in 100 mL of DI H₂O, 4.00 molar (M) sodium chloride (NaCl), Energy
22 Research and Development Administration (ERDA)-6, or Generic Weep Brine (GWB) at
23 temperatures of 25, 50, 70, and 90 °C (77, 122, 158, and 194 °F) for up to 360 days (Snider
24 2003b). ERDA-6 brine is a synthetic brine representative of fluids in brine reservoirs in the
25 Castile Formation (Popielak et al., 1983). Snider (2003c) verified that GWB is the average
26 composition of intergranular fluids collected from the Salado at the original stratigraphic horizon
27 of the repository and analyzed by Krumhansl, Kimball, and Stein (1991).

28 Based on these experiments with Premier Chemicals MgO, the most important hydration
29 reaction expected in the WIPP is



31 Reaction (MgO.6) was the only hydration reaction observed in the humid experiments.
32 Reaction (MgO.6) was also the only hydration reaction observed in the inundated runs with
33 ERDA-6 brine (Snider 2003b). In inundated experiments with GWB, hydration produced both
34 brucite and an amorphous or crystalline Mg-OH-Cl-H₂O phase (Snider 2003b). In most of the
35 runs with GWB, the Mg-OH-Cl-H₂O phase was amorphous and its exact composition was not
36 determined. In a few experiments at 25 °C (77 °F), however, a crystalline phase with the
37 composition Mg₃(OH)₅Cl·4H₂O was identified by X-ray diffraction (XRD) analysis (Snider
38 2003b). The thermodynamic speciation and solubility code Fracture-Matrix Transport (FMT)

1 (Babb and Novak 1997 and addenda; Wang 1998) also predicts that both brucite and a similar
 2 Mg-OH-Cl-H₂O phase, Mg₂(OH)₃Cl·4H₂O, would be present in GWB and Salado Primary
 3 Constituents (SPC) brine after these brines equilibrate with the solids in WIPP disposal rooms
 4 (Section MgO-5.1). SPC brine (Novak 1997) is similar to Brine A, another synthetic fluid that
 5 was used to represent intergranular Salado brines (see Section MgO-5.1.1.2 and Molecke 1983).
 6 The FMT thermodynamic database contains the phase Mg₂(OH)₃Cl·4H₂O, but not
 7 Mg₃(OH)₅Cl·4H₂O; if Mg₃(OH)₅Cl·4H₂O were in the database, FMT might predict that
 8 Mg₃(OH)₅Cl·4H₂O would be present in GWB instead of or along with Mg₂(OH)₃Cl·4H₂O.
 9 However, long-term experiments with GWB suggested that brucite might be replacing the
 10 amorphous Mg-OH-Cl-H₂O phase, possibly because the Mg(II)(aq) concentration of this brine
 11 was decreasing with time. Figure MgO-3 is a scanning electron microscope (SEM) image of
 12 Premier Chemicals MgO after hydration in GWB; Figure MgO-4 shows Premier Chemicals
 13 MgO after hydration in ERDA-6 brine. Figure MgO-3 and Figure MgO-4 provide visual
 14 evidence that the passivation of MgO will not occur in the repository.



15
 16 **Figure MgO-3. SEM Image of Premier Chemicals MgO after Hydration in GWB at 90 °C**
 17 **(194 °F) for 21 Days (SNL Experiment CC-GW-90-30-5). The Light-Gray**
 18 **Phase Inside the Large Grain at the Center of This Image is Unhydrated**
 19 **Periclase. The Bright Inclusions in this Periclase are Oxides and Silicates**
 20 **Such as Spinel, Ulvöspinel, Forsterite, and Monticellite (Section MgO-3.2.1**
 21 **and Section MgO-3.2.2). The Dark-Gray Material Surrounding and**
 22 **Penetrating the Fractures in the Periclase is a Mg-OH-Cl-H₂O Phase,**
 23 **Probably Amorphous or Crystalline Mg₃(OH)₅Cl·4H₂O (Section MgO-**
 24 **4.1.1). Abundant Fractures are Seen Penetrating the Mg-OH-Cl-H₂O**
 25 **Phase. The Dark-Gray Material Surrounding the Mg-OH-Cl-H₂O Phase is**
 26 **Brucite. This Layer of Brucite Appears to be Loosely Attached to the Mg-**
 27 **OH-Cl-H₂O Phase, Thus Facilitating the Continued Access of Brine to the**
 28 **Mg-OH-Cl-H₂O Phase and Unhydrated Periclase.**



1
2 **Figure MgO-4. SEM Image of Premier Chemicals MgO after Hydration in ERDA-6 Brine**
3 **at 70 °C (158 °F) after 21 days (SNL Experiment CC-ER-70-30-5). Two**
4 **Concentric Layers of Brucite Surround an Inner Core of Brucite. The**
5 **Outer Layers of Brucite Appear to be Loosely Attached to the Core.**

6 **MgO-4.1.2 Results since the CRA-2004 Regarding Hydration of MgO**

7 Deng, Xiong, and Nemer (2007, Section 5) carried out accelerated hydration experiments with
8 Martin Marietta MgO. The primary objective of the accelerated hydration experiments was to
9 determine which factors (see below) have a significant effect on MgO hydration and carbonation
10 kinetics. Deng, Xiong, and Nemer (2007, Section 5) also conducted experiments to assess the
11 advantages and disadvantages of different types of containers, and the utility of tracer dyes for
12 their ongoing study of the efficacy of Martin Marietta MgO (Deng, Nemer, and Xiong (2006)
13 and Deng, Nemer, and Xiong (2007)). Fernández et al. (1999) identified particle size, solid-to-
14 solution ratio, and stirring speed as important factors that affect the kinetics of carbonation of
15 MgO slurries.

16 Therefore, Deng, Xiong, and Nemer (2007, Section 5) conducted an accelerated, inundated
17 hydration study using a fractional factorial matrix to determine which of these three factors are
18 important enough to include in their long-term hydration and carbonation studies. For the study,
19 they used MgO with particle sizes less than 75 µm, which constituted about 18 wt % of their
20 as-received material (see Table MgO-4); or 1.0 to 2.0 mm, which accounted for about 32 wt % of
21 their material (Lot SL2980076 of Martin Marietta MagChem WTS-60 MgO, the material
22 currently being emplaced in the WIPP). These are the particle-size ranges with the most
23 particles in this lot of Martin Marietta WTS-60 MgO. Deng, Xiong, and Nemer (2007, Section
24 5) used MgO-to-brine ratios of 0.05, 0.4, or 1 g/mL; these values are within the range of 0.001 to
25 10 g/mL expected in the WIPP (Nemer 2006). Furthermore, the previous studies of the

1 inundated hydration and carbonation of Premier Chemicals MgO (Section MgO-4.1.1 and
2 Section MgO-4.2.1, respectively) were performed at an MgO-to-brine ratio of 0.05 g/mL;
3 inclusion of this ratio in the accelerated hydration experiments with Martin Marietta MgO thus
4 facilitated comparison with these results. Finally, the samples were placed in an oven or in a
5 water-bath shaker at a shaking speed of 150 revolutions per minute to determine the effect of
6 agitation. Deng, Xiong, and Nemer (2007, Section 5) carried out these experiments by placing
7 Martin Marietta WTS-60 MgO and DI water in 30-mL high-density polyethylene (HDPE)
8 centrifuge tubes or 125-mL HDPE serum bottles, depending on the MgO-to-brine ratio, and
9 placed these containers in a water-bath shaker or an oven at 70 °C (158 °F) for periods of up to
10 43 days.

11 Deng, Xiong, and Nemer (2007, Section 5.4, p. 33) concluded,

12 [T]he small-particle-size samples hydrated faster than the large particle size during the first few
13 days, which is probably due to the larger specific surface area ... of the small particles. However
14 for the remainder of the experiment, the large-particle-size samples hydrate faster than the small
15 particle size. There are no obvious differences between experiments that were continuously stirred
16 in a water-bath shaker and those that were kept in the oven. The MgO-water ratio did not
17 significantly influence the hydration rate either. These visual observations have been confirmed
18 by the Minitab [statistical] analysis...

19 Finally, Deng, Xiong, and Nemer (2007, Section 5.7) fitted the results of the accelerated,
20 inundated-hydration experiments described above to one kinetic model in which the hydration
21 rate is controlled by the surface area of the MgO particles, and to three models in which the rate
22 is controlled by the diffusion of H₂O through the layer of brucite that formed on the surfaces of
23 the MgO particles. They concluded that the results obtained with the Martin Marietta WTS-60
24 MgO with small particle sizes (< 75 μm) are consistent with control by diffusion, but that the
25 results obtained with the large (1.0 to 2.0 mm) particles are consistent with surface-area control.

26 **MgO-4.2 Carbonation of MgO**

27 The DOE also conducted extensive studies on the carbonation of Premier Chemicals MgO under
28 Test Plan 00-07 (Wang and Bryan 2000; Wang, Bryan, and Wall 2001; Snider and Xiong 2002b;
29 Snider, Xiong, and Nemer 2004); Section MgO-4.2.1 describes the results of these studies
30 obtained prior to the CRA-2004. Since then, the DOE completed its carbonation studies with
31 Premier Chemicals MgO (Section MgO-4.2.2) and started new work with Martin Marietta MgO
32 (Deng, Nemer, and Xiong 2006 and 2007).

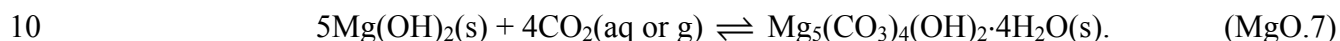
33 **MgO-4.2.1 Carbonation of Premier Chemicals MgO**

34 This section, which reviews the results of studies on the carbonation of Premier Chemicals MgO
35 completed prior to the CRA-2004, is based on the text in the CRA-2004, Appendix BARRIERS,
36 Section BARRIERS-2.3.2.2.

37 Bryan and Snider (2001a and 2001b), Snider (2002), Snider and Xiong (2002a), Xiong and
38 Snider (2003), and Xiong and Lord (2008) studied the carbonation of Premier Chemicals MgO
39 and reagent-grade materials under inundated conditions. Experiments were carried out with 5 g
40 of uncrushed Premier Chemicals MgO in 100 mL of DI H₂O, 4.00 M NaCl, ERDA-6 brine, or
41 GWB under an atmosphere of compressed, ambient, laboratory air at room temperature for up to

1 327 days (Snider and Xiong 2002a). Inundated experiments were also conducted with uncrushed
2 Premier Chemicals MgO; crushed, prehydrated Premier Chemicals MgO; Fisher reagent-grade
3 periclase; or prehydrated Fisher periclase in 100 mL of ERDA-6 brine or GWB under an
4 atmosphere containing 5% CO₂ for periods up to 91 days (Snider and Xiong 2002a). Humid
5 experiments were performed with 2.5 g of prehydrated Fisher periclase in an atmosphere
6 consisting of compressed, ambient, laboratory air at an RH of 33, 58, 75, or 95% at room
7 temperature and 40 °C (104 °F).

8 Based on these experiments, the carbonation reaction expected in the WIPP in the short term (a
9 few hundred to a few thousand years) is



11 In experiments with ERDA-6 brine and atmospheric CO₂, Snider and Xiong (2002a) detected
12 hydromagnesite with the composition Mg₅(CO₃)₄(OH)₂·4H₂O by XRD analysis. This solid is
13 referred to as “hydromagnesite (5424)” in this appendix. No other magnesium (Mg) carbonates
14 were detected in runs with ERDA-6 brine and atmospheric CO₂. Snider and Xiong (2002a)
15 detected both hydromagnesite (5424) and nesquehonite (MgCO₃·3H₂O) by XRD analysis in the
16 experiments with ERDA-6 brine and 5% CO₂, but hydromagnesite (5424) was clearly replacing
17 nesquehonite as these experiments proceeded. In experiments with GWB, hydromagnesite
18 (5424) was the only Mg carbonate detected by XRD analysis (Snider and Xiong 2002a).
19 Therefore, there is strong evidence that hydromagnesite (5424) will be the dominant Mg
20 carbonate for at least part of the 10,000-year regulatory period (the first few hundred to few
21 thousand years).

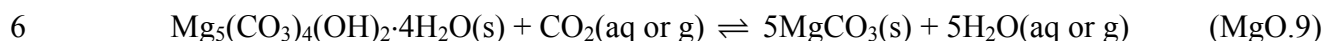
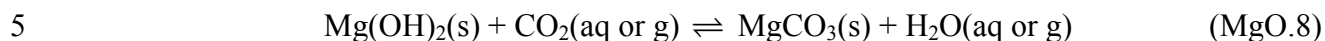
22 There are at least two forms of hydromagnesite: hydromagnesite (5424) (see above) and
23 hydromagnesite with the composition Mg₄(CO₃)₃(OH)₂·3H₂O. The latter is referred to as
24 “hydromagnesite (4323)” in this appendix. Thermodynamic data for both of these forms of
25 hydromagnesite are available; geochemical modeling carried out for the WIPP project (see
26 Section MgO-5.1) has always predicted that hydromagnesite (5424) will form under expected
27 WIPP conditions instead of hydromagnesite (4323) if magnesite is suppressed (i.e., prevented
28 from forming by switching off magnesite in the EQ36 or FMT input file). Moreover,
29 hydromagnesite (5424) was the only form of hydromagnesite produced in laboratory
30 experiments on the carbonation of Premier Chemicals MgO (i.e., hydromagnesite (4323) was not
31 reported). However, predictions of the effects of MgO on the chemical conditions in WIPP
32 disposal rooms and the solubilities of An elements under these conditions suggest that the effects
33 of hydromagnesite (5424) and hydromagnesite (4323) would be similar (compare Table MgO-7
34 and Table MgO-8 in Section MgO-5.1).

35 Section MgO-4.2.2 describes the conversion of hydromagnesite (5424) to magnesite in the
36 WIPP.

37 **MgO-4.2.2 Formation of Magnesite in the WIPP**

38 The DOE stated in the CCA, Appendix BACK and Appendix SOTERM, that magnesite would
39 be the Mg carbonate present throughout the 10,000-year regulatory period. This conclusion was
40 based on calculations by Novak et al. (1996) with the geochemical speciation component of the

1 FMT code (Babb and Novak 1995), which demonstrated that magnesite is thermodynamically
 2 stable with respect to hydromagnesite and other Mg carbonates under expected WIPP conditions.
 3 Because magnesite is the stable Mg carbonate, the DOE maintained that the brucite-magnesite or
 4 the hydromagnesite (5424)-magnesite carbonation reaction



7 would buffer f_{CO_2} in the repository at a value of 1.26×10^{-7} atmospheres (atm), and used this
 8 value of f_{CO_2} (along with other parameters) to calculate An speciation and solubilities for the
 9 CCA PA (CCA, Appendix SOTERM, p. SOTERM-6).

10 Recent thermodynamic calculations carried out by Brush and Xiong (2003a), Brush (2005), and
 11 Brush et al. (2006) with FMT (Babb and Novak 1997 and addenda; Wang 1998) and the EQ3/6
 12 geochemical software package (Daveler and Wolery 1992; Wolery 1992a and 1992b; Wolery
 13 and Daveler 1992) have also predicted that magnesite is stable with respect to hydromagnesite
 14 (5424), hydromagnesite (4323), and other Mg carbonates under expected WIPP conditions.

15 Furthermore, magnesite is commonly observed in the Salado (Lang 1939; Adams 1944;
 16 Lowenstein 1983 and 1988; Stein 1985) and in other formations in the Delaware Basin (Garber,
 17 Harris, and Borer 1990). Lowenstein (1988, p. 598) describes the siliciclastic-carbonate
 18 mudstone, in which magnesite is most abundant, as a “non-evaporitic sediment,” and attributes
 19 its origin to subaqueous “settling of fine-grained, suspended material in the center of the Salado
 20 basin where the energy of inflow waters had largely dissipated.” Therefore, the magnesite
 21 observed in the Salado did not necessarily form in situ. However, Garber, Haris, and Borer
 22 (1990), who reported that magnesite “occurs pervasively” throughout an 82-meter (m) (270-ft)
 23 interval of core recovered from a stratigraphic test well located along the subsurface trend of the
 24 Capitan Reef 27 kilometers (km) (17 miles) northeast of Carlsbad, concluded, “the most likely
 25 origin for the magnesite in the core is the downward movement of dense fluids from the Ochoan
 26 Series, Salado into the underlying, and [at the time] shallowly buried Tansil and Yates
 27 formations.” Clearly, magnesite either formed or persisted for long periods in the Delaware
 28 Basin.

29 During its review of the CCA, the EPA questioned the DOE’s conclusion that magnesite will be
 30 present throughout the entire 10,000-year regulatory period. For the CCA, the DOE based this
 31 conclusion on the fact that magnesite is the thermodynamically stable Mg carbonate under
 32 expected WIPP conditions (the CCA, Appendix BACK and Appendix SOTERM). The EPA
 33 accepted the DOE’s conclusion that magnesite is stable, but questioned whether the kinetics of
 34 the hydromagnesite (5424)-magnesite reaction are fast enough to produce enough magnesite in
 35 10,000 years for the brucite-magnesite reaction to buffer f_{CO_2} at 1.26×10^{-7} atm.

36 A literature review on the formation of dolomite and magnesite in the natural environment and
 37 laboratory studies of the formation of magnesite was completed (Sandia National Laboratories
 38 1997, Section 5.2.1, pp. 32-37). Section MgO-4.2.3 describes other aspects of this study. The
 39 literature review report (Sandia National Laboratories 1997, Section 5.2.1, pp. 32-35) provides
 40 several examples of naturally occurring dolomite and magnesite that may have formed in the last

1 several hundred to few thousand years. Nevertheless, this report states that “the most
2 quantitative rates for precipitation kinetics of magnesite come from laboratory experiments.”
3 Therefore, the data on magnesite formation from Sayles and Fyfe (1973) and Usdowski (1989
4 and 1994) obtained in laboratory experiments conducted at temperatures of 60, 126, and 180 °C
5 was used to perform an Arrhenius extrapolation to 28 °C, the temperature expected in the WIPP
6 after it is filled and sealed (Munson et al. 1987). Based on this extrapolation, it was concluded
7 “Under WIPP conditions, magnesite should form in several hundred years” (Sandia National
8 Laboratories 1997, Figure 5-4).

9 Based on this evidence, the EPA (U.S. Environmental Protection Agency 1998f) concluded:

10 The available rate data indicate that some portion, perhaps all, of the hydromagnesite will be
11 converted to magnesite over the 10,000-year period for repository performance. The exact time
12 required for complete conversion has not been established for all chemical conditions. However,
13 the available laboratory and field data clearly indicate that magnesite formation takes from
14 few hundred to, perhaps, a few thousand years. Thus, the early repository conditions can be best
15 represented by the equilibrium between brucite and hydromagnesite. These conditions will
16 eventually evolve to equilibrium between brucite and magnesite.

17 The EPA (U.S. Environmental Protection Agency 1998f) went on to describe the sequence of
18 reactions that it expected to occur in WIPP disposal rooms:

19 [T]he sequence of events resulting from brine infiltration and reaction with the MgO backfill in
20 the repository may be conceptualized by the following reactions, in order:

- 21 1. Rapid reaction (hours to days) between the brine and MgO to produce brucite.
- 22 2. Rapid carbonation (hours to days) of the brucite to produce nesquehonite and possibly
23 hydromagnesite.
- 24 3. Rapid conversion (days to weeks) of the nesquehonite to hydromagnesite.
- 25 4. Slow conversion (hundreds to thousands of years) of the hydromagnesite to magnesite”

26 However, the EPA (U.S. Environmental Protection Agency 1998f) also stated in the same
27 document:

28 These estimates of conversion rate are confounded by the fact that deposits of hydromagnesite are
29 found in some evaporite basins dated as late Quaternary in age (<23.7 million years) (Stamatakis,
30 1995), indicating that the hydromagnesite has persisted in a metastable state for a long period with
31 only partial conversion to magnesite and other magnesium carbonates.

32 Based at least in part on its interpretation of the implications of the huntite ($\text{CaMg}_3(\text{CO}_3)_4$)-
33 hydromagnesite deposits described by Stamatakis (1995) for the kinetics of the hydromagnesite-
34 magnesite reaction, the EPA stipulated that the brucite-hydromagnesite (5424) reaction be used
35 to buffer f_{CO_2} for the An-solubility calculations in the CCA PAVT (Trovato 1997a; U.S.
36 Environmental Protection Agency 1998f). This reaction would buffer f_{CO_2} at a value of
37 3.14×10^{-6} atm, a value somewhat higher than the value of 1.26×10^{-7} atm maintained by the
38 brucite-magnesite reaction that was used for the CCA PA. The DOE has used a value of
39 3.14×10^{-6} atm for f_{CO_2} in WIPP PA since the CCA PAVT. Brush and Roselle (2006)

1 reconsidered the implications of Stamatakis (1995) for the kinetics of the hydromagnesite-
2 magnesite reaction; their conclusions are described later in this section.

3 Experiments carried out for the WIPP project in the late 1990s by Zhang et al. (1999) imply that
4 magnesite will replace hydromagnesite (5424) rapidly enough to be the dominant Mg carbonate
5 for most of the 10,000-year regulatory period. Zhang et al. (1999) studied the conversion of
6 hydromagnesite (5424) to magnesite in a saturated NaCl solution and GWB at high temperatures
7 and used the Arrhenius equation to extrapolate the results to 25 °C (77 °F), close to the expected
8 WIPP temperature of 28 °C (82.4 °F) (Munson et al. 1987). Zhang et al. (1999) reacted 0.3 g of
9 reagent-grade hydromagnesite (5424) with 1.5 g of saturated NaCl solution or GWB in
10 autoclaves (type unspecified) at 110, 150, or 200 °C (230, 302, or 392 °F). They then quantified
11 the extent of conversion attained in their experiments by comparing XRD patterns for their
12 samples with XRD calibration curves obtained by running premixed samples of their reagent-
13 grade hydromagnesite (5424) and reagent-grade magnesite.

14 Conversion from hydromagnesite (5424) to magnesite took place in days to weeks at 110 and
15 150 °C (230 and 302 °F) (Zhang et al. 1999). This was preceded by an induction period that
16 persisted for nearly half of the time required for essentially complete conversion of
17 hydromagnesite (5424) to magnesite, during which only a few percent of the hydromagnesite
18 (5424) reacted to form magnesite. At 200 °C (392 °F), conversion took place in a few hours. (At
19 room temperature, formation of magnesite has not been observed in experiments carried out for
20 the WIPP project, even in experiments that lasted for a few years.) Conversion of
21 hydromagnesite (5424) to magnesite appeared to be a first-order reaction. The induction period,
22 during which about 4-5% of the hydromagnesite (5424) formed magnesite, may have resulted
23 from slow nucleation of magnesite, after which magnesite formed rapidly.

24 Zhang et al. (1999) also observed that conversion was faster in saturated NaCl than in GWB.
25 (All experiments carried out subsequently with Premier Chemicals MgO have also shown that
26 the rates of hydration and carbonation of periclase and brucite occurred faster in simpler, less
27 concentrated solutions than in complex solutions with higher ionic strengths; i.e., the rates of
28 reaction decrease in the order DI H₂O > 4 M NaCl > ERDA-6 brine > GWB.)

29 Based on their extrapolations to 25 °C (77 °F), Zhang et al. (1999) concluded that after an
30 induction period of 18 or 200 years in saturated NaCl or GWB, respectively, the “half-life” of
31 hydromagnesite (5424) (the time required for half of the hydromagnesite (5424) to convert to
32 magnesite) would be 4.7 years (saturated NaCl) or 73 years (GWB). A period of about 1000
33 years, the approximate sum of the 200-year induction period and 730 years (10 half-lives), would
34 result in conversion of over 99.9% of any hydromagnesite (5424) present to magnesite.

35 The applicability of the extrapolated results from Zhang et al. (1999) to the WIPP is probably
36 more defensible than that of the extrapolated results in Sandia National Laboratories (1997)
37 because Zhang et al. (1999) used high-ionic-strength brines—including one WIPP brine
38 (GWB)—for their experiments, but SNL (Sandia National Laboratories 1997) used only low-
39 ionic-strength (~0.05 M) results obtained from the literature.

40 Recently, Brush and Roselle (2006) reconsidered the implications of Stamatakis (1995) for the
41 kinetics of the hydromagnesite (5424)-magnesite reaction and concluded the following:

- 1 1. It is unclear—based on the poorly constrained age(s) of the huntite-hydromagnesite (4323)
2 deposits in the Kozani Basin, Greece—that the hydromagnesite (4323) there has persisted
3 longer than expected based on the results of Zhang et al. (1999).
- 4 2. It is unclear that any conclusions regarding the kinetics of the hydromagnesite (5424)-
5 magnesite reaction based on the hydromagnesite (4323) present in the Kozani Basin are
6 applicable to the conversion of the hydromagnesite (5424) produced in WIPP-relevant
7 laboratory experiments.

8 Stamatakis (1995) reported various ages or ranges of ages for the huntite-hydromagnesite
9 deposits in the Kozani Basin. He referred to the sedimentary rocks that host these deposits as
10 “late Neogene” and, on two occasions, “uppermost Neogene.” He referred to the alkaline, saline,
11 spring-fed lakes, and ponds from which these evaporite deposits precipitated as “Tertiary to
12 Recent” and “Neogene.” He did not provide any absolute (radiometric) ages for these deposits.

13 According to the current geologic time scale established by the International Commission on
14 Stratigraphy, the Neogene Period has lasted from 23.03 million years ago to the present
15 (Gradstein et al. 2005). Therefore, the ages Neogene, late Neogene, uppermost Neogene, and
16 Tertiary to Recent do not place a lower limit on the possible range of ages of these deposits,
17 especially in the absence of absolute (radiometric or astronomical) ages. Furthermore, the
18 description of the deposits provided by Stamatakis (1995) is consistent with a postdepositional
19 origin for at least some of the deposits. Therefore, it is not clear that the hydromagnesite there
20 has persisted longer than expected based on the results of Zhang et al. (1999).

21 The hydromagnesite in the huntite-hydromagnesite deposits of the Kozani Basin is
22 hydromagnesite (4323). Zhang et al. (1999) used hydromagnesite (5424) in their study on the
23 conversion of hydromagnesite to magnesite. Therefore, any conclusions regarding the rate of the
24 hydromagnesite-to-magnesite reaction based on the hydromagnesite (4323) present in the Kozani
25 Basin do not apply to the conversion of the hydromagnesite (5424) used by Zhang et al. (1999)
26 and observed in the laboratory experiments with Premier Chemicals MgO.

27 **MgO-4.2.3 Possible Passivation of MgO in the WIPP**

28 Laboratory studies on the carbonation of MgO were carried out to determine if (1) MgO would
29 rapidly neutralize the mildly acidic brines that would form if microbial consumption of CPR
30 materials in WIPP disposal rooms produces significant quantities of CO₂; and (2) reaction rims
31 would form on periclase and prevent this phase from effectively consuming all of the CO₂ that
32 could be produced by microbial consumption of CPR materials (Sandia National Laboratories
33 1997). A literature review on the formation of dolomite and magnesite in the natural
34 environment, laboratory studies on the formation of magnesite to determine the timescale on
35 which hydromagnesite (5424) would convert to magnesite, and the results of this activity are
36 described above (Sandia National Laboratories 1997 and Section MgO-4.2.2). It was
37 demonstrated that MgO would rapidly neutralize mildly acidic solutions; therefore, the
38 remainder of this discussion focuses on whether reaction rims would form on periclase and
39 prevent this phase from consuming CO₂ (Sandia National Laboratories 1997, Section 3.2, p. 7
40 and Figure 3-1, p. 8).

1 Short-term “scoping” experiments were carried out by placing MgO pellets in beakers containing
2 Salado or Castile brine and bubbling CO₂ through them for “less than a week.” (See Sandia
3 National Laboratories 1997, Section 3.2, p. 7.) The report states:

4 To provide as much latitude as possible in final materials selection, a material that had undergone
5 calcination at the higher end of the [temperature] range was chosen for testing. Because reactivity
6 typically decreases with increasing calcination temperature, selection of a material at the upper
7 end of the range will provide a worst case.

8 XRD analysis indicated that nesquehonite and hydromagnesite (polymorph unspecified) rapidly
9 formed on the surfaces of the pellets, and “After a few days of treatment, these layers coalesced
10 to cement the pellets together.” SEM analysis “suggested the presence of other phases as well.”
11 (See Sandia National Laboratories 1997, Section 3.2, p. 7)

12 Longer-term “final” experiments were also carried out (Sandia National Laboratories 1997,
13 Section 3.3.1 and Section 3.3.2, pp. 7-13). The primary objective of these experiments was “to
14 demonstrate that the formation of [Mg] carbonate surface coatings, if any, do not impact the
15 efficacy of the MgO backfill enough to impede the backfill’s ability to function as
16 conceptualized within the CCA PA.” A secondary objective was “to demonstrate that after
17 coatings form the MgO remaining inside the pellet will still be reasonably accessible to the
18 outside brine” (Sandia National Laboratories 1997, Section 3.3.1, p. 7). In the first set of these
19 longer-term experiments, about 8 g of 1- to 2-mm-diameter MgO pellets were placed in beakers
20 containing 250 mL of Salado or Castile brine and pure CO₂ was bubbled through the beakers for
21 up to 28 days, during which individual pellets were analyzed for their C content with a C
22 coulometer. In a larger, follow-on set of experiments, 0.5- to 1-mm and 2- to 4-mm-diameter
23 pellets were placed in beakers containing 100 mL of Salado or Castile brine. Manifolds were
24 used to bubble pure CO₂ through brines for up to 28 days, during which “the entire charge” was
25 removed from the beakers and analyzed for its C content. In the follow-up experiments,
26 triplicate experiments were run for every reaction time at which the C content was analyzed, and
27 triplicate C analyses were carried out on the solids in every beaker.

28 In addition, “tea-bag” experiments were conducted, in which MgO pellets (size unspecified)
29 were placed in porous bags about the size of a tea bag, the bottom third of the bags were
30 immersed in Salado or Castile brine, and pure CO₂ bubbled through the brines for periods of 3-
31 85 days. During these experiments, brine wicking moistened all of the pellets in these bags
32 (Sandia National Laboratories 1997, Section 3.3.2, p. 14).

33 “Carbonation curves” (plots of the conversion of their solids to Mg carbonates versus time) that
34 were “S-shaped” were reported (Sandia National Laboratories 1997, Section 4, pp. 17-18). The
35 data showed (1) “an initial incubation period of slow [CO₂] uptake, which is probably preceded
36 by a short period [during which] MgO actually dissolves to saturate the solution” and during
37 which the surfaces of the pellets hydrate to form brucite; (2) “a period of accelerated [CO₂]
38 uptake during which the [CO₂] content of the samples increases by several percent ... in a few
39 days”; and (3) “a long period [during which] the [CO₂] uptake rate is much slower than earlier in
40 the test, though the process does not seem to completely stop.” The incubation period was
41 correlated to dissolution of the MgO pellets, formation of a thin layer of brucite on the pellets,
42 and formation of “an incipient [Mg] carbonate phase ... consisting of fine platy crystals,”
43 possibly “protohydromagnesite.” (See Sandia National Laboratories 1997, Section 4.2, pp. 20-

29.) The period of rapid CO₂ uptake was correlated with the formation of nesquehonite needles, both on the surfaces of the pellets exposed to the brines and in the pores among the pellets. Finally, the final period of slower CO₂ uptake was correlated with reduced access of the brines to the pores caused by intergrowth of the nesquehonite needles and concomitant cementation of the pellets. However, cementation did not stop the carbonation of the pellets, even in the pores. Furthermore, “exfoliation” of nesquehonite and formation of protohydromagnesite or magnesite platy crystals was observed, possibly at the expense of nesquehonite (see Section MgO-4.2.1). Both of these processes would promote continued, albeit reduced, access of brine to the pores.

It was pointed out that, although “isolating reaction rims at high extents of conversion (15-30 mol %) were not observed,” the lower values of f_{CO_2} expected in WIPP disposal rooms would result in a lower concentration gradient of dissolved CO₂-bearing species from the brine to the surfaces of the MgO pellets, which would in turn localize the precipitation of Mg carbonates in the brines instead of on the surfaces of the pellets (see Sandia National Laboratories 1997, Section 5.1, pp. 30-32, and especially Figure 5-1). The experiments bubbled pure CO₂ through their brines (Sandia National Laboratories 1997, Section 3.3.2, pp. 8-14). This, in turn, established values of f_{CO_2} in the brines that were orders of magnitude greater than those expected in the repository, currently from 3.14×10^{-6} atm (both GWB and ERDA-6) down to 1.20×10^{-7} atm (GWB) or 1.23×10^{-7} atm (ERDA-6), the values characteristic of the brucite-hydromagnesite (5425) and the brucite-magnesite carbonation reactions (see Section MgO-5.1).

In addition to the laboratory experiments described above, MgO was added to one of the liter-scale experiments (L-28) in the WIPP Source Term Test Program (STTP) with actual TRU waste (Villarreal, Bergquist, and Leonard 2001a and 2001b; Villarreal, King, and Leonard 2001; Villarreal et al. 2001). (The STTP comprised 39 L-scale and 15 drum-scale experiments.) Because the dissolved plutonium (Pu) concentration in L-28 increased after the addition of MgO, the New Mexico Environmental Evaluation Group cited this experiment as an example of the inefficacy of MgO, possibly because of passivation (Oversby 2000). The experiment in L-28 was carried out at a CO₂ pressure of 60 bars, 7 orders of magnitude higher than that expected in the WIPP (from 3.14×10^{-6} atm down to 1.20×10^{-7} atm; see Section MgO-5.1). The partial pressure of CO₂ in the WIPP will not exceed 3.14×10^{-6} atm because the rate of CO₂ consumption by the periclase and brucite in MgO is much higher than the microbial CO₂ production rate. Therefore, the conditions in L-28 were not representative of those expected in the WIPP, and the results are irrelevant to the WIPP (Brush, Moore, and Wall 2001).

Bryan and Snider (2001b, p. 5-9) and Snider (2002, pp. 3.1 through 3.15) conducted a series of “cemented-cake” experiments to determine whether lithification of MgO will occur in the WIPP and, if so, whether it would affect the rate of MgO hydration. For the experiments, 15, 30, or 45 g of Premier Chemicals MgO were placed in 125-mL plastic containers with ERDA-6 brine or GWB. This resulted in a 5-, 10-, or 15-mm thick layer of Premier Chemicals MgO at the bottom of the containers. The containers were then placed in ovens at 25, 50, 70, or 90 °C (77, 122, 158, or 194 °F) for periods of up to about 6 months. They were not agitated. (Agitation apparently prevented any lithification of MgO in their other inundated experiments.) Snider (2002, Figure 12, Figure 13, and Figure 14) reported results from cemented-cake experiments that lasted for periods of about four to six months. She observed lithification of some samples; however, others remained “very friable,” even after inundation at 70 and 90 °C (Snider 2002, p. 3.1 through 3.15). Snider (2002, p. 3.13) had “anticipated that the thicker layers would hydrate

1 at a slower rate,” especially if lithification occurred. However, “MgO thickness has not affected
2 the hydration rate under inundated conditions in ERDA-6 brine (Figure-12)” (Snider 2002, p. 3.1
3 through 3.13); and “in GWB at 50, 70, and 90 °C (Snider 2002, Figure 13) thickness does not
4 affect hydration” (Snider 2002, p. 3.1 through 3.15). Furthermore, the 5-mm-thick samples in
5 GWB at 25 °C (77 °F) hydrated at the slowest rate, the 15-mm-thick samples hydrated at an
6 intermediate rate, and the 10-mm-thick samples hydrated at the fastest rate (Snider 2002,
7 Figure 13). Therefore, these experiments showed that lithification might occur, but, if it does, it
8 will not decrease the MgO hydration rate.

9 The results obtained all imply that the periclase in MgO and the brucite that forms from the
10 hydration of this periclase will be available to react, and will continue to react, until all CO₂ in
11 the repository has been consumed (Sandia National Laboratories (1997), Bryan and Snider
12 (2001b), and Snider (2002)). Nevertheless, Brush and Roselle (2006, Section 5.1 and Section
13 5.2) carried out a literature search for anthropogenic or natural analogs or experimental studies
14 that provide insight into whether hydration of periclase to form brucite, and carbonation of
15 brucite to form hydromagnesite and magnesite, will proceed to completion if H₂O or CO₂,
16 respectively, are present in the repository. The literature they found included studies of several
17 different types of chemical and geochemical systems:

- 18 1. Hydration of periclase in Portland cement
- 19 2. Hydration of periclase in magnesia sinters
- 20 3. Hydration of periclase formed in contact-metamorphosed dolomite and Mg-bearing
21 limestone
- 22 4. Laboratory studies of periclase hydration in metamorphic rocks formed at high pressures and
23 temperatures (these conditions are far from those expected in the WIPP, but provide valuable
24 insight because of the challenges involved in preventing periclase hydration during and after
25 “quenching” these experiments to ambient laboratory conditions)
- 26 5. Field studies of brucite carbonation during serpentinization of ultramafic rocks and the
27 weathering of the resulting serpentinites
- 28 6. The use of brucite to scrub CO₂ from the smokestacks of power plants, or for deep-geologic
29 sequestration of CO₂
- 30 7. The weathering of an approximately 4,000-year-old statue carved from a rock known as
31 predazzite, a brucite- or periclase-bearing limestone marble

32 The results of these anthropogenic- and natural-analog studies all imply that the periclase in the
33 MgO engineered barrier and the brucite that forms from the hydration of this periclase will be
34 available to react—and will continue to react—until all the CO₂ in the repository has been
35 consumed.

1 **MgO-5.0 Effects of MgO on the WIPP Disposal System**

2 This section reviews the effects of MgO on (1) brine composition, f_{CO_2} , pH, and An solubilities,
3 including changes since the CRA-2004 (Section MgO-5.1); (2) colloidal An concentrations
4 (Section MgO-5.2); (3) other near-field processes and conditions, including repository H_2O
5 content, gas generation, and room closure (Section MgO-5.3); and (4) far-field An transport
6 (Section MgO-5.4).

7 **MgO-5.1 Effects of MgO on Brine Composition, f_{CO_2} , pH, and Actinide (An)** 8 **Solubilities**

9 The DOE is emplacing MgO in the WIPP to decrease the solubilities of the An elements in TRU
10 waste by consuming all the CO_2 that would be produced by microbial activity should all the CPR
11 materials in the repository be consumed. Consumption of CO_2 will decrease An solubilities by
12 (1) buffering f_{CO_2} at a low value or within a low range of values, (2) maintaining a mildly basic
13 pH, and (3) preventing the production of significant carbonate ion (CO_3^{2-}) quantities.

14 The effects of MgO carbonation have been included in WIPP PA by removing CO_2 from the
15 gaseous phase in BRAGFLO calculations, and using the values of f_{CO_2} and pH predicted for
16 reactions among MgO, brine, and aqueous or gaseous CO_2 to calculate An solubilities.

17 Table MgO-6 provides the initial compositions of GWB and ERDA-6 brine and their
18 compositions predicted by FMT for the An-solubility calculations for the CRA-2004 PABC
19 (Brush and Xiong 2005a; 2005b; Brush 2005) after equilibration with (1) the MgO hydration and
20 carbonation products brucite ($\text{Mg}(\text{OH})_2$) and hydromagnesite (5424), respectively; (2) halite
21 (NaCl) and anhydrite (CaSO_4), two of the most abundant minerals in the Salado; and (3) the An-
22 bearing solids $\text{Am}(\text{OH})_3$; hydrous, amorphous ThO_2 ; and KNpO_2CO_3 . In addition to these
23 solids, which are specified in the input files, FMT predicted that (1) the solids
24 $\text{Mg}_2(\text{OH})_3\text{Cl}\cdot 4\text{H}_2\text{O}$ and whewellite (Ca oxalate hydrate, or $\text{CaC}_2\text{O}_4\cdot\text{H}_2\text{O}$) would precipitate from
25 GWB; and (2) glauberite ($\text{Na}_2\text{Ca}(\text{SO}_4)_2$) and whewellite would precipitate from ERDA-6 brine if
26 these brines equilibrate with brucite, hydromagnesite (5424), halite, and anhydrite. Note that,
27 although FMT predicted that $\text{Mg}_2(\text{OH})_3\text{Cl}\cdot 4\text{H}_2\text{O}$ would precipitate from GWB,
28 $\text{Mg}_3(\text{OH})_5\text{Cl}\cdot 4\text{H}_2\text{O}$ has been observed in experiments with GWB (see Section MgO-4.1.1 and
29 Figure MgO-3X). Note also that because these calculations were performed for the CRA-2004
30 PABC, oxalate (and other organic ligands) were added to these brines, which resulted in the
31 prediction that whewellite would precipitate.

32 FMT predicts equilibration of these brines with the solids listed above will (1) establish a total
33 inorganic C (TIC) concentration of 0.350 millimolar (mM) in GWB, and decrease the TIC
34 concentration from 16 to 0.428 mM in ERDA-6 brine; (2) buffer f_{CO_2} at 3.14×10^{-6} atm in both
35 brines; and (3) establish a pH of 8.69 in GWB and increase the pH from 6.17 to 8.94 in ERDA-6
36 brine.

37 Equilibration of GWB and ERDA-6 brine with these solids will also change the concentrations
38 of the major and other minor elements in these brines. In particular, the concentration of Mg in

1 GWB will decrease from 1.02 to 0.578 M, but will increase from 0.019 to 0.157 M in ERDA-6
 2 brine (Table MgO-6).

3 **Table MgO-6. Compositions of GWB and ERDA-6 Brine Predicted by FMT for the An-**
 4 **Solubility Calculations for the CRA-2004 PABC (Brush and Xiong 2005a;**
 5 **2005b; Brush 2005) (M, Unless Otherwise Noted) before and after**
 6 **Equilibration with Brucite, Hydromagnesite, Halite, Anhydrite, and Other**
 7 **Solids**

Element or Property	GWB before Reaction with Solids ^a	GWB after Reaction with Solids ^b	ERDA-6 Brine before Reaction with Solids ^c	ERDA-6 Brine after Reaction with Solids ^d
B(III)(aq)	0.158	0.166	0.063	0.0624
Na(I)(aq)	3.53	4.35	4.87	5.24
Mg(II)(aq)	1.02	0.578	0.019	0.157
K(I)(aq)	0.467	0.490	0.097	0.0961
Ca(II)(aq)	0.014	0.00895	0.012	0.0107
S(VI)(aq)	0.177	0.228	0.170	0.179
Cl(-I)(aq)	5.86	5.38	4.8	5.24
Br(-I)(aq)	0.0266	0.0278	0.011	0.0109
TIC	—	0.350 mM	16 mM	0.428 mM
Ionic strength	—	7.66 m	—	6.80 m
f _{CO₂} (atm)	—	3.14 × 10 ⁻⁶	—	3.14 × 10 ⁻⁶
pH	—	8.69	6.17	8.94
RH	—	0.732	—	0.748
Specific gravity	1.2	1.23	1.216	1.22

^a From Krumhansl et al. (1991) and Snider (2003c).
^b FMT Run 7 (Brush and Xiong 2005a; 2005b; Brush 2005).
^c From Popielak et al. (1983).
^d FMT Run 11 (Brush and Xiong 2005a; 2005b; Brush 2005).

8
 9 Table MgO-7 and Table MgO-8 show the effects of the Mg-carbonate solid produced by the
 10 carbonation of brucite on the TIC concentration, f_{CO₂}, pH, and the solubilities of An elements in
 11 the III, IV, and V oxidation states (An(III), An(IV), and An(V)) in GWB and ERDA-6 brine,
 12 respectively. Brush and Xiong (2003a; 2003b; 2003c; 2003d) carried out this sensitivity study as
 13 part of the An speciation and solubility calculations for the CRA-2004 PA. These calculations
 14 were superseded by those conducted for the CRA-2004 PABC (Brush and Xiong 2005a; 2005b;
 15 Brush 2005), which are now part of the WIPP PA baseline. However, Brush and Xiong (2005a,
 16 2005b) and Brush (2005) did not redo this sensitivity study for the CRA-2004 PABC. Therefore,
 17 Table MgO-7 and Table MgO-8 provide the results from the CRA-2004 PA, along with the
 18 results of the CRA-2004 PABC Runs 7 and 11, respectively (fourth column of Table MgO-7 and
 19 Table MgO-8). Runs 7 and 11 were also used for the CRA-2009 PA. Comparison of the CRA-
 20 2004 PA results in the third column of Table MgO-7 and Table MgO-8 with the CRA-2004
 21

1 **Table MgO-7. Effect of the Mg-Carbonate Solid on the f_{CO_2} (atm), TIC Concentration (M),**
 2 **pH (Standard Units), and An Solubilities (M) in GWB after Equilibration**
 3 **with Brucite, Halite, Anhydrite, and Other Solids**

Element or Property	Magnesite ^a	Hydro-magnesite ₅₄₂₄ ^b	Hydro-magnesite ₅₄₂₄ ^c	Hydro-magnesite ₄₃₂₃ ^d	Nesquehonite ^e
f_{CO_2}	1.20×10^{-7}	3.14×10^{-6}	3.14×10^{-6}	4.08×10^{-6}	1.42×10^{-4}
TIC	1.36×10^{-5}	3.50×10^{-4}	3.50×10^{-4}	4.56×10^{-4}	1.59×10^{-2}
pH	8.69	8.69	8.69	8.69	8.69
An(III)	3.06×10^{-7}	3.07×10^{-7}	3.87×10^{-7}	3.07×10^{-7}	2.12×10^{-6}
An(IV)	1.17×10^{-9}	1.19×10^{-8}	5.64×10^{-8}	1.52×10^{-8}	5.68×10^{-7}
An(V)	2.37×10^{-5}	1.02×10^{-6}	3.55×10^{-7}	8.06×10^{-7}	2.28×10^{-7}

^a CRA-2004 PA Run 14 (Brush and Xiong 2003a; 2003b; 2003c; 2003d).

^b CRA-2004 PA Run 18 (Brush and Xiong 2003a; 2003b; 2003c; 2003d).

^c CRA-2004 PABC Run 7 (Brush and Xiong 2005a; 2005b; Brush 2005).

^d CRA-2004 PA Run 16 (Brush and Xiong 2003a; 2003b; 2003c; 2003d).

^e CRA-2004 PA Run 20 (Brush and Xiong 2003a; 2003b; 2003c; 2003d).

4

5 **Table MgO-8. Effect of the Mg-Carbonate Solid on the f_{CO_2} (atm), TIC Concentration (M),**
 6 **pH (Standard Units), and An Solubilities (M) in ERDA-6 Brine after**
 7 **Equilibration with Brucite, Halite, Anhydrite, and Other Solids**

Element or Property	Magnesite ^a	Hydro-magnesite ₅₄₂₄ ^b	Hydro-magnesite ₅₄₂₄ ^c	Hydro-magnesite ₄₃₂₃ ^d	Nesquehonite ^e
f_{CO_2}	1.23×10^{-7}	3.14×10^{-6}	3.14×10^{-6}	4.08×10^{-6}	1.36×10^{-4}
TIC	1.87×10^{-5}	4.68×10^{-4}	4.28×10^{-4}	6.08×10^{-4}	2.00×10^{-2}
pH	9.02	9.02	8.94	9.02	9.00
An(III)	1.68×10^{-7}	1.69×10^{-7}	2.88×10^{-7}	1.70×10^{-7}	5.45×10^{-7}
An(IV)	1.72×10^{-9}	2.47×10^{-8}	6.79×10^{-8}	3.19×10^{-8}	1.01×10^{-6}
An(V)	1.19×10^{-4}	5.08×10^{-6}	8.24×10^{-7}	4.00×10^{-6}	1.10×10^{-6}

^a CRA-2004 PA Run 24 (Brush and Xiong 2003a; 2003b; 2003c; 2003d).

^b CRA-2004 PA Run 28 (Brush and Xiong 2003a; 2003b; 2003c; 2003d).

^c CRA-2004 PABC Run 11 (Brush and Xiong 2005a; 2005b; Brush 2005).

^d CRA-2004 PA Run 26 (Brush and Xiong 2003a; 2003b; 2003c; 2003d).

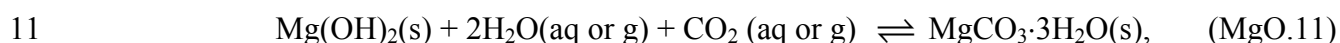
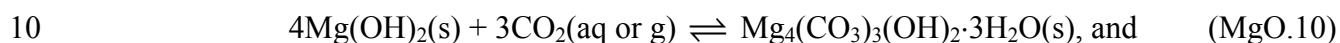
^e CRA-2004 PA Run 30 (Brush and Xiong 2003a; 2003b; 2003c; 2003d).

8

9 PABC results in the fourth column shows that the TIC concentration, $\log f_{\text{CO}_2}$, and pH predicted
 10 for GWB by the CRA-2004 PA and PABC calculations are identical to three significant figures.
 11 The TIC content, $\log f_{\text{CO}_2}$, and pH predicted for ERDA-6 by the CRA-2004 PA and PABC
 12 calculations are not identical, but are similar. The An(III), An(IV), and An(V) solubilities
 13 predicted for the CRA-2004 PA and PABC calculations are different for both brines because of
 14 changes in the thermodynamic databases for the An(III), An(IV), and An(V) models between
 15 these calculations. Although the CRA-2004 PA results were not part of the WIPP PA baseline,

1 the results of this sensitivity study still provide a reasonably accurate assessment of the effects of
2 the Mg carbonate formed in the WIPP.

3 Table MgO-7 and Table MgO-8 show that both the TIC content and the f_{CO_2} predicted for each
4 Mg-carbonate solid increase by about three orders of magnitude from magnesite to
5 hydromagnesite (5424), to hydromagnesite (4323), to nesquehonite. This is because magnesite
6 is the thermodynamically stable Mg carbonate under expected WIPP conditions; hydromagnesite
7 (5424) is metastable with respect to magnesite, hydromagnesite (4323) is metastable with respect
8 to hydromagnesite (5424), and nesquehonite is metastable with respect to hydromagnesite
9 (4323). The brucite carbonation Reactions (MgO.8), (MgO.7), as well as



12 would buffer f_{CO_2} at values of 1.20×10^{-7} atm (Reaction [MgO.8]) to 1.42×10^{-4} atm (Reaction
13 [MgO.11]) in GWB (Table MgO-7), or 1.23×10^{-7} atm (Reaction [MgO.8]) to 1.36×10^{-4} atm
14 (Reaction [MgO.11]) in ERDA-6 brine (Table MgO-8), depending on which of these reactions is
15 dominant. The TIC concentrations corresponding to these fugacities would be 1.36×10^{-5} M
16 (Reaction [MgO.8]) to 1.59×10^{-2} M (Reaction [MgO.11]) in GWB (Table MgO-8), or $1.87 \times$
17 10^{-5} M (Reaction [MgO.8]) to 2.00×10^{-2} M (Reaction [MgO.11]) in ERDA-6 brine (Table
18 MgO-8).

19 Although nesquehonite was observed in some of the DOE's carbonation experiments with
20 Premier Chemicals MgO (Section MgO-4.2.1), hydromagnesite (5424) was clearly replacing
21 nesquehonite as these experiments proceeded (Section MgO-4.2.1). Therefore, carbonation of
22 brucite to form hydromagnesite (5424) (Reaction [MgO.7]) will be the dominant carbonation
23 reaction for at least part of the 10,000-year regulatory period (the first few hundred to few
24 thousand years). The DOE has not observed the formation of hydromagnesite (4323), and has
25 not observed magnesite, except in some accelerated experiments (e.g., Zhang et al. 1999; Zhang,
26 Hardesty, and Papenguth 2001). However, these accelerated experiments (and other
27 considerations) imply that carbonation of brucite to form magnesite (Reaction [MgO.8]) will be
28 the dominant carbonation reaction for much, if not most, of the 10,000-year regulatory period
29 (Section MgO-4.2.3). Therefore, f_{CO_2} would be 3.14×10^{-6} atm in the WIPP initially while
30 hydromagnesite (5424) is the dominant Mg carbonate, but would decrease to $(1.20-1.23) \times$
31 10^{-7} atm as magnesite replaces hydromagnesite (5424) and becomes dominant. Similarly, the
32 TIC concentration would be about $(3.50-4.28) \times 10^{-4}$ M initially, but would decrease to about
33 $(1.36-1.87) \times 10^{-5}$ M.

34 Appendix SOTERM-2009, Section SOTERM-2.3.2 describes how MgO will control the pH of
35 brines in WIPP disposal rooms.

36 **MgO-5.1.1 Changes Since the CRA-2004 in Effects of MgO on Brine Composition, f_{CO_2} ,** 37 **pH, and Actinide (An) Solubilities**

38 This section describes the two changes in the predicted effects of MgO on chemical conditions in
39 the WIPP since the CRA-2004: MgO-5.1.1.1 describes the elimination of chemical conditions

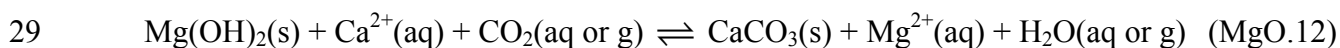
1 predicted for nonmicrobial PA vectors, and MgO-5.1.1.2 discusses the substitution of GWB for
2 Brine A.

3 The reduction of the MgO excess factor that was approved by the EPA since the CRA-2004 will
4 not affect chemical conditions in the WIPP. Therefore, it is described in Section MgO-6.2.4.

5 **MgO-5.1.1.1 Elimination of Chemical Conditions for Nonmicrobial Vectors**

6 There are large uncertainties as to whether significant microbial consumption of the CPR
7 materials emplaced in the WIPP will occur during the 10,000-year WIPP regulatory period.
8 Therefore, Brush (1995) assumed that “significant microbial consumption of CPR materials is
9 possible, but by no means certain.” To incorporate these uncertainties in the CCA PA and
10 PAVT, Wang and Brush (1996a and 1996b) developed a conceptual model for microbial activity
11 in the repository. According to this model, there is a probability of 0.50 for significant microbial
12 activity. In the event of significant microbial activity, microbes could consume 100% of the
13 cellulosic materials in the repository. Furthermore, there is a conditional probability of 0.50 that
14 microbes could consume all of the plastic and rubber materials after consumption of all of the
15 cellulosic materials. Thus, in the CCA PA and PAVT, there was no microbial activity in about
16 50% of the PA realizations (vectors); microbes could consume all of the cellulosic materials, but
17 no plastic or rubber materials, in about 25% of the vectors; and microbes could consume all of
18 the CPR materials in the remaining ~25% of the vectors. (Note that even if significant microbial
19 activity could occur in a vector, microbes did not necessarily consume 100% of the cellulosic
20 materials or 100% of the CPR materials because the quantities of these materials that the PA
21 code BRAGFLO predicted would be consumed depended on several sampled parameters.) This
22 conceptual model for microbial activity was also used in the CRA-2004 PA.

23 For the CCA PA and PAVT, it was assumed that the chemical conditions in WIPP disposal
24 rooms would be identical whether or not significant microbial activity and gas generation occur.
25 (See Brush and Xiong 2003c, Section 5, for a detailed review of how near-field chemical
26 conditions were predicted for the CCA PA and PAVT.) For the CRA-2004 PA, however, Brush
27 and Xiong (2003c, Section 5.3.2) concluded that, for the vectors without microbial activity, the
28 reaction that would buffer f_{CO_2} is



30 not the brucite-hydromagnesite (5424) carbonation reaction (Reaction [MgO.7]) (Section MgO-
31 4.2.1 and Section MgO-5.1).

32 Brush and Xiong (2003a) used FMT to establish chemical conditions for the nonmicrobial
33 vectors in the CRA-2004 PA that were slightly different than those calculated for the microbial
34 vectors. They calculated that the f_{CO_2} would be 3.31×10^{-6} and 7.08×10^{-7} atm in GWB and
35 ERDA-6 brine, respectively, for the nonmicrobial vectors; and 3.14×10^{-6} atm in both brines for
36 the microbial vectors. They also predicted that the pH would be 8.69 and 8.99 in GWB and
37 ERDA-6 brine, respectively, for the nonmicrobial vectors and 8.69 and 9.02 for the microbial
38 vectors. Despite these differences, Brush and Xiong (2003a, Table 7) calculated An solubilities
39 that were nearly identical for the nonmicrobial and microbial vectors in most cases. The only
40 exceptions were the solubilities of An(IV) in ERDA-6 brine (5.84×10^{-9} M for the nonmicrobial

1 and 2.47×10^{-8} M for the microbial vectors) and An(V) in ERDA-6 brine (2.13×10^{-5} M in the
2 nonmicrobial and 5.08×10^{-6} M in the microbial vectors).

3 During its completeness review of the CRA-2004 PA, however, the EPA (Cotsworth 2005,
4 Enclosure 1, p. 1) stated

5 In the CRA performance assessment [the CRA-2004 PA], DOE assumes that the probability that
6 microbial degradation will occur and thus produce significant gas is 50 percent [*sic*]. However,
7 based on our review to date, including DOE's response to EPA comments ..., EPA believes that
8 there are reasonable alternative interpretations to DOE's responses. It is EPA's position that
9 microbes will survive over the regulatory period and be able to produce some gas, albeit with the
10 possibility that sometimes the resulting gas generation rate may be low or near zero. The revised
11 performance assessment [the CRA-2004 PABC] must implement a change so that the modeled
12 probability of microbial degradation is 1. DOE may propose different ranges of gas production or
13 microbe effectiveness as long as it is supported by data...

14 To incorporate this change in the CRA-2004 PABC, there is now a probability of 1 that
15 significant microbial activity could occur and that microbes could consume 100% of the
16 cellulosic materials in the repository. Furthermore, there is a probability of 0.25 that microbes
17 could consume all of the CPR materials. Therefore, microbes could consume all of the cellulosic
18 materials, but no plastic or rubber materials, in about 75% of the vectors; and microbes could
19 consume all of the CPR materials in the remaining ~25% of the vectors. The microbial gas
20 generation model for the CRA-2004 PABC is the one used for CRA-2009.

21 The separate chemical conditions established for the nonmicrobial vectors were used only once
22 in WIPP PA, for the CRA-2004 PA (the CRA-2004, Appendix BARRIERS, Section
23 BARRIERS-2.3.2.4; the CRA-2004, Appendix PA, Attachment SOTERM, Section SOTERM-
24 2.2.2 and Section SOTERM-3.5).

25 **MgO-5.1.1.2 Substitution of GWB for Brine A**

26 Brush and Xiong (2003c, Section 5.3.1) proposed to the EPA that GWB (Krumhansl et al. 1991;
27 Snider 2003c) be substituted for Brine A (Molecke 1983) in future An speciation and solubility
28 calculations for WIPP PA because "this brine resembles the average composition of intergranular
29 Salado brines at or near the stratigraphic horizon of the WIPP more closely than Brine A." The
30 synthetic solution Brine A was used extensively for laboratory and modeling studies of WIPP
31 chemistry (e.g., Brush 1990; Brush 1996; Brush and Storz 1996) prior to the establishment of
32 GWB as a more representative Salado brine (Krumhansl, Kimball, and Stein 1991; Snider
33 2003c).

34 For the CRA-2004, Brush and Xiong (2003a) calculated chemical conditions and An solubilities
35 in both Brine A and GWB, as well as in ERDA-6 brine (used to represent fluids from Castile
36 brine reservoirs). The conditions and solubilities predicted for Brine A and GWB were very
37 similar, as were those predicted for Brine A or GWB and ERDA-6 brine. The solubilities
38 calculated in GWB were used for the CRA-2004 PA (the CRA-2004, Appendix PA, Attachment
39 SOTERM, Section SOTERM-3.5).

40 The EPA approved the use of GWB for An-solubility calculations for WIPP PA (U.S.
41 Environmental Protection Agency 2006). Therefore, the conditions predicted for GWB in WIPP

1 disposal rooms are now considered the baseline conditions for Salado brine. The solubilities
2 calculated in GWB were used for the CRA-2004 PABC (Leigh et al. 2005) and the CRA-2009
3 PA.

4 **MgO-5.2 Effects of MgO on Colloidal Actinide (An) Concentrations**

5 This section is based on the text in the CRA-2004, Appendix BARRIERS, Section BARRIERS-
6 2.3.3.

7 Colloids could affect the long-term performance of the WIPP because of their potential ability to
8 bind cationic metals such as the An elements in TRU waste, and because of their potential
9 mobility under expected repository conditions (Choppin 1988). Colloids are typically defined as
10 phases intermediate in size between dissolved ionic or molecular species and suspended particles
11 large enough to settle by gravity. The size range of colloids is typically on the order of
12 1 nanometer to 1 μm .

13 Humic substances, microbes, and mineral fragments could bind An elements in the WIPP.
14 Under some conditions, An elements could also form intrinsic colloids without binding to
15 humics, microbes, or minerals. Even if one or more of these four types of colloids form(s) in the
16 WIPP, they would not transport An elements out of the repository unless they remain suspended
17 in brine. If coagulation occurs, any An elements bound to these colloids would be immobilized,
18 at least with respect to direct brine releases or injection of brine into the Culebra Dolomite
19 Member of the Rustler Formation (hereafter referred to as Culebra).

20 Chemical conditions in the repository will affect the colloidal An source term. The small
21 variations in pH within the narrow range imposed by MgO will not affect the concentrations of
22 An-bearing colloids significantly. Studies carried out to quantify the colloidal source term
23 included experiments under the conditions that will be established by MgO (the CRA-2004,
24 Appendix PA, Attachment SOTERM, Section SOTERM-6.0 and Appendix SOTERM-2009).

25 **MgO-5.2.1 Results since the CRA-2004**

26 The results of Wall and Matthews (2005) imply that colloids formed by the association of
27 actinides and humic substances are highly unstable in the presence of MgO, and that these
28 colloids dissociate rapidly (i.e., within hours).

29 **MgO-5.3 Effects of MgO on Other Near-Field Processes and Conditions**

30 Section MgO-5.3.1, Section MgO-5.3.2, and Section MgO-5.3.3 are based on the text in the
31 CRA-2004, Appendix BARRIERS, Section BARRIERS-2.3.4.1, Section BARRIERS-2.3.4.2,
32 and Section BARRIERS-2.3.4.3.

33 **MgO-5.3.1 Effects of MgO on Repository H₂O Content**

34 The hydration of periclase could consume significant quantities of H₂O in the WIPP (Reaction
35 [MgO.6]). The carbonation of brucite to form hydromagnesite (5424) (Reaction [MgO.7]) or,
36 less likely, hydromagnesite (4323), will not release this H₂O unless hydromagnesite (5424) or
37 (4323) goes on to form magnesite. Furthermore, even if large quantities of magnesite form

1 during the 10,000-year regulatory period (Reaction [MgO.8]), there will still be large quantities
2 of periclase available for hydration because the DOE is emplacing more MgO than necessary to
3 consume all the CO₂ that would be produced by microbial activity should all the CPR materials
4 in TRU waste and waste containers be consumed.

5 MgO hydration is not included in PA at this time.

6 **MgO-5.3.2 Effects of MgO on Gas Generation**

7 The two gas-producing processes included in WIPP PA are anoxic corrosion of steels and other
8 Fe-base alloys, which will produce H₂, and microbial consumption of CPR materials, which will
9 produce mainly CO₂, hydrogen sulfide (H₂S), and methane (CH₄).

10 **MgO-5.3.2.1 Gas Generation from Anoxic Corrosion**

11 Telander and Westerman (1993 and 1997) studied anoxic corrosion of various metals and
12 concomitant H₂ production under expected WIPP conditions. Wang and Brush (1996a and
13 1996c) used results from three types of experiments carried out by Telander and Westerman
14 (1993 and 1997) to establish ranges and probability distributions of H₂ production rates for the
15 CCA PA:

- 16 1. Experiments with low-C steels in or above Brine A under atmospheres consisting of initially
17 pure CO₂, nitrogen (N₂), or hydrogen sulfide (H₂S) in inert (noncorroding), metallic
18 containers at low-to-intermediate pressures (about 1 to 20 atm).
- 19 2. Experiments with low-C steels in Brine A under H₂, CO₂, or N₂ in autoclaves at high
20 pressures (35 to 127 atm).
- 21 3. Runs with low-C steels in ERDA-6 brine at pH values of 2.8 to 10.6 under N₂. All these
22 experiments were conducted at 30 ± 5 °C (86 ± 9 °F). Brine A and ERDA-6 brine are
23 described above (Section MgO-4.1.1)

24 Anoxic corrosion of low-C steels in Brine A under initially pure N₂ resulted in a pH of 8.3, 8.3,
25 and 8.4 after 6, 12, and 24 months, respectively (see Telander and Westerman 1993, Table 6-3,
26 Test Containers 10, 17, and 25). Wang and Brush (1996a; 1996c) used the 12-to-24-month data
27 from these experiments to establish a range and probability distribution of inundated, anoxic-
28 corrosion rates of steels and other Fe-base alloys of 0 to 0.5 μm/year for the CCA PA. This is
29 equivalent to a range of (0-1.59) × 10⁻¹⁴ meters per second (m/s). Data on the effects of pH on
30 corrosion rates (Telander and Westerman 1997, Table 6-5) have demonstrated that rates obtained
31 at a pH of 8.3 or 8.4 are somewhat higher than those at a pH of 8.69, 8.99, or 9.02, the values
32 expected for the brucite dissolution reaction (see Reaction [MgO.3], above). Therefore, the
33 anoxic-corrosion rates established by Wang and Brush (1996a and 1996c) for the CCA
34 incorporated the effects of MgO on pH.

35 For the CCA PAVT, the EPA specified that the upper limit of the inundated anoxic-corrosion
36 rate range be increased from 1.59 × 10⁻¹⁴ m/s to 3.17 × 10⁻¹⁴ m/s (Trovato 1997b, Enclosure 2;
37 U.S. Environmental Protection Agency 1998e, Table ES-4, Section 5.15, and Table 6.3 and

1 Table 6.4; Hansen and Leigh 2003). A range of $(0-3.17) \times 10^{-14}$ m/s was also used for the CRA-
2 2004 PA (CRA-2004, Appendix PA, Section PA-5.2) and the CRA-2004 PABC (Leigh et al.
3 2005).

4 **MgO-5.3.2.2 Microbial Gas Generation**

5 Francis and Gillow (1994 and 2000), Francis, Gillow, and Giles (1997), and Gillow and Francis
6 (2001a, 2001b, 2002a, 2002b, and 2003) did not include MgO or the effects of pH in their study
7 of microbial gas generation under expected WIPP conditions. Instead, they included bentonite in
8 about half of their experiments because a backfill consisting of 70 wt % crushed salt and 30 wt %
9 bentonite had been proposed as an alternative to a backfill consisting entirely of crushed salt, the
10 design-basis backfill in January 1992 when these microbial gas-generation experiments were
11 started. No microbial experiments have been carried out with MgO since the use of this material
12 to consume CO₂ and control f_{CO_2} and pH in the WIPP was proposed in 1996.

13 Dissolution of brucite (Section MgO-5.1, Reaction [MgO.11]) will prevent the pH of any brine
14 present from decreasing below a value of about 9. This mildly basic value is somewhat higher
15 than the mildly acidic pH values produced by dissolution of microbial CO₂ in the experiments
16 described by Francis and Gillow (1994 and 2000), Francis et al. (1997), and Gillow and Francis
17 (2001a, 2001b, 2002a, 2002b, and 2003). However, emplacement of MgO in the WIPP and a
18 consequent, mildly basic pH of 9 will not in and of itself preclude significant microbial activity
19 in the repository. This conclusion is based on the common observation of viable alkalophilic
20 microbes in alkaline lakes with pH values of 9 to 10. Such alkaline lakes occur frequently in arid
21 and semiarid environments, such as southeastern New Mexico and adjacent areas of west Texas,
22 and could be one source of the halophilic microbes observed in the WIPP. However, several
23 investigators have reported that MgO and compounds derived from MgO possess inhibitory or
24 even biocidal properties (Asghari and Farrah 1993; Chapman et al. 1995; Koper et al. 2002;
25 Sawai 2003; Sawai et al. 1995a, 1995b, 1996, 2000a, and 2000b; Stoimenov et al. 2002;
26 Yamamoto et al. 1998). Some of the results of these studies may be applicable to the WIPP.

27 First, the inhibitory or biocidal effects of MgO probably result from the presence of brucite, not
28 periclase (Sawai et al. 1995a), because most of the experiments cited above were conducted in
29 aqueous solutions or in growth media that contained H₂O, and most of these experiments were
30 long enough for significant nucleation and growth of brucite on periclase surfaces exposed to
31 these solutions or media.

32 Second, the inhibitory or biocidal effects of MgO do not seem to be caused by the mildly basic
33 pH that results from the presence of brucite in aqueous solutions or growth media. Sawai et al.
34 (2000b) reported that the survival of *Escherichia coli* (*E. coli*) was unaffected by a MgO-free,
35 alkaline growth medium at pH values of 10, 10.25, and 10.5, but that *E. coli* survival decreased
36 significantly in the same medium at pH values of 10.75 and 11. This result agrees with the
37 conclusion that a mildly basic pH of about 9 (Section MgO-5.1) will not by itself preclude
38 microbial activity in the WIPP.

39 Third, inhibition of microbial activity seems to require contact between MgO particles and
40 microbes (Sawai et al. 2000a). This conclusion is based on the observation that increased
41 shaking speed of an MgO-bearing slurry increased the mortality of *E. coli* in the slurry.

1 Fourth, the inhibitory effect is inversely proportional to the size of the MgO particles (Sawai
2 et al. 1996; Koper et al. 2002; Stoimenov et al. 2002) and the temperature at which the MgO was
3 prepared (Sawai et al., 1996).

4 Application of these results to microbial activity in the WIPP is difficult in the absence of long-
5 term experiments under expected repository conditions. Biocides are often used for sterilization
6 of solid materials, but become ineffective as the volume of the material(s) to be sterilized
7 increases. This is because it becomes progressively more difficult to ensure uniform distribution
8 of the biocide throughout these materials, and hence to ensure contact between the biocide and
9 the microbes, as the volume increases. Therefore, sterilization methods such as autoclaving and
10 radiation are used for materials with large volumes. In the case of MgO, Sawai et al. (2000a)
11 reported that inhibition of microbial activity seems to require contact between MgO particles and
12 microbes. Although room closure will rupture the supersacks and disperse the MgO into the
13 interstices among and within the ruptured waste containers, this will not ensure contact between
14 MgO particles and microbes. Furthermore, survival of microbes in samples subjected to
15 treatment with an inhibitory or biocidal agent such as MgO, especially those that have had some
16 contact with particulate MgO, would probably result in the development of increased resistance
17 to MgO.

18 The results described above suggest that MgO might reduce the rate of microbial gas generation
19 in the WIPP. However, in the absence of repository-specific experiments, the potential
20 inhibitory or biocidal effects of MgO on the microbial gas-production rates are not included in
21 PA.

22 **MgO-5.3.3 Effects of MgO on Room Closure**

23 In the CCA PA, the CCA PAVT, the CRA-2004 PA, and the CRA-2004 PABC calculations,
24 room closure initially proceeded as if the rooms were open. The free air space was eliminated
25 early in the calculations by unmitigated creep closure. Eventually, the salt contacted the waste
26 and deformed it according to the waste response model. At the same time, corrosion and gas
27 production pressurized the rooms. The coupled processes involved compression owing to the
28 superincumbent rock counterbalanced by gas production, which was obtained from sampled
29 parameters. Thus, room closure was caused by salt creep modified by the structural response of
30 the waste and by gas production. MgO was not explicitly included in the PA room closure
31 calculations, and is not expected to have a significant effect on room closure.

32 **MgO-5.4 Effects of MgO on Far-Field An Transport**

33 This section is based on the text in CRA-2004, Appendix BARRIERS, Section BARRIERS-2.4.

34 MgO could affect the matrix distribution coefficients (K_{ds}) used to predict transport of dissolved
35 thorium (Th), uranium (U), Pu, and americium (Am) through the Culebra (see Brush 1996 or
36 Brush and Storz 1996 for a definition of matrix K_{ds}). For the CCA PA, data from an empirical
37 sorption study, a mechanistic sorption study, and a column-transport study were used to establish
38 ranges and probability distributions of K_{ds} for Th, U, Pu, and Am.

1 Most of these K_{ds} were obtained from 6-week, empirical sorption experiments carried out with
2 1 g of dolomite-rich rock crushed to a size range of 75 to 500 μm ; 20 mL of Brine A, ERDA-6
3 brine, AISinR, or H-17 with dissolved Th(IV), U(VI), Np(V), Pu(V), or Am(III); and a
4 controlled atmosphere containing 0.24, 1.4, or 4.1% CO_2 to simulate the expected range of f_{CO_2}
5 in the Culebra, about 3.16×10^{-4} to 3.16×10^{-2} atm (see Brush 1996; Brush and Storz 1996).
6 Brine A and ERDA-6 brine are described above (Section MgO-4.1.1); AISinR is a synthetic
7 brine representative of fluids sampled from the Culebra in the WIPP air intake shaft; and H-17
8 simulates Culebra brine from the H-17 Hydropad.

9 Brush (1996) and Brush and Storz (1996) extended the empirical K_{ds} obtained with Brine A and
10 ERDA-6 brine to a pH of about 9 or 10 with data from a mechanistic sorption study that
11 quantified the effects of f_{CO_2} , pH, and ionic strength on the sorption of Th(IV), U(VI),
12 neptunium(V) (Np(V)), Pu(V), and Am(III) from synthetic NaCl solutions by well-characterized,
13 pure dolomite. Therefore, the K_{ds} for Brine A and ERDA-6 brine used for the CCA PA included
14 the effects of MgO on pH. The K_{ds} for the Culebra brines, however, did not include the effects
15 of MgO on pH because it was assumed that if mixing is sufficient to produce fluids with
16 compositions similar to those of Culebra brines, the pH of these mixtures will also be similar to
17 those of Culebra brines (Brush 1996; Brush and Storz, 1996).

18 For the CCA PAVT, the EPA specified that the probability distributions for the K_{ds} be changed
19 from uniform to loguniform (Trovato 1997a, Enclosure 2; U.S. Environmental Protection
20 Agency 1998a, Table ES-3 and Table ES-4, Section 5.34, Section 5.3.5, Section 5.36, Section
21 5.37, and Section 5.38 and Table 6.3 and Table 6.4; Hansen and Leigh 2003). However, the
22 EPA did not change any of the K_{ds} .

23 Brush and Storz (1996) corrected some of the ranges of K_{ds} established by Brush (1996) for the
24 CCA PA. These corrections were too late for the far-field transport calculations for the CCA
25 PA, and were not included in the far-field transport calculations for the CCA PAVT. Hansen and
26 Leigh (2003), however, incorporated them in the PA database, and the CRA-2004 PA and the
27 CRA-2004 PABC used the corrected K_{ds} along with the loguniform probability distributions
28 specified by the EPA (see the CRA-2004, Appendix PA, Section PA-5.2). The K_{ds} for Brine A
29 and ERDA-6 brine used for the CRA-2004 PA and the CRA-2004 PABC included the effects of
30 MgO on pH, but the K_{ds} for the Culebra brines do not (Brush 1996; Brush and Storz 1996).

1 **MgO-6.0 The MgO Excess Factor**

2 The MgO excess factor is defined as the ratio of the total amount of MgO to be emplaced in the
3 WIPP divided by the total amount required to consume all of the CO₂ produced by microbial
4 activity should all of the CPR materials in the repository be consumed, calculated as specified by
5 the EPA (Marcinowski 2004; U.S. Environmental Protection Agency 2004). The EPA's
6 specifications for calculating the excess factor are described below.

7 Previously, the DOE referred to the MgO excess factor as the "MgO safety factor," and the EPA
8 still uses "MgO safety factor." In this appendix, "MgO excess factor" is used exclusively. For
9 the purposes of the discussions below, these terms are synonymous.

10 **MgO-6.1 Effects of Microbial Respiratory Pathways on the MgO Excess** 11 **Factor**

12 The conceptual model of sequential use of electron acceptors is based on the common
13 observation that, at any given time, (1) microbes use the best available electron acceptor
14 (oxidant) (i.e., the one that yields the most free energy per mole of organic C consumed);
15 (2) after depletion of the best available electron acceptor, these microbes—or other microbes—
16 begin to consume the next-best available electron acceptor; and (3) this process continues with
17 successively less favorable electron acceptors until all of the substrates (CPR materials in the
18 case of the WIPP) are consumed, an essential nutrient is consumed, or some other limiting
19 condition is attained. Sequential use of electron acceptors has been observed in a diverse array
20 of natural and anthropogenic environments, such as lacustrine, riverine, estuarine, and oceanic
21 sediments; soils; and landfills. In these environments, the order of use observed is oxygen (O₂)
22 (referred to as aerobic respiration), NO₃⁻ (denitrification), Mn(IV) oxides and hydroxides (Mn
23 reduction), Fe(III) oxides and hydroxides (Fe reduction), SO₄²⁻ (SO₄²⁻ reduction), and CO₂
24 (fermentation and methanogenesis) (Froelich et al. 1979; Berner 1980; Criddle, Alvarez, and
25 McCarty 1991; Chapelle 1993; Wang and Van Cappellen 1996; Schlesinger 1997; Hunter,
26 Wang, and P. Van Cappellan 1998; Fenchel, King, and T.H. Blackburn 2000). (In the following
27 discussion, fermentation and methanogenesis are usually referred to as "methanogenesis" for
28 simplicity.) Sequential use of electron acceptors by microbes is included in the conceptual
29 model for gas generation in the WIPP, one of the four conceptual models for long-term chemical
30 evolution of WIPP disposal rooms implemented in WIPP PA (Sandia National Laboratories
31 1996; U.S. Department of Energy 1996a, Chapter 6, Section 6.4.3.3; CRA-2004, Chapter 6.0,
32 Section 6.4.3.3).

33 In the WIPP, the quantities of O₂, Mn(IV) oxides and hydroxides, and Fe(III) oxides and
34 hydroxides will be small relative to that of CPR materials (Brush 1990 and 1995; Wang and
35 Brush 1996a). Therefore, aerobic respiration, manganese (Mn) reduction, and Fe reduction can
36 be ignored from the standpoint of their potential effects on the long-term chemical behavior of
37 the repository.

38 However, several potentially useful electron acceptors will be present in and/or around WIPP
39 disposal rooms: (1) some NO₃⁻ and SO₄²⁻ will be present in the waste; (2) SO₄²⁻ is present in
40 SO₄²⁻-bearing minerals such as anhydrite, gypsum (CaSO₄·2H₂O), and polyhalite

1 denitrification, SO_4^{2-} reduction, and methanogenesis would consume 4.89, 0.84, and 94.27 mol
2 %, respectively, of the CPR materials in the repository; the overall CO_2 yield would be
3 0.529 mol of CO_2 per mol of organic C.

4 However, it is possible that microbial SO_4^{2-} reduction could continue after microbes consume all
5 the SO_4^{2-} in the waste. Microbial SO_4^{2-} reduction could continue by using the SO_4^{2-} dissolved in
6 Salado or Castile brines, or by using SO_4^{2-} released by the dissolution of anhydrite, gypsum, and
7 polyhalite in the disturbed rock zone (DRZ) surrounding WIPP disposal rooms (Section MgO-
8 6.2.3.1, Section MgO-6.2.3.2, and Section MgO-6.2.3.3).

9 **MgO-6.2 History of the MgO Excess Factor**

10 This section reviews (1) the establishment of the MgO excess factor (Section MgO-6.2.1); (2) the
11 reduction of the MgO excess factor from 1.95 to 1.67 (Section MgO-6.2.2), which occurred
12 concomitantly with the EPA's approval of the DOE's request to eliminate the emplacement of
13 minisacks (Section MgO-2.1.2); (3) additional developments relevant to the MgO excess factor
14 prior to the CRA-2004 (Section MgO-6.2.3); and (4) changes since the CRA-2004 (Section
15 MgO-6.2.4), which included the EPA's approval of the DOE's request to reduce the MgO excess
16 factor from 1.67 to 1.2.

17 **MgO-6.2.1 Establishment of the MgO Excess Factor**

18 Just prior to the submittal of the CCA, Peterson (1996) calculated the quantity of MgO required
19 to consume all of the CO_2 produced should microbes consume all of the CPR materials in the
20 WIPP. Peterson (1996) assumed that (1) microbes would consume all of the CPR materials in
21 the WIPP TRU waste inventory (U.S. Department of Energy 1996b), and (2) the CO_2 yield
22 would be 1 mol of CO_2 per mol of organic C in the CPR materials (i.e., there would be no
23 methanogenesis).

24 The DOE stated in the CCA that it would emplace 85,600 short tons (77,640 metric tons) of
25 MgO in the WIPP (U.S. Department of Energy 1996a, Chapter 3, Section 3.3.3). However, it did
26 not specify an MgO excess factor. Instead, it said that "Since the MgO backfill is being added in
27 large excess, any quantity of brine that may enter the repository will be saturated with respect to
28 the appropriate MgO reaction products" (the CCA, Appendix BACK, p. BACK-3).

29 The MgO excess factor was first established by an EPA request for additional information during
30 its review of the CCA, and by the DOE's response to that request. The portion of the EPA
31 request relevant to the establishment of the MgO excess factor was that the DOE "... provide
32 information which demonstrates that the excess volume proposed to be emplaced can actually be
33 accommodated and whether it covers the uncertainties in the actual geochemical process"
34 (Nichols 1996, Enclosure 2, p. 11). The pertinent portion of the DOE's response (Dials 1997)
35 was the following:

36 The quantity of MgO required to be emplaced to assure removal of CO_2 from the gas phase is
37 based on calculations that consider all processes that might contribute to CO_2 production. These
38 calculations are very conservative in that they utilize a maximum extent of CO_2 production, a
39 quantity that is unlikely to be attained. Based on the [Baseline Inventory Report, or BIR] and
40 memoranda in the Records Center, the total number of moles of MgO required to react with the

1 maximum possible amount of CO₂ generated is 9.85×10^8 mol. Using the appropriate conversion
 2 factors (40.3 g/mol, 0.001 kg/g, 2.202 kg/lb, 0.0005 lb/ton) a total of 43,700 tons of MgO are
 3 required to react with this maximum estimate of [CO₂] production. Section 3.3.3 of the CCA
 4 documents that approximately 85,600 tons of backfill will be emplaced in the repository.
 5 Therefore, by dividing the mass of backfill to be emplaced (85,600 tons) by the maximum mass of
 6 MgO required to react with the maximum possible [CO₂] production (43,700 tons), a 1.95 factor
 7 of safety results. In other words, 95% more MgO will be emplaced than is required to react with a
 8 conservative estimate of the maximum quantity of CO₂ production.

9 The EPA included this calculation of the MgO excess factor in its review of the CCA (U.S.
 10 Environmental Protection Agency 1998a, Section 44.A.5 and Section 44.A.6).

11 This excess factor of 1.95 is consistent with the conservative assumptions that (1) microbes
 12 would consume all of the CPR materials in the inventory (U.S. Department of Energy 1996b),
 13 and (2) the CO₂ yield would be 1 mol of CO₂ per mol of organic C in the CPR materials (i.e.,
 14 there would be no methanogenesis even if all of the CPR materials in the repository were
 15 consumed).

16 The DOE assumed that the CO₂ yield would be 1 mol of CO₂ per mol of organic C in the CPR
 17 materials because at the time that Wang and Brush (1996a and 1996b) established the conceptual
 18 model and parameters for microbial gas generation in the CCA PA, Francis and Gillow (1994)
 19 and Francis, Gillow, and Giles (1997) had observed aerobic respiration and denitrification, but
 20 not methanogenesis, in their microbial gas-generation experiments at Brookhaven National
 21 Laboratory (BNL). By the time Wang and Brush (1996a and 1996b) established the model and
 22 parameters for the CCA PA, BNL had carried out their experiments for up to 1,228 days (3.36
 23 years). Therefore, there was no experimental evidence at the time of the CCA PA or the CCA
 24 PAVT that methanogenesis would actually occur in the WIPP. There were at least four possible
 25 reasons why methanogenesis had not been observed by the time of the CCA and the CCA
 26 PAVT:

- 27 1. Halophilic methanogens capable of metabolizing complex, organic substrates such as
 28 cellulosic materials under expected WIPP conditions do not exist.
- 29 2. Halophilic methanogens capable of metabolizing complex, organic substrates exist, but were
 30 not present in the materials used to inoculate these experiments (laboratory dust; brine and
 31 mud from the salt lakes in Nash Draw; and brine collected from G Seep in G Drift, a drift
 32 located in the northern end of the WIPP underground workings).
- 33 3. Methanogens were present in the materials used to inoculate these experiments, but had not
 34 survived collection, storage, and inoculation of the BNL experiments.
- 35 4. Methanogens had survived collection, storage, and inoculation of these experiments, but
 36 there had not been enough time for other microbes to consume all of the NO₃⁻ and SO₄²⁻ and
 37 allow the methanogens to become active.

38 **MgO-6.2.2 Reduction of the MgO Excess Factor from 1.95 to 1.67**

39 In 2001, the MgO excess factor decreased from 1.95 to 1.67 when the EPA approved the DOE's
 40 2000 request to eliminate the emplacement of minisacks among the waste containers and

1 between the waste containers and the ribs (Triay 2000; U.S. Department of Energy 2000;
2 Marcinowski 2001; U.S. Environmental Protection Agency 2001). Section MgO-2.1.2 describes
3 the DOE's request to eliminate the minisacks and the EPA's approval of this request.

4 The DOE's 2000 request to eliminate the minisacks proposed a less-conservative assumption for
5 the calculation of the MgO excess factor: that methanogenesis would be the dominant microbial
6 respiratory pathway in the WIPP should all of the CPR materials in the repository be consumed,
7 and therefore, microbes would not convert all of the organic C in the CPR materials to CO₂.

8 The DOE proposed this less-conservative assumption because Francis and Gillow (2000, pp. 2,
9 3, and 10) observed CH₄ in the headspaces of their long-term, inundated microbial gas-
10 generation experiments carried out at BNL for 2,718 days (7.44 years) under most combinations
11 of conditions. However, Francis and Gillow (2000) did not observe CH₄ in the inundated
12 experiments to which excess NO₃⁻ had been added at the start of the experiments. The addition
13 of excess NO₃⁻ to some of the experiments appears to have prevented the onset of
14 methanogenesis. Wang (2000a) used the results of Francis and Gillow (2000) to support the
15 DOE's request to eliminate the minisacks (Section MgO-2.1.2).

16 Therefore, it was clear that the absence of experimental evidence for methanogenesis at the time
17 of the CCA was because microbial activity in the initially aerobic inundated experiments had not
18 progressed through aerobic respiration, denitrification, and SO₄²⁻ reduction to methanogenesis;
19 and that microbial activity in the initially anaerobic inundated experiments had not progressed
20 through denitrification and SO₄²⁻ reduction to methanogenesis. The requirement that these steps
21 be completed prior to the onset of methanogenesis is a consequence of the observation of the
22 sequential use of electron acceptors (Section MgO-6.1), according to which methanogenesis does
23 not start until any and all NO₃⁻ and SO₄²⁻ are depleted. Although methanogenesis had not been
24 observed by the time of the CCA in experiments carried out for up to 1,228 days (3.36 years),
25 Francis and Gillow observed CH₄ in inundated experiments after 2,718 days (7.44 years).

26 It was also clear from these results by the time of the DOE's 2000 request to eliminate the
27 minisacks that (1) there exist communities of halophilic methanogens capable of metabolizing
28 complex organic substrates, such as cellulosic materials, under expected WIPP conditions;
29 (2) these microbes are present and viable in one or more of the materials used to inoculate these
30 experiments; and (3) these microbes are capable of surviving exposure to O₂. Methanogens are
31 obligate anaerobes and, as such, are extremely sensitive to exposure to O₂. The fact that they
32 produced CH₄ after exposure to O₂ implies that they are capable of producing resistant forms that
33 can survive initially oxic conditions in these experiments.

34 Furthermore, results from the BNL microbial gas-generation study have confirmed that viable
35 halophilic methanogens capable of metabolizing cellulosic materials under expected near-field
36 conditions are present in the WIPP underground workings. Francis and Gillow (2000, pp. 2 and
37 10) detected CH₄ in initially oxic, unamended, and uninoculated experiments, and in initially
38 anoxic, unamended, and uninoculated experiments. The most likely explanation for microbial
39 gas production in these uninoculated experiments is that G Seep, the brine used for these
40 inundated experiments, was collected from the WIPP underground workings. This brine
41 contained a small but viable microflora, including methanogens, and was not sterilized prior to
42 use. The fact that these microbes produced CH₄ after exposure to O₂ in the air used to ventilate

1 G Drift and in initially oxic experiments implies that they are capable of producing resistant
2 forms that can withstand initially oxic conditions in the repository.

3 However, the presence of viable halophilic methanogens in the WIPP does not preclude the
4 possibility that similar communities of microbes are also present in the other materials used to
5 inoculate these experiments, especially brine and mud from the salt lakes in Nash Draw. It is
6 quite possible that methanogens in these lakes are also capable of producing resistant forms that
7 can survive the oxic conditions encountered during eolian transport from Nash Draw to the
8 WIPP air intake shaft, and initially oxic conditions in the repository. Therefore, the presence of
9 viable methanogens in the WIPP does not depend on the claim that microbes have survived in
10 the Salado since the Permian Period (Vreeland, Rosenzweig, and Powers 2000) a claim that is
11 controversial (see, for example, Hazen and Roedder 2001; Parkes 2000; Powers, Vreeland, and
12 Rosenzweig 2001; Satterfield et al. 2005).

13 Based on the results of Francis and Gillow (2000) and the analysis of Wang (2000a), the DOE's
14 2000 request to eliminate the minisacks proposed that, if methanogenesis were the dominant
15 respiratory pathway, it would increase the MgO excess factor from values of 1.95 prior to and
16 1.67 after the proposed elimination of the minisacks to values of 3.73 prior to and 3.23 after
17 minisack elimination (U.S. Department of Energy 2000, Table 1).

18 The EPA's approval of the DOE's request to eliminate the minisacks included the results of
19 several of the DOE's calculations regarding excess MgO, but did not acknowledge the proposed
20 excess factors of 3.73 prior to and 3.23 after minisack elimination (U.S. Environmental
21 Protection Agency 2001, Table 1).

22 **MgO-6.2.3 Additional Developments Relevant to the MgO Excess Factor Prior to the** 23 **CRA-2004**

24 In March 2004, the EPA approved emplacing supercompacted waste from the AMWTP at the
25 INEEL in the WIPP (Marcinowski 2004; Trinity Engineering Associates 2004; U.S.
26 Environmental Protection Agency 2004). However, the EPA specified that the DOE maintain an
27 MgO excess factor of 1.67. Because much of the AMWTP waste contains high concentrations
28 of CPR materials, the DOE anticipated the need to emplace additional MgO in the repository,
29 and began to explore various possible approaches to support a Planned Change Request (PCR)
30 for EPA approval of a reduction in the MgO excess factor.

31 **MgO-6.2.3.1 Additional Evidence for Microbial Methanogenesis under Expected WIPP** 32 **Conditions**

33 Gillow and Francis (2001b) reported additional CH₄ in the inundated, initially anaerobic
34 experiments in which Francis and Gillow (2000, pp. 2, 3, and 10) had first detected this gas.
35 Furthermore, Gillow and Francis (2001b, pp. 3-4 and 3-5) detected CH₄ in experiments to which
36 excess NO₃⁻ had been added at the start of these experiments. These results were from
37 experiments sampled after 3462 days (9.48 years). After 2,718 days (7.44 years), Francis and
38 Gillow (2000, pp. 2, 3, and 10) had not observed CH₄ in the experiments to which excess NO₃⁻
39 had been added. Therefore, this excess NO₃⁻ had delayed, but did not permanently prevent, the

1 onset of methanogenesis. This seemed to make the case stronger for methanogenesis as a
2 potential microbial respiratory pathway in the WIPP.

3 Consequently, the DOE emphasized the likely dominance of methanogenesis during microbial
4 consumption of the CPR materials in the WIPP (CRA-2004, Appendix BARRIERS, Section
5 BARRIERS-2.5.1). Based on the CRA-2004 PA inventory (CRA-2004, Appendix DATA,
6 Attachment F) and calculations by Snider (2003d), the DOE concluded that (1) 4.72 mol % of
7 the CPR materials would be consumed by denitrification, 0.82 mol % by SO_4^{2-} reduction, and
8 94.46 mol % by methanogenesis; (2) the overall CO_2 yield would be 0.528 mol of CO_2 per mol
9 of organic C consumed; and (3) the MgO excess factor would be 2.45.

10 However, during a DOE-EPA technical exchange in January 2004, the EPA expressed concern
11 that naturally occurring SO_4^{2-} could delay or even prevent methanogenesis in the WIPP after
12 microbes consume the SO_4^{2-} in the waste. Dissolved SO_4^{2-} is present in both Salado and Castile
13 brines (see Table MgO-6), so advective transport of SO_4^{2-} into WIPP disposal rooms via seepage
14 of intergranular Salado brines (i.e., GWB) from the DRZ, or inflow of brines from the Castile
15 (i.e., ERDA-6 brine) could delay or prevent methanogenesis. Furthermore, diffusive transport of
16 dissolved SO_4^{2-} from DRZ minerals such as anhydrite, gypsum, and polyhalite—all of which
17 contain SO_4^{2-} —to WIPP disposal rooms could become important as microbial consumption of
18 SO_4^{2-} in the waste creates a concentration gradient from the DRZ to the repository.

19 **MgO-6.2.3.2 The DOE's Analysis of Transport of Naturally Occurring SO_4^{2-} into WIPP** 20 **Disposal Rooms**

21 Kanney et al. (2004) analyzed the effects of CPR materials in a panel and transport of naturally
22 occurring SO_4^{2-} on the extent of microbial methanogenesis in the WIPP and the MgO excess
23 factor for different assumed loadings of AMWTP supercompacted waste in a panel.

24 Kanney et al. (2004) used the four loadings of AMWTP supercompacted waste in a hypothetical
25 "Panel X" developed by Leigh (2003, 2004a, and 2004b) for the DOE's analysis of the effects of
26 this waste on the long-term performance of the WIPP (Hansen et al. 2004). The four loadings
27 assumed for Panel X were (1) the "DOE homogeneous Panel X," based on the assumption that
28 the AMWTP supercompacted waste would be homogeneously emplaced throughout the entire
29 10-panel repository (Panel X would comprise ~11-12 volume % (vol %) AMWTP
30 supercompacted waste, the same as the other 9 panels); (2) the "DOE realistic Panel X," which
31 would comprise 14 vol % AMWTP supercompacted waste; (3) the "DOE conservative Panel X,"
32 which would consist of 27 vol % AMWTP supercompacted waste; and (4) the "EPA
33 conservative Panel X," which would contain 50 vol % AMWTP supercompacted waste. In all
34 four cases, the remaining waste in the WIPP inventory was assumed to be distributed
35 homogeneously throughout the other nine panels.

36 Kanney et al. (2004, Section 3.2.1, pp. 20-22, and especially Figure 4 and Figure 5) used the
37 BRAGFLO results from the PA calculations of Hansen et al. (2004) to demonstrate that

38 In all but a few vectors, CPR biodegradation has ceased after about 2000 years. In most vectors,
39 this is because all of the CPR has been consumed. For a few vectors the consumption of CPR
40 [materials] has ceased even though there [are] CPR [materials] remaining. This is likely caused by
41 very low brine saturations. For those few vectors that still show some activity, the rate of ...

1 consumption is only a fraction of the inundated rate. Thus, a value [of] 2000 years for the
2 biodegradation time scale T_{bio} is appropriate for this analysis.

3 Kanney et al. (2004, Section 3.1.1, p. 19; and Section 3.2.2, p. 22) then used a dissolved SO_4^{2-}
4 concentration of 182 mM, the highest concentration predicted by Brush and Xiong (2003a) for
5 GWB or ERDA-6 brine before or after equilibration with the solids in WIPP disposal rooms (see
6 Section MgO-5.1), and a brine volume of $7.74 \times 10^4 \text{ m}^3$, the largest volume predicted after 2,000
7 years in all of the 100 vectors of Replicate 1 of Hansen et al. (2004), to calculate the quantity of
8 SO_4^{2-} that could enter the repository via advective transport.

9 To calculate the quantity that could enter via diffusive transport in 2,000 years, Kanney et al.
10 (2004, Section 2.2.2, pp. 5-7; Section 3.1.2, p. 18) used a concentration of 1.7 wt % each for
11 anhydrite, gypsum, and polyhalite (Stein 1985; Brush 1990) to calculate the concentration of
12 SO_4^{2-} in the Salado at or near the stratigraphic horizon of the WIPP. Kanney et al. (2004,
13 Section 2.3.3, pp. 13-16; Section 3.2.3, p. 23) then assumed that all the SO_4^{2-} in these minerals
14 within 1.06 m (3.5 ft) of the excavated surfaces of a panel would diffuse into the repository in
15 2000 years. They calculated this “effective diffusion length” using (1) a value of 9.84×10^{-10}
16 meters squared per second (m^2/s) for the free-solution tracer diffusion coefficient of SO_4^{2-} (Li
17 and Gregory 1974), (2) a value of 0.05 for the porosity of the Salado DRZ, (3) a value of 1.8 for
18 the cementation factor (Deal et al. 1989), (4) a tortuosity of 0.091, and (5) a value of $4.48 \times$
19 $10^{-12} \text{ m}^2/\text{s}$ for the effective diffusion coefficient of SO_4^{2-} .

20 For these parameter values, Kanney et al. (2004) predicted that a maximum quantity of $1.35 \times$
21 10^6 kg of SO_4^{2-} would be advected into Panel X in Castile brine and a total of $2.37 \times 10^6 \text{ kg}$ of
22 SO_4^{2-} would dissolve from anhydrite, gypsum, and polyhalite and diffuse into Panel X from the
23 DRZ surrounding Panel X. These quantities are much greater than those in this panel’s waste,
24 just $(1.40\text{-}4.40) \times 10^4 \text{ kg}$. Therefore, the total quantity of SO_4^{2-} available to SO_4^{2-} -reducing
25 microbes would be $\sim 3.74 \times 10^6 \text{ kg}$ ($1.35 \times 10^6 \text{ kg} + 2.37 \times 10^6 \text{ kg} + 1.4 \times 10^4 \text{ kg}$).

26 Finally, Kanney et al. (2004, Section 3.3, pp. 24-26) used the waste-material parameters from
27 Leigh (2004a, 2004b), the CRA-2004 PA inventory (the CRA-2004, Appendix DATA,
28 Attachment F), and the methods of Snider (2003d) to predict the quantities of CPR materials in
29 the DOE homogeneous Panel X, the DOE realistic Panel X, the DOE conservative Panel X, and
30 the EPA conservative Panel X that would be consumed by microbes in 2000 years via
31 denitrification, SO_4^{2-} reduction using SO_4^{2-} in the waste, SO_4^{2-} reduction using naturally
32 occurring SO_4^{2-} (Castile-brine SO_4^{2-} and SO_4^{2-} in DRZ minerals), and methanogenesis. They
33 also determined the MgO excess factors for these panels.

34 Table MgO-9 provides the results of these calculations. They show that, for a given panel
35 loading (i.e., for a given quantity of CPR materials), including naturally occurring SO_4^{2-}
36 decreased the MgO excess factor relative to that calculated using only the SO_4^{2-} in the waste
37 (e.g., the MgO safety factor for the DOE homogeneous Panel X decreased from 2.45 to 1.37).
38 Kanney et al. (2004, Section 3.3, pp. 25-26) also concluded,

1 **Table MgO-9. Effects of Panel Loading and the Source of SO₄²⁻ on Microbial Respiratory**
 2 **Pathways and the MgO Excess Factor—Base Case. Adapted from Kanney**
 3 **et al. (2004).**

Loading of Panel X and Source of SO ₄ ²⁻	Denitrification (% of CPR Materials Consumed)	SO ₄ ²⁻ Reduction (% of CPR Materials Consumed)	Methanogenesis (% of CPR Materials Consumed)	MgO Excess Factor
DOE Homogeneous:^a				
Waste SO ₄ ²⁻	4.75	0.82	94.46	2.45
Waste + Natural SO ₄ ²⁻	4.75	70.57	24.68	1.37
DOE Realistic:^b				
Waste SO ₄ ²⁻	4.48	0.66	94.87	2.44
Waste + Natural SO ₄ ²⁻	4.48	63.27	32.26	1.40
DOE Conservative:^c				
Waste SO ₄ ²⁻	3.00	0.16	96.84	1.71
Waste + Natural SO ₄ ²⁻	3.00	42.98	54.03	1.13
EPA Conservative:^d				
Waste SO ₄ ²⁻	1.03	0.23	98.75	1.21
Waste + Natural SO ₄ ²⁻	1.03	32.31	66.66	0.94

^a Panel X would comprise ~11-12 vol % AMWTP supercompacted waste.

^b Panel X would comprise 14 vol % AMWTP supercompacted waste.

^c Panel X would consist of 27 vol % AMWTP supercompacted waste.

^d Panel X would contain 50 vol % AMWTP supercompacted waste.

4
 5 In spite of the decreases noted above, these results show that the MgO [excess]¹F factor is not
 6 very sensitive to the amount of [SO₄²⁻]. For the DOE homogeneous [P]anel X, the amount of
 7 [SO₄²⁻] increased by about 8500% while the ... [excess] factor decreased by about 44%. For the
 8 DOE realistic [P]anel X, the amount of [SO₄²⁻] increased by about 9500% and the [MgO excess]
 9 factor decreased by about 43%. For the DOE conservative case, the amount of [SO₄²⁻] increased
 10 by about 26,500% and the [excess] factor decreased by about 34%. For the EPA conservative
 11 scenario, the amount of [SO₄²⁻] increased by about 14000% and the ... [excess] factor decreased by
 12 about 22%.

13 The MgO [excess] factor is much more sensitive to the amount of CPR [materials]. Keeping in
 14 mind that there is roughly the same amount of [SO₄²⁻] available in each [panel], one can observe
 15 how the [excess] factor change[d] as more CPR [materials were] added by comparing [excess]
 16 factors for different [loadings]. In going from the DOE realistic [Panel X] to the EPA
 17 conservative [Panel X], the [mass of] CPR [materials] increase[d] by about 95% and the MgO
 18 safety factor decrease[d] by about 33%.

19 Note that the fraction of CPR [materials consumed] by [SO₄²⁻] reduction in the EPA conservative
 20 [P]anel X ... [was] actually less than for the DOE conservative [P]anel X, while the MgO [excess]
 21 factor [was] lower than that of [the] DOE conservative [P]anel X. This [was] caused by the larger
 22 amount of CPR [materials] in the EPA conservative [P]anel X...

23 Kanney et al. (2004, Section 4, pp. 27-34) also carried out an uncertainty analysis of the effects
 24 of the brine volume that enters a panel following a human intrusion, the time required for

¹ Explanatory text appears in brackets.

1 microbial consumption of all of the CPR materials, and the effective diffusion coefficient for
 2 SO_4^{2-} on these results.

3 Kanney et al. (2004, Section 4, Table 13) pointed out that the probability of a large volume of
 4 brine flowing into a panel from a reservoir in the Castile (the only way that large volumes of
 5 brine can enter the repository) is quite low; about 0.006. Therefore, Kanney et al. (2004, Section
 6 4.1, pp. 27-29) recalculated the effects of panel loading and the source of SO_4^{2-} on microbial
 7 methanogenesis in the absence of Castile brine. This change (1) decreased the maximum volume
 8 of brine that could enter Panel X by about 75%, from 7.74×10^4 to $1.91 \times 10^4 \text{ m}^3$; (2) decreased
 9 the maximum quantity of SO_4^{2-} advected into this panel by the same percentage, from 1.35×10^6
 10 to $3.34 \times 10^5 \text{ kg}$; and (3) decreased the total quantity of SO_4^{2-} available to microbes in the panel
 11 by 27%, from $(3.74\text{-}3.77) \times 10^6$ to $(2.72\text{-}2.75) \times 10^6 \text{ kg}$. The absence of Castile brine from
 12 Panel X increased the percentage of CPR materials consumed by methanogenesis by about 13%
 13 in the case of the EPA conservative Panel X to 77% for the DOE homogeneous Panel X, and
 14 increased the MgO excess factor for the same panels by about 6-11% (see Table MgO-10).

15 **Table MgO-10. Effects of Panel Loading and the Source of SO_4^{2-} on Microbial**
 16 **Methanogenesis and the MgO Excess Factor—Effects of Having no Castile**
 17 **Brine Intrude Panel X. Adapted from Kanney et al. (2004).**

Loading of Panel X and Source of SO_4^{2-}	Denitrification (% of CPR Materials Consumed)	SO_4^{2-} Reduction (% of CPR Materials Consumed)	Methanogenesis (% of CPR Materials Consumed)	MgO Excess Factor
DOE Homogeneous:^a				
Castile brine present	4.75	70.57	24.68	1.37
No Castile brine	4.75	51.47	43.77	1.52
DOE Realistic:^b				
Castile brine present	4.48	63.27	32.26	1.40
No Castile brine	4.48	46.13	49.40	1.55
DOE Conservative:^c				
Castile brine present	3.00	42.98	54.03	1.13
No Castile brine	3.00	31.26	65.75	1.22
EPA Conservative:^d				
Castile brine present	1.03	32.31	66.66	0.94
No Castile brine	1.03	23.53	75.44	1.00

^a Panel X would comprise ~11-12 vol % AMWTP supercompacted waste.

^b Panel X would comprise 14 vol % AMWTP supercompacted waste.

^c Panel X would consist of 27 vol % AMWTP supercompacted waste.

^d Panel X would contain 50 vol % AMWTP supercompacted waste.

18

19 Kanney et al. (2004, Section 4.2, pp. 29-32) then predicted the effects of doubling the time
 20 required for microbial consumption of all CPR materials from 2,000 to 4,000 years. This change

- 1 1. Increased the maximum volume of Castile brine that could enter Panel X by about 32%, from
2 7.74×10^4 to 1.02×10^5 m³
 - 3 2. Increased the maximum quantity of SO₄²⁻ advected into this panel by the same percentage,
4 from 1.35×10^6 to 1.78×10^6 kg
 - 5 3. Increased the effective diffusion length by 42%, from 1.06 to 1.50
 - 6 4. Increased the quantity of SO₄²⁻ that diffused into the panel by 41%, from 2.37×10^6 to $3.35 \times$
7 10^6 kg
 - 8 5. Increased the total quantity of SO₄²⁻ available in this panel by 37%, from $(3.74-3.77) \times 10^6$ to
9 $(5.14-5.17) \times 10^6$ kg
- 10 Doubling the time required for microbial consumption of all of the CPR materials decreased the
11 percentage of CPR materials consumed by methanogenesis by about 18% in the case of the EPA
12 conservative Panel X to 100% for the DOE homogeneous Panel X, and decreased the MgO
13 excess factor for the same panels by about 9-12% (Table MgO-11).

14 **Table MgO-11. Effects of Panel Loading and the Source of SO₄²⁻ on Microbial Respiratory**
15 **Pathways and the MgO Excess Factor—Effects of Doubling the Time**
16 **Required for Consumption of All CPR Materials. Adapted from Kanney**
17 **et al. (2004).**

Loading of Panel X and Source of SO ₄ ²⁻	Denitrification (% of CPR Materials Consumed)	SO ₄ ²⁻ Reduction (% of CPR Materials Consumed)	Methanogenesis (% of CPR Materials Consumed)	MgO Excess Factor
DOE Homogeneous:^a				
2,000 years	4.75	70.57	24.68	1.37
4,000 years	4.75	95.25	0.00	1.21
DOE Realistic:^b				
2,000 years	4.48	63.27	32.26	1.40
4,000 years	4.48	86.98	8.54	1.25
DOE Conservative:^c				
2,000 years	3.00	42.98	54.03	1.13
4,000 years	3.00	59.20	37.81	1.02
EPA Conservative:^d				
2,000 years	1.03	32.31	66.66	0.94
4,000 years	1.03	44.47	54.51	0.86

^a Panel X would comprise ~11-12 vol % AMWTP supercompacted waste.

^b Panel X would comprise 14 vol % AMWTP supercompacted waste.

^c Panel X would consist of 27 vol % AMWTP supercompacted waste.

^d Panel X would contain 50 vol % AMWTP supercompacted waste.

1 Finally, Kanney et al. (2004, Section 4.3, pp. 32-34) predicted the effects of approximately
 2 doubling the effective diffusion coefficient for SO_4^{2-} , from 4.48×10^{-12} to 1.00×10^{-11} m^2/s . This
 3 change (1) increased the effective diffusion length by 50%, from 1.06 to 1.59 m (3.5 to 5.2 ft);
 4 (2) increased the quantity of SO_4^{2-} that diffused into the panel by 49%, from 2.37×10^6 to $3.54 \times$
 5 10^6 kg; and (3) increased the total quantity of SO_4^{2-} available by 31%, from $(3.74\text{-}3.77) \times 10^6$ to
 6 $(4.91\text{-}4.94) \times 10^6$ kg. Doubling the effective diffusion coefficient for SO_4^{2-} decreased the
 7 percentage of CPR materials consumed by methanogenesis by about 15% in the case of the EPA
 8 conservative Panel X to 89% for the DOE homogeneous Panel X, and decreased the MgO excess
 9 factor for the same panels by about 6-10% (Table MgO-12).

10 **Table MgO-12. Effects of Panel Loading and the Source of SO_4^{2-} on Microbial Respiratory**
 11 **Pathways and the MgO Excess Factor—Effects of Doubling the Effective**
 12 **Diffusion Coefficient for SO_4^{2-} . Adapted from Kanney et al. (2004).**

Loading of Panel X and Source of SO_4^{2-}	Denitrification (% of CPR Materials Consumed)	SO_4^{2-} Reduction (% of CPR Materials Consumed)	Methanogenesis (% of CPR Materials Consumed)	MgO Excess Factor
DOE Homogeneous:^a				
Base Case	4.75	70.57	24.68	1.37
Doubling D_{eff}	4.75	92.48	2.76	1.23
DOE Realistic:^b				
Base Case	4.48	63.27	32.26	1.40
Doubling D_{eff}	4.48	82.94	12.58	1.27
DOE Conservative:^c				
Base Case	3.00	42.98	54.03	1.13
Doubling D_{eff}	3.00	56.44	40.57	1.04
EPA Conservative:^d				
Base Case	1.03	32.31	66.66	0.94
Doubling D_{eff}	1.03	42.40	56.58	0.88

^a Panel X would comprise ~11-12 vol % AMWTP supercompacted waste.

^b Panel X would comprise 14 vol % AMWTP supercompacted waste.

^c Panel X would consist of 27 vol % AMWTP supercompacted waste.

^d Panel X would contain 50 vol % AMWTP supercompacted waste.

13

14 **MgO-6.2.3.3 The EPA’s Response to the DOE’s Analysis of Transport of Naturally**
 15 **Occurring SO_4^{2-} into the WIPP**

16 The EPA concluded that the analysis of Kanney et al. (2004) did not adequately bound the
 17 quantity of naturally occurring SO_4^{2-} that could enter WIPP disposal rooms. In its review of the
 18 issues associated with the emplacement of AMWTP supercompacted waste in the WIPP, Trinity
 19 Engineering Associates (TEA) (2004, pp. 31-33) concluded,

20 TEA agrees that advection, dissolution, and diffusion in brine are the major mechanisms for
 21 transporting natural $[\text{SO}_4^{2-}]$ into the repository. TEA also agrees that basing the quantity of
 22 available $[\text{SO}_4^{2-}]$ on the maximum available brine volume and ignoring mass transfer limitations in

1 dissolution and diffusion are conservative. However, TEA questions certain details of the
2 approach that should be resolved before [the DOE's] calculations can be accepted as adequately
3 bounding sulfate availability. These questions primarily concern the questionable basis for the
4 assumed rate of room closure and the associated degree of DRZ healing, a lack of consideration of
5 the anhydrite-rich beds immediately above the repository, and a lack of consideration of the effect
6 of increased [Fe] surface area or the conservatism of the microbial degradation rates in
7 determining an appropriate time scale for the sulfate reduction reaction.

8 The timing of room closure and the associated degree of DRZ healing cited by Kanney et al.
9 [2004] are related to the accuracy of SANTOS model predictions which are currently being
10 reviewed by the Agency... If the SANTOS model predictions are found to be inaccurate, the
11 conclusions cited by Kanney et al. [2004] may not be supported. In addition, the belief that the
12 vertical DRZ would essentially heal within fewer than 100 years may be inconsistent with the
13 approved conceptual model implemented in the CCA and PAVT [PAs], which incorporate a DRZ
14 that endures for 10,000 years with permeabilities that can be orders of magnitude higher than for
15 intact halite. Even if the vertical DRZ rapidly heals to the extent that additional vertical brine flow
16 is not of concern, [the DOE's] diffusion length of about 1 m is not consistent with the
17 approximately 3 m cited extent of the lateral DRZ. The lateral DRZ includes stress fracturing,
18 provides advective access to Anhydrite B, and will endure significantly longer than the vertical
19 DRZ (Kanney et al. 2004, p. 9).

20 TEA agrees that pressure-induced fractures are more likely to conduct brine away from the
21 repository rather than toward it, and that brine flow into the repository from the thinner anhydrite
22 layers immediately above the waste rooms is likely to be small compared with the volume of brine
23 inflow assumed in [the DOE's] calculations. However, TEA believes that structural disruptions
24 during room closure, such as a roof collapse that would bring [SO₄²⁻]-bearing minerals such as
25 anhydrite into direct contact with waste room brines, cannot be ruled out. Additional [SO₄²⁻]
26 could be derived in this manner from Anhydrite Interbeds A and B, and from the anhydrite-rich
27 halite between these interbeds (Stein 1985). As the [SO₄²⁻] in the brine is consumed by the
28 reduction reaction, the tendency of the system to maintain chemical equilibrium requires that
29 sulfates present in minerals accessible to repository brines dissolve. These sources of additional
30 natural [SO₄²⁻] were not considered in [the DOE's] analysis.

31 The assumption that all [SO₄²⁻] around the repository within an approximately 1 m diffusion
32 length would be available for reaction was considered by [the DOE] to account for [SO₄²⁻] that
33 may be dissolved from the Salado as well as [SO₄²⁻] that may diffuse from the Salado (Kanney
34 et al. 2004, p. 13). The approximately 1 m diffusion length was based in part on the assumption
35 that CPR degradation would be essentially complete within 2,000 years (Kanney et al. 2004,
36 Sections 2.3.1 and 3.2.1). The 2,000-year time scale is used by [the DOE] to establish limits for
37 the volume of brine inflow and diffusion length that need to be considered as sources of [SO₄²⁻].
38 However, the assumption that CPR degradation would be essentially complete within 2,000 years
39 does not hold for waste panels with the increased iron surface areas that would be present with
40 supercompacted AMWTF waste. Stein and Zelinski (2003, Figure 2) show that CPR
41 biodegradation endures for over 10,000 years for an increasing number of vectors because of
42 decreased brine saturation as the iron surface area increases. TEA has agreed that the effects of
43 increased iron surface areas can be ignored in [PA] for purposes of gas generation impacts because
44 the prolonged CPR degradation reaction conservatively results in less overall gas generation (see
45 Section 5.2.2 [of TEA, 2004]). However, ignoring a prolonged CPR degradation reaction for
46 purposes of limiting the [SO₄²⁻]-reduction reaction is not conservative and inappropriate. In
47 addition, the microbial degradation rates used in BRAGFLO are consistent with the higher initial
48 reaction rates observed in microbial degradation experiments. Use of these higher initial rates is
49 conservative from the standpoint of estimating gas generation rates, but use of the lower, long-
50 term rates would be more conservative for the purpose of determining the length of time available
51 for [SO₄²⁻] diffusion.

1 The MgO safety factors calculated by [the DOE] fall below the Agency-approved value of 1.67
 2 (EPA, 2001) for *every* [TEA's italics] waste loading scenario considered in [the DOE's] analysis
 3 when natural sulfates are included. [The DOE's] calculated safety factors range from 0.94 for the
 4 EPA loading scenario (50 percent supercompacted AMWTF waste and 50 percent standard waste)
 5 to 1.40 for the DOE realistic Panel X scenario described in Section 5.2.1.2 [of TEA, 2004]
 6 (Kanney et al. 2004, Table 12). TEA believes that uncertainties in the quantities of CPR
 7 [materials] present in a waste panel and in the extent to which [SO₄²⁻] reduction will occur are
 8 sufficiently great that the Agency-approved safety factor of 1.67 is the minimum that should
 9 be maintained...

10 TEA concludes that the aforementioned DOE study by Kanney et al. (2004) provides useful
 11 information but clearly demonstrates that reductions in the effect of methanogenesis due to the
 12 availability of natural [SO₄²⁻] can have a significant adverse effect on MgO safety factors. TEA
 13 also believes that not all potential sources for natural [SO₄²⁻] to enter the repository were
 14 considered in [the DOE's] analysis and that an acceptable bounding analysis has therefore not been
 15 performed...

16 Furthermore, U.S. EPA (2004, pp. 7-8) concluded that

17 [The] DOE's analysis may be correct but uncertainties remain in the quantities of CPR [materials]
 18 present in a waste panel and in the extent to which sulfate reduction will occur. More [SO₄²⁻] may
 19 be present in the waste or waste area environment than currently estimated. More waste with high
 20 CPR may be placed in a panel than currently anticipated. Because of these uncertainties, [the]
 21 DOE needs to ensure that these uncertainties are accounted for in the calculation of the MgO
 22 safety factor, even if it appears that there is enough MgO for [PA] calculations.

23 Methanogenesis may not occur because of the presence of excess [SO₄²⁻] in the system, so MgO
 24 safety factor calculations need to assume all [C] could be converted to [CO₂] until the Department
 25 provides adequate evidence that methanogenesis is the dominant process...

26 **MgO-6.2.4 Changes since the CRA-2004 in the MgO Excess Factor**

27 In March 2004, the EPA approved the DOE's request to dispose of supercompacted waste in the
 28 WIPP (Marcinowski 2004; Trinity Engineering Associates 2004; U.S. Environmental Protection
 29 Agency 2004). As part of its approval, the EPA specified that the DOE maintain an MgO excess
 30 factor of 1.67, calculated assuming that there would be no microbial methanogenesis in the
 31 repository. The elimination of methanogenesis from consideration in WIPP PA is discussed in
 32 Leigh et al. (2005, Section 2.4) and Cotsworth (2005). In some cases, maintaining an excess
 33 factor of 1.67 has, in turn, required that the DOE emplace additional MgO in place of TRU waste
 34 (Section MgO-2.1.1). Therefore, the DOE continued to explore various possible approaches to
 35 support a PCR for EPA approval of a reduction in the MgO excess factor.

36 **MgO-6.2.4.1 The RSI's Expert Review of the DOE's Use of MgO**

37 In 2005 and 2006, the Institute for Regulatory Science (RSI) of Alexandria, VA, reviewed the
 38 DOE's use of MgO in the WIPP, especially the need to emplace additional MgO in rooms with
 39 supercompacted waste.

40 The RSI carries out studies; assesses regulatory actions; conducts peer reviews of studies by
 41 other organizations; and provides training and other services to federal, state, and local
 42 governments in the biological, chemical, health, and physical sciences, and in all areas of
 43 engineering. The RSI was established in 1985 and received nonprofit status in 1986. From 1989

1 until mid-1995, the RSI operated through the University of Maryland at Baltimore and Temple
2 University in Philadelphia, PA. Since then, the RSI has operated as an independent organization.
3 The RSI has a small in-house staff and utilizes individuals in other organizations, especially for
4 peer reviews (Institute for Regulatory Science [RSI] 2008).

5 In 2005, the RSI assembled an expert panel chaired by Edward Abbott, Professor of Chemistry at
6 Montana State University in Bozeman, MT. The other members of this panel were Gudmundur
7 S. (“Bo”) Bodvarsson, Director of the Earth Sciences Division at Lawrence Berkeley National
8 Laboratory in Berkeley, CA; R. Ian Miller, President of the GoldSim Technology Group, LLC,
9 in Issaquah, WA; Dade W. Moeller, President of Dade Moeller and Associates, Inc., and
10 Professor Emeritus at Harvard University in Cambridge, MA; and Richard Wilson, Mallinckrodt
11 Research Professor of Physics at Harvard University. The GoldSim Technology Group, LLC,
12 develops, maintains, and applies the GoldSim software package for decision analysis and PA
13 calculations for radioactive waste repositories and other environmental studies. Dade Moeller
14 and Associates provides services in the environmental and occupational sciences. A. Alan
15 Moghissi, President of the RSI, oversaw the operation of the expert panel during its review.
16 Sorin R. Straja, Vice President for Science and Technology of the RSI, served as the technical
17 secretary for the expert panel.

18 The RSI expert panel met for two days in July 2005 in Carlsbad, NM. Several DOE and DOE-
19 contractor personnel made detailed presentations to the panel on

- 20 1. The methodology used for WIPP PA
- 21 2. The history of engineered barriers in the WIPP disposal system, especially MgO
- 22 3. Aspects of WIPP chemistry and geochemistry related to MgO
- 23 4. Calculation of the MgO excess factor
- 24 5. Preliminary PA calculations pertinent to possible reductions in the amount of excess MgO
25 emplaced in the repository
- 26 6. Possible approaches to support a PCR for EPA approval of a reduction in the MgO excess
27 factor

28 The members of the panel prepared a summary of their initial impressions and identified issues
29 to be addressed at the next meeting (Institute for Regulatory Science [RSI] 2006).

30 The RSI expert panel met again for two days in September 2005 in Albuquerque, NM. DOE and
31 DOE contractor personnel responded to several issues raised during the first meeting of the
32 panel, including the following:

- 33 1. The history of implementing and using MgO in the WIPP disposal system and its description
34 in WIPP regulatory-compliance documents
- 35 2. MgO-related assumptions in WIPP PA

- 1 3. Issues that arose while scoping PA calculations for possible reductions in the amount of
2 excess MgO
- 3 4. Issues pertinent to the availability of naturally occurring SO_4^{2-} in and around the repository
- 4 5. Possible approaches to support a PCR for EPA approval of a reduction in the MgO excess
5 factor

6 The panel also met in a closed session to discuss a possible PCR (Institute for Regulatory
7 Science [RSI] 2006).

8 Subsequent to the September 2005 meeting, Abbott prepared a set of draft findings and
9 recommendations, which were modified and included in Institute for Regulatory Science (RSI)
10 2006. At the same time, R. Patterson, D. Mercer, T. W. Thompson, and M. B. Gross assembled
11 brief summaries of the WIPP disposal system and its use of MgO as the engineered barrier from
12 previous WIPP regulatory-compliance documents; these summaries also appeared in Institute for
13 Regulatory Science (RSI) 2006. The report of the expert panel also included excerpts from the
14 EPA's regulations related to natural and engineered barriers in the WIPP (Institute for
15 Regulatory Science [RSI] 2006).

16 The RSI expert panel reported nine findings. The first three findings dealt with possible
17 generation of CO_2 from microbial consumption of CPR materials in the WIPP.

18 The first question posed to the panel ("Criterion 1") was, "Is the assumption that *cellulosic*
19 materials [in TRU waste] could be consumed by microbes, under conditions prevailing at WIPP,
20 consistent with scientific and engineering principles, standards, and practices?" (Institute for
21 Regulatory Science [RSI] 2006, p. 19).

22 In response to this question, the Institute for Regulatory Science (RSI) (2006, p. 19) found

23 The assumption that *cellulosic* materials [the RSI's italics] could be consumed by microbes under
24 conditions prevailing at WIPP is consistent with scientific and engineering principles, standards,
25 and practices. Because a small portion of the material will be incorporated into the microbial
26 biomass, biodegradation is unlikely to reach 100%. An extensive review by staff members ... led
27 to the conclusion that communities of halophilic, fermentative, and methanogenic are potentially
28 capable of metabolizing cellulosic materials, under expected WIPP conditions.

29 The biodegradation of cellulosic materials could progress under at least two scenarios:

- 30 1. During the initial phases of emplacement of waste at WIPP when $[\text{O}_2]$ is available; and
- 31 2. As a consequence of human intrusion that resulted in brine reaching and interacting with
32 the waste.

33 However, the RSI expert panel also agreed with two of the conclusions reached by the U.S.
34 National Academy of Sciences' Committee on the Waste Isolation Pilot Plant (National Research
35 Council [NRC] Committee on the Waste Isolation Pilot Plant 1996 and 2001), which RSI
36 (Institute for Regulatory Science [RSI] 2006, p. 19) stated as

37 Two committees of the National Research Council (NRC, 1996; 2001) came to the conclusion that

- 1 1. The biodegradation of cellulosic materials is expected to be minimal; but
- 2 2. For that portion that does undergo biodegradation, the rate is expected to be maximum
- 3 3 during the pre-closure period.

4 Finally, the RSI expert panel stated that they “made no attempt to independently quantify the
5 extent and rate of biodegradation of *cellulosic* materials” (Institute for Regulatory Science [RSI]
6 2006, p. 10).

7 The second question posed to the panel (“Criterion 2”) was, “Is the assumption that *plastic*
8 materials ... in TRU waste could be consumed by microbes, under conditions prevailing at
9 WIPP, consistent with scientific and engineering principles, standards, and practices?” (Institute
10 for Regulatory Science [RSI] 2006, p. 10).

11 In response, the Institute for Regulatory Science (RSI) (2006, pp. 10–11) found

12 The assumption that *plastic* materials [the RSI’s italics] will be completely metabolized by
13 microbes under conditions prevailing at WIPP is not consistent with scientific and engineering
14 principles, standards, and practices. However, partial metabolization of such materials is possible,
15 but if it occurs at all, then its rate and extent of reaction is expected to be significantly lower than
16 that for cellulosic materials. Under WIPP conditions, neither thermo-oxidation nor photo-
17 oxidation can occur, and therefore the biodegradation of polymers, such as polyethylene, will be
18 highly unlikely. It is of particular interest to note that, in its regulations [U.S. EPA, 1992a,
19 p. 54,460; U.S. EPA, 1992b, p. 54,461], the EPA ... defined the following polymers as
20 nonbiodegradable:

- 21 • polyethylene,
- 22 • high density polyethylene (HDPE),
- 23 • polypropylene, polystyrene,
- 24 • polyurethane,
- 25 • polyacrylate,
- 26 • polynorborene,
- 27 • polyisobutylene,
- 28 • ground synthetic rubber,
- 29 • cross-linked allylstyrene,
- 30 • tertiary butyl copolymers.

31 The EPA regulations, cited above, which were developed as an outgrowth of experience with land
32 disposal facilities, as well as laboratory studies, involved significant public participation.

33 The rate of biodegradation of a polymer depends on the mechanism of degradation; its structure;
34 and the presence of the required microbial populations and environmental conditions that enhance
35 their growth. Although the understanding of polymer degradation is limited, there is sufficient
36 information indicating that critical parameters include oxygen, temperature, and water.

1 In recent years there has been an increasing recognition of a need to develop polymers that would
2 be biodegradable. Through modifications, such as changing the chemical structure of certain
3 plastic materials so as to initiate and accelerate the biodegradation process, this goal has been
4 achieved. In fact, many polymers on the market today, that heretofore were considered not to be
5 subject to biodegradation, are now degradable. However, the polymers likely to be disposed at
6 WIPP are not expected to belong to the new classes of biodegradable polymers. In addition, any
7 biodegradable polymers that may have been present in the initial TRU waste should have been
8 biodegraded by the time it was disposed at WIPP.

9 On the basis of the information that was provided, the [RSI expert panel] concluded that the
10 fraction of plastics that is expected to be biodegraded under the conditions existing within the
11 WIPP is small. This conclusion is consistent with the assessment of the NRC (2001) and the
12 regulatory decisions of the EPA. However, the [RSI expert panel] made no attempt to
13 independently quantify the extent and the rate of biodegradation of *plastic* materials [the RSI's
14 italics].

15 The third question ("Criterion 3") was, "Is the assumption that *rubber* materials will be
16 consumed by microbes, under the conditions prevailing at WIPP, consistent with scientific and
17 engineering principles, standards, and practices?" (Institute for Regulatory Science [RSI] 2006,
18 p. 11).

19 The Institute for Regulatory Science (RSI) (2006, pp. 11–12) found

20 The assumption that commercial *rubber* materials [the RSI's italics] will be completely
21 metabolized by microbes, under conditions prevailing at WIPP, is not consistent with scientific
22 and engineering principles, standards, and practices. The extent of biodegradation of rubber
23 materials, if it occurs, is likely to be significantly lower than that for plastic materials, and very
24 much less than that for cellulosic materials.

25 Raw *natural* rubber [the RSI's italics] obtained from the latex of *Hevea brasiliensis* trees, contains
26 more than 90% poly(cis-1,4-isoprene). The remaining constituents include proteins, lipids,
27 carbohydrates, resins, and inorganic salts. Raw *synthetic* rubber [the RSI's italics] consists
28 essentially of poly(cis-1,4-isoprene) rubber with the addition of antioxidants to prevent ageing.
29 The monomer units of natural rubber contain unsaturated bonds that are susceptible to thermo-
30 oxidative degradation, attack by ozone, or degradation by [ultraviolet]-light. In contrast, the
31 synthetic alternatives to the natural rubber can withstand elevated temperatures for long times
32 even under relatively aggressive conditions. Commercial rubber (natural or synthetic) is usually
33 vulcanized (crosslinked) by heating in the presence of sulfur. The lack of biodegradability of
34 commercial rubber products is the consequence of inhibition of the oxidation process by
35 antioxidants.

36 On the basis of the information that was provided, the [RSI expert panel] concluded that the
37 fraction of rubber that is expected to be biodegraded under the conditions existing within the
38 WIPP is small. The conclusion is consistent with the assessment of the NRC (2001) and the
39 regulatory decisions of the EPA. However, the level and the rate of biodegradation of *rubber*
40 materials [the RSI's italics], as small as they may be, were not independently quantified by [the
41 RSI expert panel].

42 The fourth finding of the RSI expert panel dealt with the performance of MgO in the WIPP. The
43 fourth question ("Criterion 4") was, "Under conditions prevailing at WIPP, is the assumption
44 that all the MgO, as presently emplaced, will be available to react with CO₂ consistent with
45 scientific and engineering principles, standards, and practices?" (Institute for Regulatory Science
46 [RSI] 2006, p. 12).

1 The Institute for Regulatory Science (RSI) (2006, pp. 12-13) found

2 Under conditions prevailing at WIPP, [the RSI expert panel] has concluded that the assumption
3 that 100% of the MgO will be available to react with CO₂ is not consistent with scientific and
4 engineering principles, standards, and practices.

5 The processes that will occur in the emplacement rooms are very complex. They will involve the
6 interplay of multiple processes, including the mechanical creep of the salt formation; the
7 development of a gaseous phase consisting mostly of CO₂; and the gradual inflow of brine from
8 the surrounding saturated salt. These processes will likely result in a very heterogeneous
9 hydrological and chemical environment within the emplacement rooms. Although hydrological
10 and chemical gradients in the gas and liquid phases within the rooms will tend to equilibrate
11 thermodynamic and chemical conditions, local pockets of unreacted MgO are likely to be present
12 for long periods of time. For these reasons, the [RSI expert panel] believes that 100% reaction of
13 the MgO with CO₂ is not likely to occur. Nonetheless, the [RSI expert panel] has concluded that
14 most of the MgO will be active in chemical reactions.

15 The fifth and sixth findings of the RSI expert panel involved the performance of the WIPP in the
16 hypothetical absence of MgO. (The DOE has never requested that the EPA approve eliminating
17 MgO from the WIPP, only that the EPA approve reducing the amount of excess MgO that the
18 DOE must emplace.)

19 The fifth question (“Criterion 5”) was, “Assuming that only cellulosic materials are consumed by
20 microbes, is it consistent with scientific and engineering principles, standards, and practices to
21 conclude that, in the absence of MgO, the solubility of actinides will be such that releases to the
22 accessible environment will still be below the EPA limits?” (Institute for Regulatory Science
23 [RSI] 2006, p. 13).

24 The Institute for Regulatory Science (RSI) (2006, p. 13) found

25 “On the basis of the information received by the [RSI expert panel], it is likely that releases to the
26 accessible environment will be below the EPA regulatory limits. However, the evidence received
27 by the [RSI expert panel] is not sufficient to definitely support this conclusion.

28 The sixth question (“Criterion 6”) was, “Assuming that all cellulosic, plastic and rubber
29 materials are consumed by microbes, is it consistent with scientific and engineering principles,
30 standards, and practices to conclude that, in the absence of MgO, the solubility of the actinides
31 will be such that releases to the accessible environment will still be below the EPA limits?”
32 (Institute for Regulatory Science [RSI] 2006, p. 13).

33 The Institute for Regulatory Science (RSI) (2006, pp. 13–14) found

34 On the basis of the information received by the [RSI expert panel], it is likely that releases to the
35 accessible environment will be below the EPA regulatory limits. However, the evidence received
36 by the [RSI expert panel] is not sufficient to definitely support this conclusion.

37 The seventh criterion and finding dealt with the application of “acceptable knowledge” to the
38 characterization of the concentrations of CPR materials in TRU waste, and will not be discussed
39 herein.

1 The eighth question (“Criterion 8”) was, “Is the requirement to emplace a 67% MgO excess
2 consistent with as low as reasonably achievable (ALARA) scientific and engineering principles,
3 standards, and practices? Is the associated increased and real risk to the affected workers and the
4 general public imposed by this requirement offset by the potentially reduced risk to future
5 generations?” (Institute for Regulatory Science [RSI] 2006, p. 15).

6 The Institute for Regulatory Science (RSI) (2006, p. 15) found

7 In reference to Finding 4, the [RSI expert panel] has concluded that most of the MgO will be
8 available for chemical reaction. In reference to Findings 1-3, the [RSI expert panel] has concluded
9 that only a small fraction of the CPR materials is likely to be biodegraded to produce CO₂. In
10 reference to Findings 5-6, the [RSI expert panel] believed that it is likely that the EPA release
11 standards would be met, even if the amount of MgO is less than the quantity required to consume
12 all the CO₂ produced. Therefore, the [RSI expert panel] concludes that 67% MgO excess (i.e.,
13 67% in excess of the stoichiometric quantity required assuming complete biodegradation of
14 CPR materials to CO₂) is not necessary.

15 The ninth criterion and finding dealt with whether it would be reasonable for the DOE to
16 convene another expert panel to “reach a consensus on the potential extent of consumption of
17 various components of CPR materials” and, if so, if other issues should be considered. The RSI
18 expert panel’s response to this criterion is included below in the discussion of its
19 recommendations.

20 The Institute for Regulatory Science (RSI) (2006, p. 16) made two recommendations:

- 21 1. The DOE should consider convening an Expert Elicitation Panel to provide a more
22 realistic and accurate estimate of the potential extent of biodegradation of various
23 components of CPR materials likely to be emplaced in the WIPP.
- 24 2. The DOE should consider performing a single-room realistic analysis of the complex
25 processes involved, including gas generation, chemical reactions, biodegradation, and
26 mechanical creep.

27 In its ninth finding, the RSI expert panel recommended that, in addition to providing “more
28 realistic and accurate estimate[s]” of the fractions of the CPR materials that would be consumed
29 by microbial activity in the WIPP, the expert elicitation panel should also estimate the “fraction
30 of the emplaced MgO [that] is likely to react with the CO₂” and “the performance consequences
31 of a partial or complete shortfall in MgO buffering capacity” (Institute for Regulatory Science
32 [RSI] 2006, p. 16).

33 The RSI expert panel did not provide any details on how the DOE should perform “a single-
34 room realistic analysis of the complex processes involved” in the WIPP.

35 **MgO-6.2.4.2 The DOE’s PCR for EPA Approval of Reducing the MgO Excess Factor** 36 **from 1.67 to 1.2**

37 In April 2006, the DOE submitted a PCR for EPA approval of reducing the MgO excess factor
38 from 1.67 to 1.2 (Moody 2006). To justify its request, the DOE used reasoned arguments
39 regarding health-related transportation risks to the public, the cost of emplacing MgO, and the

1 uncertainties inherent in predicting the extent of microbial consumption of CPR materials during
2 the 10,000-year WIPP regulatory period.

3 The EPA responded by requesting that the “DOE needs to address the uncertainties related to
4 MgO effectiveness, the size of the uncertainties, and the potential impact of the uncertainties on
5 long-term performance” (Gitlin 2006). In particular, the EPA instructed the DOE to identify all
6 of the uncertainties related to the calculation of the MgO excess factor, and quantify these
7 uncertainties, if possible.

8 **MgO-6.2.4.3 The EPA’s Review of the Consumption of CPR Materials in the WIPP and** 9 **Its Effects on the MgO Excess Factor**

10 As the DOE began to address the uncertainties related to the MgO excess factor, S. Cohen and
11 Associates (SCA) carried out a review of the possible consumption of CPR materials in the
12 WIPP for the EPA (S. Cohen and Associates 2006). The objectives of this report were the
13 following:

14 [T]o identify specific technical questions that must be answered and uncertainties that must be
15 addressed before EPA can consider changing the amounts of MgO backfill that must be placed in
16 the repository to maintain the effectiveness of the engineered barrier. Therefore, a preliminary
17 review of the available data relevant to a number of issues related to the MgO backfill was carried
18 out. This review included chemistry-related issues such as the potential CO₂-generating microbial
19 degradation reactions that could occur within the repository, the extent to which these reactions
20 could occur, and the reactivity of MgO in the repository environment. These issues were
21 addressed by consulting the available scientific literature, including data generated by the WIPP
22 program and a survey of other relevant information. The possibility of conducting experiments to
23 better define the reaction rates and possible extent of the microbial degradation reactions was also
24 considered. Regulatory requirements related to engineered barriers in the WIPP and ways in
25 which uncertainties must be addressed were evaluated as well, and are summarized in this report
26 [SCA, 2006, pp. 1-1 to 1-2].

27 In addition, the SCA report (S. Cohen and Associates 2006) responded to the findings and
28 recommendations of the RSI expert panel, and to its assessment of the EPA regulations relevant
29 to MgO.

30 In its first three findings, the RSI expert panel stated that “[t]he assumption that *cellulosic*
31 materials could be consumed by microbes under conditions prevailing at WIPP is consistent with
32 scientific and engineering principles, standards, and practices” (Institute for Regulatory Science
33 [RSI] 2006, p. 9), but that the fraction of plastic and rubber materials “that is expected to be
34 biodegraded under the conditions existing within the WIPP is small” (Institute for Regulatory
35 Science [RSI] 2006, pp. 11 and 12). With regard to the RSI expert panel’s first three findings,
36 SCA (S. Cohen and Associates 2006, p. 4-2) stated

37 The rates and extent of CPR degradation during the 10,000-year WIPP regulatory period are likely
38 to be influenced by the following:

- 39 • Composition of the CPR materials
- 40 • Microbial population

- 1 • Chemical and physical environment, including the quantity and salinity of the repository
- 2 brines, redox conditions, pH, and temperature
- 3 • Radiation dose to the CPR materials and associated brines
- 4 • Interactions of different processes.

5 SCA (S. Cohen and Associates 2006, pp. 4-2 through 4-8) reviewed some of the literature
 6 pertaining to these factors. SCA described its review as “preliminary.” It then reviewed results
 7 obtained by the WIPP project and results in the literature pertaining to the possible microbial
 8 consumption of CPR materials (S. Cohen and Associates 2006, pp. 4-8 through 4-18).

9 With regard to the possible extent of microbial consumption of cellulosic materials in the WIPP,
 10 SCA (S. Cohen and Associates 2006, pp. 4-11 through 4-12) stated

11 A number of factors contribute to the high likelihood that cellulose will be completely degraded
 12 in the WIPP repository. These factors include the variety of microorganisms that can degrade
 13 cellulosic materials, the general adaptability of microbes to their environment and available [C]
 14 sources, the abundant [SO₄²⁻] in the repository, and the long regulatory time period.

15 Although relatively little data appear to be available regarding the chemical effects of radiation on
 16 cellulose, it appears low-level radiation may decrease polymer chain length and alter physical and
 17 chemical properties of cellulose. It is expected that radiation-induced degradation of cellulose in
 18 the WIPP will occur through direct and indirect interaction with ionizing radiation from
 19 radionuclides in the waste. The direct interactions, which are interactions of the ionizing radiation
 20 with the solid cellulose, initiate scissions on the backbone of the molecules leading to degradation;
 21 however, a very small yield of branching also can occur. The presence of oxygen in the repository
 22 environment is not required for these scission reactions. Indirect interactions will occur through
 23 the radiolysis of water. As mentioned above in Section 4.1.4, the radiolysis of water produces
 24 hydroxyl radicals (•OH). Hydroxyl radicals can cause hydrolytic cleavage of glycoside linkages in
 25 cellulose, which would be expected to facilitate microbial degradation.

26 Although some radiation-induced effects could act to limit cellulose biodegradation, on balance,
 27 the overall effects of radiation on cellulose appear to increase the likelihood of microbial
 28 degradation of cellulose through cleavage of the polymer backbone and decreased molecular
 29 weight. The available literature appears to indicate that microbial and radiation-induced
 30 degradation of cellulose may proceed virtually to completion over 10,000 years if water is
 31 present in the WIPP repository.

32 With regard to the possible extent of microbial consumption of plastic materials, SCA (S. Cohen
 33 and Associates 2006, p. 4-15) stated

34 Literature data are available regarding both microbial degradation and radiation-induced
 35 degradation of plastics such as polyethylene and [polyvinylchloride]. Microbial degradation of
 36 plastics generally is less extensive in the short term than microbial degradation of cellulosic
 37 materials, based on the data identified in the literature. Radiolytic processes may degrade plastics
 38 directly, and also may indirectly contribute to the long-term biodegradability of plastics by
 39 altering their chemical and physical properties. The likelihood of significant radiolytic effects on
 40 plastics degradation would depend on the dose. The dose to WIPP waste can be calculated from
 41 the DOE’s inventory projections (Leigh and Trone 2005). The presence of oxygen in the
 42 repository before closure and for a period of time after closure could affect both radiolytic and
 43 microbial processes. This preliminary evaluation of the data indicates that plastic degradation may
 44 occur over 10,000 years in the WIPP repository.

1 SCA (S. Cohen and Associates 2006, pp. 3-4 through 3-6) also responded to the RSI expert
 2 panel's statement in its second finding (Institute for Regulatory Science [RSI] 2006, pp. 10–11)
 3 that the EPA had defined polymers such as polyethylene, HDPE, and polypropylene as
 4 nonbiodegradable:

5 RSI (2006) cited EPA's RCRA [Resource Conservation and Recovery Act] regulations at 40 CFR
 6 264.314 and 40 CFR 265.314 to support the contention that 'the fraction of plastics that is
 7 expected to be biodegraded under conditions existing within the WIPP is small' (Finding 2). For
 8 example, 40 CFR 264.314 lists a number of high molecular weight polymers, such as
 9 polyethylene, polypropylene, and ground synthetic rubber, as non-biodegradable sorbents to
 10 sequester free liquids prior to disposal in surface hazardous landfills. EPA has listed in its *Federal*
 11 *Register* notice 'Final Rule Regarding Liquids in Hazardous Waste Landfills' [U.S. EPA, 1992a;
 12 1992b] on November 18, 1992, of certain high-density polymers as non-biodegradable sorbents in
 13 RCRA landfills. The *Federal Register* notice did not, however, provide any background
 14 information supporting the contention that such high molecular weight polymers were non-
 15 biodegradable. The Agency merely stated that such materials 'have proved to be highly resistant
 16 to biodegradation.' In an earlier *Federal Register* notice of June 1987, when EPA first proposed
 17 the use of high-molecular weight polymers as nonbiodegradable sorbents, the notice stated the
 18 following [U.S. EPA, 1987, p. 23,696]:

19 *[T]he Agency now believes that a different criterion should be used to determine*
 20 *if an organic polymer is biodegradable. The Agency proposes to determine this*
 21 *alternative criterion by using tests which involve incubating the absorbent*
 22 *materials with prepared stock cultures of various microorganisms under ideal*
 23 *conditions for their growth. This incubation demonstrates the fungal resistance*
 24 *of polymers and is used by the American Society for ... Testing [and] Materials*
 25 *laboratory test ASTM Method G21-70... [SCA's italics].*

26 The relevance of the fact that certain plastics and rubbers are defined as non-biodegradable for use
 27 as sorbents in RCRA surface landfills to the assumption that such materials are nonbiodegradable
 28 in the context of the WIPP environment is questionable based on the following considerations:

- 29 • Under 40 CFR 264.117, post-closure monitoring is limited to 30 years unless extended by the
 30 EPA Regional Administrator, while at the WIPP, regulatory compliance must be
 31 demonstrated through PA for 10,000 years.
- 32 • Under 40 CFR 264.314, EPA offers three tests to demonstrate that materials not specifically
 33 listed as non-biodegradable sorbents in §264.314(e)(1)(i) and (ii) can be used as non-
 34 biodegradable sorbents. Two of the tests are American Society for Testing and Materials
 35 (ASTM) procedures and one is an Organisation for Economic Co-operation and Development
 36 (OECD) procedure. In 1995, EPA decided to add the OECD test to §264.314(e)(2) as
 37 described in its *Federal Register* notice [U.S. EPA, 1995]. In the *Federal Register* notice,
 38 EPA noted that:

39 *[T]he OECD [T]est 301B is a test for biodegradability in an aerobic*
 40 *environment, as are the two ASTM tests that were promulgated in the November*
 41 *18, 1992 rule. The Agency also recognizes that the actual environment in which*
 42 *the sorbents will be used, i.e., in a container in a landfill, will be anaerobic. The*
 43 *Agency does not know, however, of any published widely accepted tests for the*
 44 *biodegradability of materials in anaerobic conditions that would be practical*
 45 *for purposes of this rule. The Agency believes, however, that OECD 301B is an*
 46 *acceptable surrogate for determining if a sorbent will biodegrade in*
 47 *containerized liquids in a hazardous waste landfill [SCA's italics].*

1 The environment in the WIPP will become anaerobic shortly after closure and will remain so
2 throughout the regulatory period. Therefore, the assumption that high molecular weight
3 polymers will not biodegrade may not be valid at WIPP.

- 4 • While materials may be judged functionally as non-biodegradable sorbents in RCRA surface
5 landfills, they can achieve that functionality even if limited biodegradation actually occurs. In
6 the WIPP, on the other hand, at least one mol of MgO backfill must be provided for each mol
7 of CO₂ generated from CPR decomposition. This places a greater burden on defining
8 quantitatively the extent to which biodegradation occurs at the WIPP.

9 The Resource Conservation and Recovery Act (RCRA) definition of some plastic sorbents as
10 nonbiodegradable is based mainly on observations over relatively short time frames and testing
11 in aerobic environments. These conditions do not appear relevant to the long-term WIPP
12 environment or regulatory period of performance. Therefore, the RCRA definition of some
13 plastic sorbents as nonbiodegradable appears to have essentially no relevance to the
14 determination of whether plastic and rubber materials are likely to be substantially biodegraded
15 in the WIPP repository.

16 With respect to the possible extent of microbial consumption of rubber materials, SCA (S. Cohen
17 and Associates 2006, p. 4-18) stated

18 Available WIPP and literature data indicate that rubber materials likely to be present in the WIPP
19 repository will be partially degraded by microbes. Radiation appears to affect both the physical
20 and chemical properties of rubber, and in WIPP experiments appeared to enhance microbial
21 degradation. The presence of oxygen in the repository before closure and immediately after
22 closure could affect the physical and chemical properties of the rubber. This preliminary
23 evaluation of the data indicates that rubber degradation may occur over 10,000 years in the WIPP
24 repository.

25 The RSI expert panel's fourth finding was that, "100% reaction of the MgO with CO₂ is not
26 likely to occur. Nonetheless ... most of the MgO will be active in chemical reactions" (Institute
27 for Regulatory Science [RSI] 2006, p. 13). SCA (S. Cohen and Associates 2006, p. 5-1) agreed
28 with this finding:

29 Review of the available information related to MgO reactivity indicates that MgO is likely to react
30 in the repository to control CO₂ concentrations in the brine. However, it is possible that a small
31 fraction of the MgO could become unavailable for reaction because of physical segregation. This
32 relatively small source of uncertainty has been adequately accounted for by using an MgO safety
33 factor greater than one.

34 With regard to the RSI expert panel's fourth finding, SCA (S. Cohen and Associates 2006,
35 p. 6-1) also stated

36 [T]he MgO backfill is likely to perform as designed and control brine pH and CO₂ concentrations
37 in the repository. Incomplete reaction of the MgO with brine and CO₂ is unlikely to occur unless
38 the MgO is physically segregated from the brine or CO₂; if such physical segregation should
39 occur, the effective MgO safety factor would be decreased by a commensurate amount. The
40 recent changes in MgO placement methods, with a constant safety factor calculated for each
41 disposal room, limit the potential effects of inhomogeneous distribution of CPR in the waste, and
42 are likely to minimize the uncertainties associated with possible physical segregation of the MgO
43 from brine and CO₂. However, the small remaining uncertainty related to physical segregation
44 should be addressed by the MgO safety factor.

1 The RSI expert panel’s fifth and sixth findings, which responded to the question, “Assuming that
2 only cellulosic materials [or all of the CPR materials] are consumed by microbes, is it consistent
3 with scientific and engineering principles, standards, and practices to conclude that, in the
4 absence of MgO, the solubility of actinides will be such that releases to the accessible
5 environment will still be below the EPA limits?” (Institute for Regulatory Science [RSI] 2006,
6 p. 13), were that: “On the basis of the information received by the [RSI expert panel], it is likely
7 that releases to the accessible environment will be below the EPA regulatory limits. However,
8 the evidence received by the [RSI expert panel] is not sufficient to definitely support this
9 conclusion” (Institute for Regulatory Science [RSI] 2006, pp. 13–14).

10 SCA did not specifically address whether, in the absence of MgO, the WIPP would continue to
11 meet the EPA’s containment requirements, given microbial consumption of cellulosic materials,
12 or microbial consumption of all of the CPR materials. However, SCA (S. Cohen and Associates
13 2006, p. 3-4) stated

14 The use of at least one engineered barrier at WIPP is required by 40 CFR 194.44 to ‘prevent or
15 substantially delay the movement of water or radionuclides toward the accessible environment.’
16 For the CCA, DOE identified and EPA approved MgO backfill in the disposal rooms as the only
17 WIPP engineered barrier (DOE 1996[b]). MgO backfill was designed to maintain alkaline pH and
18 mitigate the effects of CO₂ generation in the disposal rooms, thereby controlling actinide
19 solubilities in intruding brines ([U.S.] EPA 1997). The inclusion of MgO backfill as an
20 engineered barrier remained unchanged for the CRA, although the required safety factor and
21 backfill emplacement strategy have changed since the CCA....

22 Furthermore, in response to a recommendation by the NRC (2001) that “The committee
23 recommends that the net benefit of MgO used as backfill be reevaluated. The option to
24 discontinue emplacement of MgO should be considered,” SCA (S. Cohen and Associates 2006,
25 p. 3-1) stated that

26 Removing the MgO backfill from the repository design will likely affect predictions of gas
27 generation and actinide solubilities. Additional information would be necessary before EPA could
28 consider elimination of, or significant modifications to, the MgO backfill. EPA regulations
29 require assurance requirements (40 CFR 191.14), including an engineered barrier, to compensate
30 for uncertainties in the prediction of future repository performance and provide increased
31 confidence in the disposal system. The MgO backfill is the only engineered barrier in the WIPP
32 repository and an engineered barrier is required by regulation....

33 The RSI expert panel’s seventh finding, which dealt with the application of “acceptable
34 knowledge” to the characterization of the concentrations of CPR materials in TRU waste, and
35 SCA’s response to this finding are not discussed herein.

36 In its eighth finding, the RSI expert panel stated that “[a] 67% MgO ... is not necessary”
37 (Institute for Regulatory Science [RSI] 2006, p. 15). SCA (S. Cohen and Associates 2006,
38 p. 5-1) responded by stating that

39 In the original certification review (EPA 1997), EPA accepted MgO as the only engineered barrier
40 (40 CFR 194.44). This acceptance was predicated on the assumption that MgO was necessary to
41 control chemical conditions in disposal rooms. [U.S.] EPA (1997) also stated that excess MgO,
42 i.e., the MgO safety factor, was a conservative measure, an assurance requirement, necessary to
43 overcome the uncertainty associated with predicting the expected future(s) of the WIPP disposal
44 system. The engineered barrier is of critical importance because of a number of uncertainties

1 associated with repository performance over the long regulatory time period. Assuming that all
 2 CPR [C] could be converted to CO₂ was a conservative assumption associated with the engineered
 3 barrier's performance. If this conservative assumption is no longer included in the determination
 4 of the MgO safety factor, the potential significance of other uncertainties would increase, such as
 5 those related to CPR inventory, CPR degradation rates and extents, and the possible physical
 6 segregation of small amounts of MgO. The MgO safety factor must account for these
 7 uncertainties in the absence of conservative assumptions regarding the extent of CPR degradation
 8 to form CO₂. Because of the importance of the MgO backfill, an understanding of the potential
 9 effects of a shortfall would be necessary before the technical feasibility of significantly reducing
 10 the MgO safety factor could be assessed.

11 In its summary and conclusions, SCA listed “a number of potential technical issues ... related to
 12 whether the amount of MgO placed in the repository can be reduced without affecting repository
 13 safety” (S. Cohen and Associates 2006, p. 6-1). These included (1) the availability of MgO,
 14 which could be reduced by the possible physical segregation of small quantities of MgO from
 15 brine; (2) uncertainties in the quantities of CPR materials in the inventory; and (3) the extent of
 16 microbial consumption of CPR materials during the 10,000-year regulatory period.

17 SCA (S. Cohen and Associates 2006, pp. 6-1 to 6-2) also identified several issues that could
 18 affect the possible extent of microbial consumption of CPR materials. These included the
 19 following:

- 20 1. The adaptability of microbes to different substrates and environments
- 21 2. The short-term effects of microbial consumption of CPR materials by aerobic bacteria and
 22 fungi
- 23 3. The short-term effects of α radiolysis of CPR materials (i.e., radiolysis under oxic
 24 conditions) on the biodegradability of these materials
- 25 4. The length of time that molecular oxygen (O₂) will be present
- 26 5. The long-term effects of α radiolysis of CPR materials (i.e., radiolysis under anoxic
 27 conditions) on the biodegradability of these materials
- 28 6. The long-term, integrated radiation dose to CPR materials
- 29 7. Uncertainties associated with the predicted availability of brine in the repository

30 In its ninth finding and its first recommendation, the RSI expert panel stated that (1) “[t]he DOE
 31 should consider convening an Expert Elicitation Panel to provide a more realistic and accurate
 32 estimate of the potential extent of biodegradation of various components of CPR materials likely
 33 to be emplaced in the WIPP”; (2) the Expert Elicitation Panel should estimate the “fraction of
 34 the emplaced MgO [that] is likely to react with the CO₂”; and (3) that the Expert Elicitation
 35 Panel should estimate “the performance consequences of a partial or complete shortfall in MgO
 36 buffering capacity” (Institute for Regulatory Science [RSI] 2006, p. 16). SCA (S. Cohen and
 37 Associates 2006, p. 3-4), responded

1 Requirements related to the elicitation of expert judgment for use in compliance applications are
2 provided in 40 CFR 194.26. With regard to the circumstances under which expert judgment can
3 be used for compliance applications, the regulation states [40 CFR 194.26(a)]:

4 *Expert judgment, by an individual expert or panel of experts, may be used to*
5 *support any compliance application, provided that expert judgment does not*
6 *substitute for information that could reasonably be obtained through data*
7 *collection or experimentation [SCA's italics].*

8 In its summary and conclusions, SCA (S. Cohen and Associates 2006, pp. 6-2 through 6-3) went
9 on to describe the “information that could reasonably be obtained through data collection or
10 experimentation” with regard to the possible extent of microbial consumption of CPR materials:

11 The results of the preliminary review described in this report indicate that cellulose may be
12 completely degraded in the repository environment over the 10,000-year regulatory period. The
13 preliminary review of information regarding the possible extent of plastics and rubber degradation
14 in the repository is less conclusive; therefore, additional literature review and experimental
15 investigations may be necessary to determine the likely extent of radiolytic and microbial
16 degradation of plastics and rubber during the 10,000-year regulatory period. Processes likely to
17 affect waste during use, storage, transport, and the early disposal period include degradation by
18 aerobic bacteria and fungi, and radiolysis in the presence of [O₂]. Estimation of the length of time
19 [O₂] will persist in the repository and the radiation doses to waste could be used to determine the
20 likely effects of these processes. Although these processes may not significantly affect short-term
21 rates and extents of degradation of CPR, their effects could influence mechanisms, rates, and
22 extents of CPR degradation over the long WIPP regulatory time period. The available literature
23 should be reviewed to determine whether these early degradation processes and long-term
24 radiolysis under anaerobic conditions are likely to make CPR more susceptible to microbial
25 degradation in the longer-term anaerobic WIPP environment.

26 Any assessment of the extents of degradation of CPR should include an estimation of associated
27 uncertainties, which should be incorporated in the MgO safety factor. These estimated
28 uncertainties should reflect all possible physical and chemical processes that might occur over
29 10,000 years including:

- 30 • The adaptability of microbes to different substrates and environments
- 31 • Potential physical segregation of small quantities of MgO from brine
- 32 • CPR inventory uncertainties
- 33 • Effects of short-term aerobic radiolysis and biodegradation reactions on long-term microbial
34 degradation of CPR
- 35 • Effects of long-term anaerobic radiolytic processes on CPR biodegradation
- 36 • Uncertainties associated with the predicted availability of brine in the repository

37 EPA regulations require that expert judgment should not be substituted for available experimental
38 data or data that could be obtained from a reasonable set of experiments (40 CFR 194.26). The
39 results of this review have indicated that literature describing experimental data is available that
40 might be used to reduce the uncertainties associated with the extent of CPR degradation in the
41 WIPP repository and improve understanding of WIPP's future performance. Consequently, use of
42 expert judgment to assess the likely extents of CPR degradation in the WIPP repository may not
43 be justified at this time and would require adequate justification by DOE. If the use of expert
44 judgment is justified, this judgment should include not only the likely extents of CPR degradation,
45 but also the associated uncertainties, taking into account the factors listed above.

1 A more extensive evaluation of the available WIPP and non-WIPP literature should be carried out
 2 to determine whether the data are sufficient for estimating the likely extent of CPR degradation
 3 during the 10,000-year regulatory period, or whether experiments might be designed to determine
 4 the probable extents of degradation of the various materials over this long regulatory time period.
 5 The goal of the literature review and experimental studies would be to adequately quantify or
 6 capture system uncertainties, including both the uncertainties associated with the quantities of
 7 CPR in the repository and the chemical uncertainties related to the CPR degradation reactions and
 8 reactions of the MgO backfill. Sufficient excess MgO (an adequate safety factor) needs to be
 9 emplaced in each disposal room to compensate for the range of uncertainties related to CPR
 10 degradation and the effective performance of the MgO engineered barrier, thereby ensuring
 11 WIPP's expected safe performance in the future.

12 Finally, SCA noted that the RSI expert panel recommended that “[t]he DOE should consider
 13 performing a single-room realistic analysis of the complex processes involved, including gas
 14 generation, chemical reactions, biodegradation, and mechanical creep” (Institute for Regulatory
 15 Science [RSI] 2006, p. 16). However, SCA did not comment on this recommendation.

16 **MgO-6.2.4.4 The DOE’s Assessment of the Uncertainties Related to the MgO Excess**
 17 **Factor**

18 The DOE carried out an analysis (Vugrin, Nemer, and Wagner 2006) and several supporting
 19 analyses (Brush and Roselle 2006; Brush et al. 2006; Clayton and Nemer 2006; Deng et al. 2006;
 20 Kanney and Vugrin 2006; Kirchner and Vugrin 2006) to respond to the EPA’s request for
 21 additional information on “the uncertainties related to MgO effectiveness, the size of the
 22 uncertainties, and the potential impact of the uncertainties on long-term performance” (Gitlin
 23 2006).

24 Vugrin, Nemer, and Wagner (2006, p. 2) defined the MgO effective excess factor as “a quantity
 25 that incorporates uncertainties into the current definition of the MgO excess factor.” The results
 26 of the supporting analyses cited above were used to quantify these uncertainties whenever
 27 possible and incorporate them in the effective excess factor.

28 Vugrin, Nemer, and Wagner (2006, p. 8) recognized four categories of uncertainties that could
 29 affect the MgO effective excess factor:

- 30 1. Uncertainties in the quantities of CPR materials that will be consumed during the 10,000-
 31 year WIPP regulatory period
- 32 2. Uncertainties in the number of moles of CO₂ produced per mole of organic C in CPR
 33 materials (i.e., the CO₂ yield)
- 34 3. Uncertainties in the quantity of MgO that will be available to consume CO₂
- 35 4. Uncertainties in the number of moles of CO₂ consumed per mole of available MgO

36 Although Vugrin, Nemer, and Wagner (2006, Appendix A) reviewed previous discussions of the
 37 uncertainties inherent in predicting the extent of microbial consumption of CPR materials in
 38 10,000 years (Brush 1995; Gillow and Francis 2003; Brush 2004; the CRA-2004, Appendix
 39 BARRIERS), they did not attempt to incorporate them in the MgO effective excess factor.

1 Therefore, they used the conservative assumption that microbes will consume 100% of the CPR
2 materials to calculate the MgO effective excess factor.

3 **MgO-6.2.4.4.1 Uncertainties in the CO₂ Yield From Microbial Consumption of CPR** 4 **Materials**

5 Vugrin, Nemer, and Wagner (2006, Section 4) included two sources of the uncertainties inherent
6 in predicting the CO₂ yield per mole of organic C in CPR materials: (1) uncertainty in the
7 quantities of CPR materials emplaced in WIPP disposal rooms, and (2) uncertainty as to the
8 microbial respiratory pathways involved in consumption of the CPR materials (see Section
9 MgO-6.1).

10 Kirchner and Vugrin (2006) quantified the uncertainties in the estimates of the quantities of CPR
11 materials emplaced in WIPP disposal rooms. Their analysis was based on the differences
12 between the masses of CPR materials measured by real-time radiography (RTR) and visual
13 examination (VE), paired by waste container. They assumed that the VE measurements were the
14 more accurate values and, because they observed no significant bias in the RTR measurements,
15 that the sum of the RTR measurements best estimate the true value of the CPR material quantity
16 in a room. Kirchner and Vugrin (2006) then used Monte Carlo methods “to simulate potential
17 errors in the RTR measurements and to construct a distribution representing the uncertainty in
18 the ... CPR [materials] in a room” and concluded “that the uncertainty [standard deviation] on
19 the total mass of CPR [materials] in a room would be less than 0.3%.” See Kirchner and Vugrin
20 (2006) for a detailed explanation of this analysis, and Vugrin, Nemer, and Wagner (2006) for an
21 explanation of how the results were incorporated in the MgO effective excess factor.

22 Vugrin, Nemer, and Wagner (2006) reviewed previous discussions on the effects of microbial
23 respiratory pathways on the CO₂ yield per mole of organic C in CPR materials (Wang and Brush
24 1996a; Snider 2003d; and Section MgO-6.1). However, Vugrin, Nemer, and Wagner (2006) did
25 not include the effects of possible methanogenesis on the CO₂ yield, because the EPA concluded
26 that Kanney et al. (2004) did not adequately bound the quantity of naturally occurring SO₄²⁻ that
27 could enter WIPP disposal rooms (TEA 2004, pp. 31-33; U.S. EPA 2004, pp. 7-8) and specified
28 that methanogenesis not be included in PA. Therefore, Vugrin, Nemer, and Wagner (2006)
29 included only denitrification and SO₄²⁻ reduction in their analysis. They calculated that microbes
30 would consume 4.89 mol % of the organic C in the CPR materials in the CRA-2004 PABC
31 inventory via denitrification and 0.84 mol % via SO₄²⁻ reduction using SO₄²⁻ in the waste
32 (Vugrin, Nemer, and Wagner 2006, p. 11). The remainder of the organic C, 94.27 mol %, would
33 be consumed via SO₄²⁻ reduction using naturally occurring SO₄²⁻.

34 Vugrin, Nemer, and Wagner (2006) quantified the effects of the source of SO₄²⁻ on the MgO
35 effective excess factor. There are three potential sources of SO₄²⁻ for microbial consumption of
36 CPR materials via SO₄²⁻ reduction: (1) SO₄²⁻ in the waste; (2) SO₄²⁻ dissolved in Salado or
37 Castile brines; and (3) SO₄²⁻ contained in DRZ minerals such as anhydrite, gypsum, or
38 polyhalite. Microbes would consume 0.84 mol % of the organic C in the CPR materials in the
39 CRA-2004 PABC inventory via SO₄²⁻ reduction using SO₄²⁻ in the waste, and produce CO₂ with
40 a yield of 1 mol per mol of organic C consumed. The CO₂ yield from the SO₄²⁻ dissolved in
41 WIPP brines would be 1 mol per mol of organic C consumed (see below), but the amount of
42 organic C in the CPR materials that would be consumed via SO₄²⁻ reduction using SO₄²⁻ in brines

1 had never been calculated. Furthermore, neither the amount of organic C in the CPR materials
2 that would be consumed via SO_4^{2-} reduction using SO_4^{2-} in DRZ minerals nor the CO_2 yield from
3 this process had previously been calculated.

4 Therefore, Clayton and Nemer (2006) calculated the quantities of dissolved SO_4^{2-} that could
5 enter the repository in brine, and Brush et al. (2006) calculated the CO_2 yield from microbial
6 consumption of CPR materials via SO_4^{2-} reduction using DRZ minerals. The analysis of Clayton
7 and Nemer will be described first because Vugrin, Nemer, and Wagner (2006) assumed that
8 microbes would use SO_4^{2-} from the waste and brine before using the SO_4^{2-} from DRZ minerals.
9 This assumption was conservative because SO_4^{2-} reduction with SO_4^{2-} from the waste and brine
10 would have a higher CO_2 yield than SO_4^{2-} reduction using SO_4^{2-} from DRZ minerals (see below).

11 Clayton and Nemer (2006) determined at the outset of their analysis that it was conservative to
12 assume that Salado brine will not be a significant source of SO_4^{2-} for microbial consumption of
13 CPR materials. Microbial SO_4^{2-} reduction produces 2 mol of CO_2 per mol of SO_4^{2-} consumed
14 (see Equation MgO.14 in Section MgO-6.1). For every mol of SO_4^{2-} dissolved in GWB, there
15 are about 5.76 mol of dissolved Mg before equilibration with the solids in WIPP disposal rooms
16 (Section MgO-5.1) and 2.54 mol of dissolved Mg after equilibration with these solids (Table
17 MgO-6). Therefore, GWB will always contain enough dissolved Mg to consume all of the CO_2
18 that would be produced via SO_4^{2-} reduction using the SO_4^{2-} dissolved in this brine.

19 Clayton and Nemer (2006) then established a probability distribution for the quantities of SO_4^{2-}
20 dissolved in Castile brines that could enter a panel during the 10,000-year regulatory period.
21 They used a Monte Carlo simulation to generate 1,000 possible human-intrusion (drilling)
22 futures. Each of these futures consisted of possible intrusion sequences into all 10 panels of the
23 repository. For each future, they identified the “worst-case” panel: the panel with the most
24 boreholes that intersected a Castile brine reservoir and hence the largest volume of Castile brine
25 in that future. Clayton and Nemer (2006) then used the results from the BRAGFLO calculations
26 for the CRA-2004 PABC (Nemer and Stein 2005) to calculate a probability distribution of the
27 quantities of SO_4^{2-} that could enter a panel from a single intrusion that penetrated a Castile brine
28 reservoir. Finally, Clayton and Nemer (2006) combined the uncertainties in the drilling futures
29 with those in the quantities of Castile-brine SO_4^{2-} from a single intrusion to create a probability
30 distribution of the quantities of SO_4^{2-} that could enter the worst-case panel in 10,000 years.
31 Clayton and Nemer (2006, Figure 1) obtained a complementary cumulative distribution function
32 (CCDF) for the quantities of Castile SO_4^{2-} that could enter a panel in 10,000 years. The mean
33 value of this CCDF was consumption of 2.4 mol % of the organic C in CPR materials via SO_4^{2-}
34 reduction using Castile-brine SO_4^{2-} , with a standard deviation of 5.1 mol %. The mean value
35 was small because almost 30% of the drilling futures did not have intrusions that penetrated a
36 brine reservoir and thus did not have any Castile-brine SO_4^{2-} . Vugrin, Nemer, and Wagner
37 (2006) incorporated these values into the MgO effective excess factor.

38 Brush et al. (2006) calculated the CO_2 yield from microbial consumption of CPR materials via
39 SO_4^{2-} reduction using DRZ minerals. If microbes consume all the SO_4^{2-} in the waste and in
40 brines that enter WIPP disposal rooms, the resulting concentration gradient from the
41 intergranular brines in the DRZ to the brine(s) in the repository would drive diffusive transport
42 of SO_4^{2-} from the DRZ through saturated voids to the waste. This would in turn decrease the
43 SO_4^{2-} concentration in the brines in the DRZ, which would lead to the dissolution of SO_4^{2-} -

1 bearing minerals such as anhydrite, gypsum, and polyhalite present in both the marker beds and
2 the nearly pure halites in the Salado (Stein 1985). Because all of these SO_4^{2-} -bearing minerals
3 also contain Ca, dissolution of these minerals would release Ca^{2+} to these intergranular brines
4 and (after transport) to the repository. This Ca^{2+} would remove CO_2 from both the aqueous and
5 gaseous phases by precipitating it as minerals such as calcite (CaCO_3); metastable polymorphs of
6 calcite like aragonite, vaterite, or ikaite; monohydrocalcite ($\text{CaCO}_3 \cdot \text{H}_2\text{O}$), amorphous CaCO_3
7 ($\text{CaCO}_3(\text{amorphous} [\text{am}])$), or pirssonite ($\text{Na}_2\text{Ca}(\text{CO}_3)_2 \cdot 2\text{H}_2\text{O}$). Consumption of CO_2 by
8 precipitation of CaCO_3 -bearing minerals would reduce the amount of MgO that must be
9 emplaced, thus impacting the calculation of the MgO effective excess factor.

10 Brush et al. (2006) used the reaction-path code EQ6 (Wolery and Daveler 1992), part of the
11 EQ3/6 geochemical software package (Daveler and Wolery 1992; Wolery 1992a and 1992b), to
12 simulate the precipitation of CaCO_3 -bearing minerals via the process described above. Brush
13 et al. (2006) quantified the sensitivity of the CO_2 yield to factors such as

- 14 1. The initial brine composition and the brine volume
- 15 2. Whether carbonation of brucite produces hydromagnesite (5424) or magnesite
- 16 3. The effects of organic ligands
- 17 4. The effects of precipitation of $\text{CaCO}_3(\text{am})$ instead of calcite

18 They assumed that microbes will consume all of the CPR materials in WIPP disposal rooms, and
19 calculated that microbes would consume 4.89 mol % of the organic C in the CPR materials in the
20 CRA-2004 PABC inventory via denitrification using NO_3^- in the waste and produce CO_2 with a
21 yield of 1 mol per mol of organic C consumed; 0.84 mol % of the organic C via SO_4^{2-} reduction
22 using SO_4^{2-} in the waste with a yield of 1 mol of CO_2 per mol of organic C; and 94.27 mol % of
23 the organic C via SO_4^{2-} reduction using SO_4^{2-} from DRZ minerals. Brush et al. (2006) did not
24 include any SO_4^{2-} reduction using Castile-brine SO_4^{2-} because this was an uncertain parameter,
25 the effects of which were incorporated later by Vugrin, Nemer, and Wagner (2006).

26 Brush et al. (2006) calculated that the effective CO_2 yield from SO_4^{2-} reduction using SO_4^{2-} from
27 DRZ minerals would be 0.54-0.60 mol per mol of organic C in the CPR materials consumed.
28 The overall CO_2 yield, which included denitrification and SO_4^{2-} reduction using SO_4^{2-} from the
29 waste, but not Castile-brine SO_4^{2-} , would be 0.57-0.62 mol per mol of organic C.

30 A potential concern evaluated by Brush et al. (2006) is that certain elements or compounds in
31 WIPP disposal rooms could inhibit or even prevent calcite precipitation. Dissolved Mg, for
32 example, could inhibit or prevent the precipitation of calcite, depending on its concentration.
33 However, the literature reviewed for this analysis suggested that if an element or compound
34 inhibits or prevents the precipitation of one CaCO_3 -bearing mineral, another, less-stable CaCO_3 -
35 bearing mineral precipitates instead. Thus, if dissolved Mg inhibits or prevents the formation of
36 calcite, aragonite would precipitate (Fernández-Díaz et al. 1996), possibly with coprecipitation of
37 as much as 20% MgCO_3 in addition to CaCO_3 (Morse 1983). The most important point,
38 however, is that if precipitation of CaCO_3 -bearing minerals were prevented, microbial SO_4^{2-}
39 reduction would cease after the consumption of 4.89 mol % of the organic C in the CPR
40 materials in the CRA-2004 PABC inventory via denitrification, 0.84 mol % via SO_4^{2-} reduction

1 using SO_4^{2-} in the waste, and 2.4 mol % via SO_4^{2-} reduction using Castile-brine SO_4^{2-} . Any
2 additional consumption of CPR materials could only occur via methanogenesis, which has a CO_2
3 yield of 0.5 mol per mol of organic C consumed. This is because failure of CaCO_3 to precipitate
4 would prevent additional dissolution of SO_4^{2-} -bearing minerals and result in rapid microbial
5 depletion of SO_4^{2-} .

6 Vugrin, Nemer, and Wagner (2006) accounted for the possibility of magnesian calcite formation
7 in the WIPP by conservatively assuming that any CO_2 not consumed by hydromagnesite (5424)
8 or magnesite in the simulations of Brush et al. (2006) would be incorporated in a solid solution
9 or two-phase mixture with the composition $\text{Mg}_{0.22}\text{Ca}_{0.78}\text{CO}_3$, rather than a polymorph of CaCO_3
10 or pirssonite as predicted by EQ6. Magnesian calcite with the composition $\text{Mg}_{0.22}\text{Ca}_{0.78}\text{CO}_3$
11 (Meldrum and Hyde 2001) was the most Mg-rich calcite that Brush et al. (2006) found, if
12 dissolved SO_4^{2-} were present, in their literature review of elements or compounds that could
13 inhibit CaCO_3 precipitation. Vugrin, Nemer, and Wagner (2006) implemented this assumption
14 by adjusting the effective CO_2 yield from SO_4^{2-} reduction using SO_4^{2-} from DRZ minerals from
15 0.54-0.60 mol per mol of organic C consumed (Brush et al. 2006) to 0.62-0.69 mol per mol of
16 organic C. They added additional conservatism by using only the upper end of this range, or
17 0.69 mol of CO_2 per mol of organic C in their calculation of the MgO effective excess factor.

18 Finally, Vugrin, Nemer, and Wagner (2006, Section 5.2.3, pp. 51-52) combined the yields for
19 each step of the possible microbial consumption of CPR materials as follows:

- 20 1. Consumption of 4.89% of the organic C in the CPR materials via denitrification using NO_3^-
21 in the waste, with a yield of 1 mol of CO_2 per mol of organic C
- 22 2. Consumption of 0.84% of the organic C via SO_4^- reduction using SO_4^{2-} in the waste, with a
23 yield of 1 mol of CO_2 per mol of organic C
- 24 3. Consumption of 2.4 mol % of the organic C via SO_4^{2-} reduction using Castile-brine SO_4^{2-} ,
25 with a yield of 1 mol of CO_2 per mol of organic C
- 26 4. Consumption of the remaining 91.87 mol % of the organic C via SO_4^{2-} reduction using SO_4^{2-}
27 from DRZ minerals, with a yield of 0.69 mol of CO_2 per mol of organic C

28 The overall yield for this combination of microbial respiratory pathways and these sources of
29 electron acceptors is 0.715 mol of CO_2 per mol of organic C, with a standard deviation of
30 0.016 mol of CO_2 per mol of organic C.

31 **MgO-6.2.4.4.2 Uncertainties in the Quantity of MgO that will be Available to Consume** 32 **CO_2**

33 Vugrin, Nemer, and Wagner (2006, Section 5.0, p. 19) divided these uncertainties into two
34 categories: (1) uncertainties related to the characteristics and performance of MgO, and (2) those
35 related to the characteristics and performance of the WIPP.

36 Vugrin, Nemer, and Wagner (2006, Section 5.1, p. 20) identified three uncertainties related to
37 MgO: (1) the concentration of reactive constituents in MgO, (2) the extent to which these

1 reactive constituents react with atmospheric CO₂ prior to emplacement in the repository, and
2 (3) the extent to which they react with CO₂ after emplacement.

3 Vugrin, Nemer, and Wagner (2006, Section 5.1.1) incorporated the results of Deng et al. (2006a)
4 and Deng, Xiong, and Nemer (2007b) in the MgO effective excess factor because these were the
5 first results obtained directly for Martin Marietta WTS-60, the MgO currently being emplaced in
6 the WIPP. Deng et al. (2006) and Deng, Xiong, and Nemer (2007b) reported that WTS-60
7 contains 96 ± 5 mol % periclase and lime (see Section MgO-3.3.2). Vugrin et al. (2006, Section
8 5.1.1) selected these results based on the review by Brush and Roselle (2006, Section 2) of the
9 characterization of the MgO that has been emplaced in the WIPP since it opened in March 1999
10 (see also Section MgO-3.0).

11 Vugrin, Nemer, and Wagner (2006, Section 5.1.2, p. 21) assumed that “due to carbonation of
12 periclase prior to emplacement, 0.1% of the emplaced MgO will be unavailable to sequester CO₂
13 after closure of the repository.” This assumption is based on a DOE analysis carried out during
14 the EPA’s review of the CCA demonstrating that less than 0.1% of the MgO would be
15 carbonated in 30 years by CO₂ that penetrates the bag over 30 years, and the WTS specification
16 for MgO that states, “The super sack shall function as a barrier to atmospheric moisture and CO₂,
17 which is equivalent to or better than that provided by a standard commercial cement bag”
18 (Washington TRU Solutions 2005, Section 3.3.2 E.).

19 Vugrin, Nemer, and Wagner (2006, Section 5.1.3, p. 22) also assumed “that all of the periclase
20 will be available to react and will continue to react until all of the CO₂ [in the repository] is
21 consumed.” This assumption is based on the conclusion by Brush and Roselle (2006, Section
22 3.2, p. 8):

23 Because all results to date imply that the periclase and lime present in MgO will be available to
24 react – and will continue to react – until all CO₂ in the repository has been consumed, the MgO
25 effective excess factor need not be reduced to account for incomplete reaction. This is consistent
26 with multiplication of the excess factor by 1.

27 However, Vugrin, Nemer, and Wagner (2006, Section 5.1.3, p. 22) also stated that they did not
28 include uncertainty in the MgO effective excess factor because they could not quantify it.

29 Vugrin, Nemer, and Wagner (2006, Section 5.2, p. 22) identified five uncertainties in the
30 quantity of MgO that will be available to consume CO₂ related to the characteristics and
31 performance of the WIPP:

- 32 1. The probability that the supersacks will rupture and expose MgO to the repository
33 environment (i.e., aqueous and gaseous CO₂)
- 34 2. The loss of dissolved MgO from the repository via brine outflow
- 35 3. The mass of MgO in individual supersacks
- 36 4. The probability that CO₂ will be transported to MgO via brine-mixing processes
- 37 5. The probability of physical segregation of MgO from CO₂

1 Vugrin, Nemer, and Wagner (2006, Section 5.2.1, p. 23) assumed “that all MgO supersacks
2 will rupture due to either microbial degradation or lithostatic loading, making the MgO available
3 for consumption of CO₂.”

4 Clayton and Nemer (2006) established a probability distribution for the fraction of MgO that
5 could be lost via brine outflow during the 10,000-year regulatory period. They used methods
6 similar to those for calculating the probability distribution for the quantities of SO₄²⁻ dissolved in
7 Castile brines that could enter a panel in 10,000 years. Clayton and Nemer (2006) used a Monte
8 Carlo simulation to generate 1,000 possible drilling futures, the brine-outflow results from the
9 BRAGFLO calculations for the CRA-2004 PABC (Nemer and Stein 2005), and an MgO excess
10 factor of 1.2 to calculate a CCDF for the quantities of MgO that could be lost in 10,000 years.
11 The mean of this CCDF was 0.8% of the quantity of MgO initially emplaced, with a standard
12 deviation of 1.9%. The mean value was small because almost 30% of the drilling futures did not
13 have intrusions that penetrated a brine reservoir, and thus did not have any Castile-brine SO₄²⁻.
14 Vugrin, Nemer, and Wagner (2006, Section 5.2.2, p. 23) incorporated these results into the MgO
15 effective excess factor.

16 Kanney and Vugrin (2006) updated the analysis of Wang (2000b), which demonstrated that, in
17 the absence of minisacks, molecular diffusion in WIPP brines would be fast enough for MgO to
18 control chemical conditions in the repository (see Section MgO-2.1.2). Kanney and Vugrin
19 (2006) updated Wang’s (2000b) work by modifying it to be consistent with the CRA-2004
20 PABC, and applying it in a modified form to the results of analysis of the effects of
21 supercompacted waste on the long-term performance of the WIPP (Hansen et al. 2004). Neither
22 of these modifications changed the conclusion reached by Wang (2000b), that diffusive transport
23 alone is sufficient to mix CO₂ in the aqueous phase over length scales corresponding to the
24 postclosure height of WIPP disposal rooms and time scales appropriate to that of maximum
25 average brine flows. Both analyses (Wang 2000b; Kanney and Vugrin 2006) conservatively
26 omitted advective and dispersive mixing in the aqueous phase, which would be more effective
27 than diffusion; and diffusive transport of CO₂ in the gaseous phase, which would be very fast
28 relative to that in brine. Therefore, Vugrin, Nemer, and Wagner (2006, Section 5.2.3, p. 25)
29 “assume[d] that the mixing processes expected in the repository will be sufficient to maintain a
30 well-mixed brine.”

31 Vugrin, Nemer, and Wagner (2006, Section 5.2.4, p. 25) assumed that none of the MgO
32 emplaced in WIPP disposal rooms would become physically segregated from the repository
33 environment. The report stated

34 Physical segregation of a quantity of MgO from brine or CO₂ due to roof collapse could
35 potentially impact the quantity of MgO available to sequester CO₂; however, the probability of
36 this segregation and the potential impact is negligible. It is probable that any roof failure will
37 occur by lowering of a roof beam onto the waste/MgO stack so that the failed material will not
38 intrude into the stack. Secondly, any failed roof which might occur in smaller blocks will be
39 fractured and will maintain a fairly high permeability to brine and gas for a significant amount of
40 time. Finally, any small scale spalling of the roof into the interstices of the stacks will also
41 probably maintain a high permeability either because grains will not re-cement easily, or if they
42 do, they will form a coherent mass with brine, MgO, and gas outside of them.

43 Furthermore, the current method that DOE uses to emplace the MgO and calculation of the MgO
44 excess factor on a room basis likely minimizes the possible physical segregation of MgO from

1 brine and CO₂. Operational controls guarantee one MgO supersack is emplaced on each stack of
 2 waste. If this quantity is not sufficient to meet the required MgO [excess factor] for a room,
 3 additional MgO is emplaced. These EPA audited operations are detailed in WIPP technical
 4 procedures (WTS, 2006).

5 Vugrin, Nemer, and Wagner (2006, Section 5.2.4, p. 25) also stated that “The uncertainty with
 6 this assumption cannot presently be quantified, so the uncertainty will not be included in [the]
 7 calculations of the MgO effective excess factor.”

8 Vugrin, Nemer, and Wagner (2006, Section 5.2.5, pp. 25-26) carried out a statistical analysis of
 9 the uncertainty in the mass of MgO in the supersacks and concluded that they could use a mean
 10 value of 4200 lbs, the value specified by WTS (Washington TRU Solutions 2005, Section 3.4.1,
 11 p. 3) for the mass of MgO in a supersack, and a standard deviation of 0.037%.

12 **MgO-6.2.4.4.3 Uncertainties in the Number of Moles of CO₂ Consumed per Mole of**
 13 **Available MgO**

14 Vugrin, Nemer, and Wagner (2006) recognized four uncertainties that could affect the number of
 15 moles of CO₂ that would be consumed per mole of available MgO:

- 16 1. The extent to which consumption of CO₂ by brucite produces hydromagnesite (5424) or
 17 magnesite in WIPP disposal rooms
- 18 2. Possible consumption of CO₂ by materials other than MgO
- 19 3. Dissolution of CO₂ in WIPP brines
- 20 4. Incorporation of CO₂ in biomass

21 The extent to which carbonation of brucite produces hydromagnesite (5424) or magnesite will
 22 affect the MgO effective excess factor (Brush and Roselle 2006, Section 4; Vugrin, Nemer, and
 23 Wagner 2006, Section 6.1). The brucite-hydromagnesite (5424) carbonation reaction consumes
 24 0.8 mol of CO₂ per mol of MgO consumed; the brucite-magnesite reaction consumes 1 mol of
 25 CO₂ per mol of MgO (compare Reactions [MgO.7] and [MgO.8] in Section MgO-5.1). Brush
 26 and Roselle (2006, Section 4.1, Section 5.2, and Section 5.3) reviewed the results of laboratory
 27 and natural-analog studies of brucite carbonation. Based on their review, Brush and Roselle
 28 (2006, Section 4.1, p. 12) concluded

29 Any hydromagnesite formed prior to 9,000 years after the WIPP is filled and sealed would convert
 30 completely to magnesite, which – along with the initially formed hydromagnesite – would
 31 consume 1 mol of CO₂ per mol of periclase. Furthermore, much of the hydromagnesite formed
 32 after 9,000 years would react to form magnesite.

33 Brush and Roselle (2006, Section 4.2, pp. 12-13) also concluded

34 Incorporation of the ratio of the number of moles of CO₂ consumed per mol of periclase in MgO
 35 into the effective excess factor necessitates multiplication of this factor by a value close to 1. The
 36 number of moles of CO₂ consumed per mol of periclase will be close to 1 because: (1) magnesite
 37 will be the dominant Mg carbonate throughout most of the 10,000-year regulatory period; and (2)
 38 formation of magnesite from brucite (or periclase), and formation of hydromagnesite followed by

1 conversion of hydromagnesite to magnesite would both consume 1 mol of CO₂ per mol of
2 periclase. The exact ratio of CO₂ consumed per mol of periclase will depend on how much CO₂ is
3 produced by microbial activity prior to 9,000 years. Therefore, this ratio might have to be
4 computed on a vector-by-vector basis.

5 The laboratory and some of the natural-analog studies on which these conclusions are based are
6 also reviewed in Section MgO-4.2.2 (see above).

7 Vugrin, Nemer, and Wagner (2006, Section 6.1, p. 29) carried out an analysis that demonstrated
8 that “as long as the half life for the conversion of hydromagnesite [5424] to magnesite is less
9 than 3,000 years, uncarbonated Mg[O] will remain.” Their analysis was based on the results of
10 Zhang et al. (1999), but introduced additional conservatisms that are not required to apply these
11 results to the formation of magnesite in the WIPP (see Section MgO-4.2.2). Vugrin, Nemer, and
12 Wagner (2006, Table 5, p. 35) also assumed that carbonation of brucite will consume 1 mol of
13 CO₂ per mol of MgO, consistent with conversion of all of the hydromagnesite (5424) in WIPP
14 disposal rooms to magnesite (Reaction [MgO.9] in Section MgO-4.2.2).

15 Brush and Roselle (2006, Section 6) reviewed the results of studies relevant to the possible
16 consumption of CO₂ by materials other than MgO in the WIPP. Brush and Roselle (2006,
17 Section 6.6, p. 25) concluded

18 Inclusion of the effects of consumption of CO₂ by Fe-base metals and their corrosion products,
19 lead (Pb)-base metals and their corrosion products, and CaO and Ca(OH)₂ in Portland cement
20 would be difficult at present because of the uncertainties associated with these processes in the
21 WIPP ... However, these materials could consume 36.1, 1.36, and 0.177% of the CO₂ that would
22 be produced by complete microbial consumption of all CPR materials in the repository.

23 Therefore, Vugrin, Nemer, and Wagner (2006, Section 6.2, p. 31) decided

24 Because of these uncertainties, this analysis will use the conservative assumption that CO₂ will not
25 be consumed by Fe-base metals or their corrosion products, Pb-base metals or their corrosion
26 products, or lime and portlandite in portland cements. However, if it were possible to quantify the
27 expected quantities of CO₂ that would be consumed by these materials and the associated
28 uncertainty in calculation of the [MgO effective excess factor], it would increase the mean [MgO
29 effective excess factor] and possibly the ... uncertainty. The magnitude of these increases is not
30 known.

31 Brush and Roselle (2006, Section 6.4, p. 24) demonstrated

32 Dissolution of CO₂ in WIPP brines cannot consume significant quantities of CO₂ relative to the
33 quantity that would be produced by microbial consumption of all CPR materials in the repository.
34 This is because the solubility of CO₂ in brines is too low, and the volumes of brines that could
35 flow through the repository are too low to dissolve significant amounts of CO₂. The CO₂
36 solubility is too low because the brucite-magnesite or brucite-hydromagnesite carbonation
37 reactions will buffer f_{CO₂} at values of [1.26 × 10⁻⁷ or 3.16 × 10⁻⁶ atm], respectively.

38 For example, Brush and Roselle (2006, Section 6.4, p. 24) calculated that “the amounts of CO₂
39 dissolved in 10,011 m³ of GWB, 100,000 m³ of ERDA-6 brine, or 1,000,000 m³ of ERDA-6
40 brine are just 0.000318%, 0.00389%, and 0.0389%, respectively, of the total quantity of CO₂ that
41 would be produced by microbial consumption of all [of the] CPR materials in the repository.”
42 Therefore, Vugrin, Nemer, and Wagner (2006, Section 6.3, p. 32) “assume[d] that no CO₂ is
43 consumed by dissolution in brine.”

1 Brush et al. (2006, Section 6.5, p. 24) stated

2 Some of the organic C in CPR materials would be sequestered in biomass (cellular material)
3 instead of being oxidized to CO₂ if significant microbial consumption of these materials occurs in
4 the WIPP. However, it would be difficult to predict defensibly how much C would be sequestered
5 in biomass.

6 Therefore, Vugrin, Nemer, and Wagner (2006, Section 6.4, p. 32) concluded

7 Because the uncertainty in the quantity of organic [C] that might be sequestered in biomass cannot
8 presently be quantified, this analysis will conservatively assume that no organic [C] in CPR
9 materials will be incorporated into biomass. If it [were] possible to quantify this uncertainty and
10 the uncertainty was included in calculation of the [MgO effective excess factor], it would have the
11 impact of increasing the mean [MgO effective excess factor] and increasing the standard
12 deviation. The magnitudes of these changes are not known.

13 **MgO-6.2.4.4 Conclusions Regarding the Uncertainties Related to the MgO Excess** 14 **Factor**

15 Vugrin, Nemer, and Wagner (2006, Section 7) used the mean values and standard deviations of
16 the uncertainties that could be quantified (see above) to calculate an MgO effective excess factor
17 for an MgO excess factor of 1.2. They summarized the values of these parameters for the
18 uncertainties in the number of moles of CO₂ produced per mole of organic C in CPR materials,
19 the uncertainties in the quantity of MgO that will be available to consume CO₂, and the
20 uncertainties in the number of moles of CO₂ consumed per mole of available MgO in their Table
21 3, Table 4, and Table 5. Vugrin, Nemer, and Wagner (2006) summarized their calculation of the
22 MgO effective excess factor in their Equation 7-1 and provided details on their calculations of
23 the means and uncertainties (standard deviations) for their random variables and the MgO
24 effective excess factor in Appendix C of their report.

25 Vugrin, Nemer, and Wagner (2006, Section 7.1, pp. 35-36) calculated that, for an MgO excess
26 factor of 1.2, the MgO effective excess factor has a mean value of 1.60 and that the uncertainty
27 (standard deviation) is 0.0819. Based on the assumption that the distribution of the effective
28 excess factor is lognormal, Vugrin, Nemer, and Wagner (2006, Section 7.1, p. 36) calculated

29 [T]here is a 3×10^{-5} probability that the [MgO effective excess factor] will be less than 1.30
30 (Table 7), which is 30% higher than the minimum [MgO effective excess factor] required to
31 maintain chemical conditions assumed in PA. Furthermore, there is only a 10^{-19} probability that
32 the [MgO effective excess factor] will be less than 1.01.

33 As long as the MgO effective excess factor is greater than or equal to 1.00, there would be
34 enough MgO present in WIPP disposal rooms to consume all the CO₂ produced by complete
35 consumption of all of the CPR materials in the repository.

36 **MgO-6.2.4.5 Revision of the DOE's Assessment of the Uncertainties Related to the MgO** 37 **Excess Factor**

38 Vugrin, Nemer, and Wagner (2007) revised the uncertainties used by Vugrin, Nemer, and
39 Wagner (2006) because of EPA-mandated changes to the PA technical baseline for the CRA-
40 2004 PABC. Vugrin, Nemer, and Wagner (2007) (1) changed the overall yield for microbial

1 consumption of all of the CPR materials in the repository from 0.715 mol of CO₂ per mol of
2 organic C, with a standard deviation of 0.0158 mol of CO₂ per mol of organic C, to a constant
3 value of 1 mol of CO₂ per mol of organic C; and (2) changed the assumption that carbonation of
4 brucite will consume 1 mol of CO₂ per mol of MgO, consistent with conversion of all of the
5 hydromagnesite (5424) in WIPP disposal rooms to magnesite, and introduced a random variable
6 with a uniform distribution between 0.8 and 1 mol of CO₂ per mol of MgO, consistent with an
7 equal likelihood of forming hydromagnesite (5424) or magnesite.

8 Vugrin, Nemer, and Wagner (2006, Section 5.2.3, pp. 51-52) combined the yields for each step
9 of the possible microbial consumption of CPR materials in the repository and obtained an overall
10 yield of 0.715 mol of CO₂ per mol of organic C, with a standard deviation of 0.016 mol of CO₂
11 per mol of organic C (see the discussion above of the uncertainties in the number of moles of
12 CO₂ produced per mole of organic C in CPR materials). Vugrin et al. (2007, Section 4.2.3,
13 p. 13) changed the overall yield from 0.715 mol of CO₂ per mol of organic C, with a standard
14 deviation of 0.016 mol of CO₂ per mol of organic C, to a constant value of 1 because

15 [T]he current PA technical baseline (established by the CRA-2004 PABC) includes only
16 denitrification and [SO₄²⁻] reduction as microbial [respiratory] pathways for the consumption of
17 organic [C]. Methanogenesis was not included in the CRA-2004 PABC. The current baseline
18 also does not include consumption of CO₂ by [Mg] in Salado brines or by precipitation of CaCO₃-
19 bearing minerals. Consequently, the effective CO₂ yield corresponding to the baseline
20 assumptions is 1 mol of CO₂ per mol of consumed organic [C]. This value represents the
21 maximum yield that could occur.

22 Because of the complexity involved with quantifying the uncertainty in the effective CO₂ yield,
23 this analysis will model the yield in a conservative manner consistent with the CRA 2004 PABC.
24 That is, it will be assumed that:

- 25 (1) Denitrification and [SO₄²⁻] reduction [would be] the only microbial [respiratory]
26 pathways or the consumption of organic [C].
- 27 (2) Methanogenesis [would not] occur.
- 28 (3) No CO₂ [would be] consumed by precipitation of CaCO₃-bearing minerals.
- 29 (4) No CO₂ [would be] consumed by [Mg] in Salado brines.

30 Consequently, this analysis will assume that the effective CO₂ yield is 1 mol of CO₂ per mol of
31 consumed organic [C]. This value represents the maximum effective yield that could occur, so
32 modeling the yield in this manner is conservative. The variable y_{yield} represents the effective CO₂
33 yield in this analysis, and it will be assigned a constant value of 1 mol of CO₂ per mol of
34 consumed organic [C]. If it [were] possible to quantify this uncertainty and the uncertainty [were]
35 included in [the] calculation of the [MgO effective excess factor], it would have the impact of
36 increasing the mean [effective excess factor] and increasing the standard deviation.

37 Vugrin, Nemer, and Wagner (2006, Table 5, p. 35) also assumed that carbonation of brucite will
38 consume 1 mol of CO₂ per mol of MgO, consistent with conversion of all of the hydromagnesite
39 (5424) in WIPP disposal rooms to magnesite (Reaction MgO.9 in Section MgO-4.2.2). They
40 based this assumption on the review by Brush and Roselle (2006, Section 4.1, Section 5.2, and
41 Section 5.3) of laboratory studies carried out for the WIPP project, laboratory studies carried out
42 for other applications, and studies of anthropogenic and natural analogs. However, Vugrin,

1 Nemer, and Wagner (2007, Section 6.1, p. 22) abandoned this assumption and introduced a
2 random variable:

3 As noted above, there is some uncertainty in the length of time required for hydromagnesite to
4 convert to magnesite. Thus, this analysis includes an approach that does not require the rate of
5 magnesite formation to model the uncertainty in the moles of CO₂ consumed per mol of MgO.
6 Two bounding scenarios are considered for modeling purposes:

7 **Scenario 1.** No hydromagnesite converts to magnesite. In this scenario, each
8 mol of MgO can consume 0.8 mol of CO₂, and this value represents the lower
9 bound for the moles of CO₂ sequestered per mol of MgO.

10 **Scenario 2:** All hydromagnesite converts to magnesite. In this scenario, each
11 mol of MgO can consume 1 mol of CO₂, and this value represents the upper
12 bound for the moles of CO₂ sequestered per mol of MgO.

13 For the [MgO effective excess factor] calculation, the moles of CO₂ sequestered per mol of MgO
14 are modeled as a random variable with a uniform distribution on [0.8,1]. Representing the
15 quantity in this manner incorporates the lower and upper bounds associated with Scenarios 1 and 2
16 and maximizes the uncertainty since the distribution is not weighted towards any particular value
17 on [0.8,1].

18 Vugrin, Nemer, and Wagner (2007, Section 7) used the mean values and standard deviations of
19 the uncertainties that could be quantified to recalculate an MgO effective excess factor for an
20 MgO excess factor of 1.2. They summarized the values of these parameters for the uncertainties
21 in the number of moles of CO₂ produced per mole of organic C in CPR materials, the
22 uncertainties in the quantity of MgO that will be available to consume CO₂, and the uncertainties
23 in the number of moles of CO₂ consumed per mole of available MgO in their Table 2, Table 3,
24 and Table 4. Vugrin, Nemer, and Wagner (2007) summarized their calculation of the MgO
25 effective excess factor in their Equation 7-1 and provided details on their calculations of the
26 means and uncertainties (standard deviations) for their random variables and the MgO effective
27 excess factor in their Appendix B.

28 Vugrin, Nemer, and Wagner (2007, Section 7.1, pp. 27-28) calculated that, for an MgO excess
29 factor of 1.2, the MgO effective excess factor has a mean value of 1.03 and the uncertainty
30 (standard deviation) is 0.072.

31 Because the MgO effective excess factor is greater than 1.00, there would be enough MgO
32 present in WIPP disposal rooms to consume all of the CO₂ produced by complete consumption
33 of all of the CPR materials in the repository.

34 **MgO-6.2.4.6 The EPA's Approval of the DOE's Planned Change Request to Reduce the** 35 **MgO Excess Factor from 1.67 to 1.2**

36 The EPA approved the reduction of the MgO excess factor to 1.2 in February 2008 (Reyes
37 2008). However, the EPA imposed two conditions in its approval letter (Reyes 2008, p. 1):

38 First, [the] DOE must continue to calculate and track both the [C] disposed and the required MgO
39 needed on a room-by-room basis. Second, [the] DOE must annually verify the reactivity of MgO
40 and ensure that it is maintained at 96 [mol] % as assumed in [the] DOE's supporting
41 documentation. These conditions ensure that the WIPP will continue to meet the assurance
42 requirements in our radioactive waste disposal regulations.

1 The EPA's approval (Reyes 2008, p. 1) went on to state

2 As a result of this evaluation, it is our opinion that further reductions in the MgO safety factor are
3 not warranted given the current state of knowledge. We believe that reducing the safety factor
4 below 1.2, based on our current understanding of the disposal system, would not be sufficient to
5 comply with the assurance requirement that MgO is intended to address.

6 The EPA (U.S. Environmental Protection Agency 2008) summarized its review of the DOE's
7 PCR for a reduction in the MgO excess factor from 1.67 to 1.2. SCA (2008) carried out a
8 detailed review of the uncertainties related to the use of MgO as the engineered barrier in the
9 WIPP. Langmuir (2007) reviewed the results of the analysis published by SCA (2008), and SCA
10 (2007) responded to this review. Finally, PECOS Management Services, Inc. reviewed the use
11 of MgO as an engineered barrier, and concluded that reducing the MgO excess factor from 1.67
12 to 1.2 would be appropriate and that the excess factor could be reduced even more (PMS 2007).
13 Langmuir (2007), PMS (PECOS Management Services, Inc. 2007), SCA (S. Cohen and
14 Associates 2007), SCA (S. Cohen and Associates 2008), and U.S. Environmental Protection
15 Agency (2008) were all included in Reyes (2008) as attachments.

1 **MgO-7.0 References**

- 2 Adams, J.E. 1944. "Upper Permian Ochoa Series of Delaware Basin, West Texas and
3 Southeastern New Mexico." *American Association of Petroleum Geologists Bulletin*, vol. 28:
4 1596-1625.
- 5 Asghari, A., and S.R. Farrah. 1993. "Inactivation of Bacteria by Solids Coated with Magnesium
6 Peroxide," *Journal of Environmental Science and Health*, vol. A28: 779-93.
- 7 Babb, S.C., and C.F. Novak. 1995. *User's Manual for FMT, Version 2.0*. ERMS 228119.
8 Albuquerque: Sandia National Laboratories, WIPP Performance Assessment.
- 9 Babb, S.C., and C.F. Novak. 1997. *User's Manual for FMT Version 2.3: A Computer Code
10 Employing the Pitzer Activity Coefficient Formalism for Calculating Thermodynamic
11 Equilibrium in Geochemical Systems to High Electrolyte Concentrations*. ERMS 243037.
12 Albuquerque: Sandia National Laboratories, WIPP Performance Assessment.
- 13 Bates, R.L., and J.A. Jackson, eds. 1984. *Dictionary of Geological Terms*. 3rd ed. New York:
14 Anchor-Doubleday.
- 15 Berner, R.A. 1980. *Early Diagenesis: A Theoretical Approach*. Princeton: Princeton UP.
- 16 Brush, L.H. 1990. *Test Plan for Laboratory and Modeling Studies of Repository and
17 Radionuclide Chemistry for the Waste Isolation Pilot Plant*. SAND90-0266. ERMS 226015.
18 Albuquerque: Sandia National Laboratories.
- 19 Brush, L.H. 1995. *Systems Prioritization Method—Iteration 2 Baseline Position Paper: Gas
20 Generation in the Waste Isolation Pilot Plant* (March 17). ERMS 228740. Albuquerque:
21 Sandia National Laboratories.
- 22 Brush, L.H. 1996. Memorandum to M.S. Tierney (Subject: Ranges and Probability
23 Distributions of K_d s for Dissolved Pu, Am, U, Th, and Np in the Culebra for the PA Calculations
24 to Support the CCA). 10 June 1996. ERMS 238801. U.S. Department of Energy, Sandia
25 National Laboratories, Albuquerque, NM.
- 26 Brush, L.H. 2004. *Implications of New (Post-CCA) Information for the Probability of
27 Significant Microbial Activity in the WIPP* (July 28). ERMS 536205. Carlsbad, NM: Sandia
28 National Laboratories.
- 29 Brush, L.H. 2005. *Results of Calculations of Actinide Solubilities for the WIPP
30 Performance Assessment Baseline Calculations* (May 18). ERMS 539800. Carlsbad, NM:
31 Sandia National Laboratories.
- 32 Brush, L.H., R.C. Moore, and N.A. Wall. 2001. *Response to EEG-77, Plutonium Chemistry
33 under Conditions Relevant for WIPP Performance Assessment: Review of Experimental Results
34 and Recommendations for Future Work, by V.M. Oversby* (March 15). ERMS 517373.
35 Albuquerque: Sandia National Laboratories.

- 1 Brush, L.H., and G.T. Roselle. 2006. Memorandum to E.D. Vugrin (Subject: Geochemical
2 Information for Calculation of the MgO Effective Excess Factor). 17 November 2006. ERMS
3 544840. U.S. Department of Energy, Sandia National Laboratories, Carlsbad, NM.
- 4 Brush, L.H., and L.J. Storz. 1996. Memorandum to M.S. Tierney (Subject: Revised Ranges and
5 Probability Distributions of K_{ds} for Dissolved Pu, Am, U, Th, and Np in the Culebra for the PA
6 Calculations to Support the CCA). 24 July 1996. ERMS 238231. U.S. Department of Energy,
7 Sandia National Laboratories, Albuquerque, NM.
- 8 Brush, L.H., and Y. Xiong. 2003a. *Calculation of Actinide Solubilities for the WIPP*
9 *Compliance Recertification Application* (May 8). ERMS 529131. Carlsbad, NM: Sandia
10 National Laboratories.
- 11 Brush, L.H., and Y. Xiong. 2003b. *Calculation of Actinide Solubilities for the WIPP*
12 *Compliance Recertification Application* (March 20). AP-098. ERMS 526862. Carlsbad, NM:
13 Sandia National Laboratories.
- 14 Brush, L.H., and Y. Xiong. 2003c. *Calculation of Actinide Solubilities for the WIPP*
15 *Compliance Recertification Application* (Rev. 1). AP 098. ERMS 527714. Carlsbad, NM:
16 Sandia National Laboratories.
- 17 Brush, L.H., and Y. Xiong. 2003d. *Calculation of Organic Ligand Concentrations for the WIPP*
18 *Compliance Recertification Application*. ERMS 527567. Carlsbad, NM: Sandia National
19 Laboratories.
- 20 Brush, L.H., and Y. Xiong, 2005a. *Calculation of Actinide Solubilities for the WIPP*
21 *Performance-Assessment Baseline Calculations* (Rev 0, April 4). AP-120. ERMS 539255.
22 Carlsbad, NM: Sandia National Laboratories.
- 23 Brush, L.H., and Y. Xiong, 2005b. *Calculation of Organic-Ligand Concentrations for the WIPP*
24 *Performance-Assessment Baseline Calculations* (May 4). ERMS 539635. Carlsbad, NM:
25 Sandia National Laboratories.
- 26 Brush, L.H., Y. Xiong, J.W. Garner, A. Ismail, and G.T. Roselle. 2006. *Consumption of Carbon*
27 *Dioxide by Precipitation of Carbonate Minerals Resulting from Dissolution of Sulfate Minerals*
28 *in the Salado Formation in Response to Microbial Sulfate Reduction in the WIPP*. ERMS
29 544785. Carlsbad, NM: Sandia National Laboratories.
- 30 Bryan, C.R., and A.C. Snider. 2001a. "MgO Hydration and Carbonation at SNL/Carlsbad."
31 *Sandia National Laboratories Technical Baseline Reports; WBS 1.3.5.4, Repository*
32 *Investigations; Milestone RI010; January 31, 2001* (pp. 66–83). ERMS 516749. Carlsbad, NM:
33 Sandia National Laboratories.
- 34 Bryan, C.R., and A.C. Snider. 2001b. "MgO Experimental Work Conducted at SNL/CB:
35 Continuing Investigations with Premier Chemicals MgO." *Sandia National Laboratories*
36 *Technical Baseline Reports; WBS 1.3.5.4, Repository Investigations; Milestone RI020; July 31,*
37 *2001* (pp. 5-1 through 5-15). ERMS 518970. Carlsbad, NM: Sandia National Laboratories.

- 1 Chapelle, F.H. 1993. *Ground-Water Microbiology and Geochemistry*. New York: Wiley.
- 2 Chapman, M.A.S., J. Abercrombie, D.M. Livermore, and N.S. Williams. 1995. “Antibacterial
3 Activity of Bowel-Cleansing Agents: Implications of Antibacteroides Activity of Senna.”
4 *British Journal of Surgery*, vol. 82: 1053.
- 5 Choppin, G.R. 1988. “Humic and Radionuclide Migration.” *Radiochimica Acta*, vol. 44/45:
6 23–28.
- 7 Clayton, D.J., and M.B. Nemer. 2006. Memorandum to E.D. Vugrin (Subject: Normalized
8 Moles of Castile Sulfate Entering the Repository and Fraction of MgO Lost Due to Brine Flow
9 Out of the Repository). 9 October 2006. ERMS 544385. U.S. Department of Energy,
10 Sandia National Laboratories, Carlsbad, NM.
- 11 Cotsworth, E. 2005. Letter to I. Triay (1 Enclosure). 4 March 2005. ERMS 538858. U.S.
12 Environmental Protection Agency, Office of Radiation and Indoor Air, Washington, DC.
- 13 Crawford, B.A. 2005a. *Determination of Waste Stream Oxyanions using TWBID Revision 2.1,*
14 *Version 3.13, Data Version 4.15* (February 24). ERMS 538811. Carlsbad, NM: Los Alamos
15 National Laboratory.
- 16 Crawford, B.A. 2005b. *Waste Material Densities in TRU Waste Streams from TWBID Revision*
17 *2.1, Version 3.13, Data Version D.4.15* (April 13). ERMS 539323. Carlsbad, NM: Los Alamos
18 National Laboratory.
- 19 Criddle, C.S., L.A. Alvarez, and P.L. McCarty. 1991. “Microbial Processes in Porous Media.”
20 *Transport Processes in Porous Media* (pp. 639–91) eds. J. Bear and M.Y. Corapcioglu.
21 Amsterdam: Kluwer.
- 22 Daveler, S.A., and T.J. Wolery. 1992. *EQPT, A Data File Preprocessor for the EQ3/6 Software*
23 *Package: User’s Guide and Related Documentation* (Version 7.0). UCRL-MA-110662 PT II.
24 Livermore, CA: Lawrence Livermore National Laboratory.
- 25 Deal, D.E., R.J. Abitz, D.S. Belski, J.B. Case, M.E. Crawley, R.M. Deshler, P.E. Drez,
26 C.A. Givens, R.B. King, B.A. Lauctes, J. Myers, S. Niou, J.M. Pietz, W.M. Roggenthen, J.R.
27 Tyburski, and M.G. Wallace. 1989. *Brine Sampling and Evaluation Program 1988 Report*.
28 DOE-WIPP-89-015. Carlsbad, NM: U.S. Department of Energy, WIPP Project Office.
- 29 Deng, H., S.R. Johnsen, G.T. Roselle, and M.B. Nemer. 2006. *Analysis of Martin Marietta*
30 *MagChem 10 WTS-60 MgO* (November 14). ERMS 544712. Carlsbad, NM: Sandia National
31 Laboratories.
- 32 Deng, H., M.B. Nemer, and Y. Xiong. 2006. *Experimental Study of MgO Reaction Pathways*
33 *and Kinetics* (Rev. 0, June 6). TP 06-03. ERMS 543633. Carlsbad, NM: Sandia National
34 Laboratories.

- 1 Deng, H., M.B. Nemer, and Y. Xiong. 2007. *Experimental Study of MgO Reaction Pathways*
2 *and Kinetics* (Rev. 1, January 10). TP 06-03. ERMS 545182. Carlsbad, NM: Sandia National
3 Laboratories.
- 4 Deng, H., Y. Xiong, and M.B. Nemer. 2007. *Experimental Work Conducted on MgO*
5 *Characterization and Hydration, Milestone Report*. ERMS 546570. Carlsbad, NM: Sandia
6 National Laboratories.
- 7 Dials, G. 1997. Letter to R. Trovato (Enclosure: Fifth Set of Responses to the Letter of Nichols
8 1996). 7 March 1997. Carlsbad, NM: U.S. Department of Energy, Carlsbad Area Office.
- 9 Fenchel, T., G.M. King, and T.H. Blackburn. 2000. *Bacterial Biogeochemistry: The*
10 *Ecophysiology of Mineral Cycling*. 2nd ed. San Diego: Academic.
- 11 Fernández, A.I., J.M. Chimenos, M. Segarra, M.A. Fernández, and F. Espiell. 1999. “Kinetic
12 Study of Carbonation of MgO Slurries.” *Hydrometallurgy*, vol. 53: 155-67.
- 13 Fernández-Díaz, L., A. Putnis, M. Prieto, and C.V. Putnis. 1996. “The Role of Magnesium in
14 the Crystallization of Calcite and Aragonite in a Porous Medium.” *Journal of Sedimentary*
15 *Research*, vol. 66, no. 3: 482-91.
- 16 Francis, A.J., and J.B. Gillow. 1994. *Effect of Microbial Processes on Gas Generation under*
17 *Expected Waste Isolation Pilot Plant Repository Conditions: Progress Report through 1992*.
18 SAND93-7036. Albuquerque: Sandia National Laboratories.
- 19 Francis, A.J., and J.B. Gillow. 2000. Memorandum to Y. Wang (Subject: Progress Report:
20 Microbial Gas Generation Program). 6 January 2000. ERMS 509352. Brookhaven National
21 Laboratory, Upton, NY.
- 22 Francis, A.J., J.B. Gillow, and M.R. Giles. 1997. *Microbial Gas Generation under Expected*
23 *Waste Isolation Pilot Plant Repository Conditions*. SAND96-2582. Albuquerque: Sandia
24 National Laboratories.
- 25 Froelich, P.N., G.P. Klinkhammer, M.L. Bender, N.A. Luedtke, G.R. Heath, D. Cullen,
26 P. Dauphin, D. Hammond, B. Hartman, and V. Maynard. 1979. “Early Oxidation of Organic
27 Matter in Pelagic Sediments of the Eastern Equatorial Atlantic: Suboxic Diagenesis.”
28 *Geochimica et Cosmochimica Acta*, vol. 43: 1075–90.
- 29 Garber, R.A., P.M. Harris, and J.M. Borer. 1990. “Occurrence and Significance of Magnesite in
30 Upper Permian (Guadalupian) Tansil and Yates Formations, Delaware Basin, New Mexico.”
31 *American Association of Petroleum Geologists Bulletin*, vol. 74, no. 2: 119-34.
- 32 Gillow, J.B., and A.J. Francis. 2001a. “Re-Evaluation of Microbial Gas Generation under
33 Expected Waste Isolation Pilot Plant Conditions: Data Summary Report, January 24, 2001.”
34 *Sandia National Laboratories Technical Baseline Reports; WBS 1.3.5.4, Repository*
35 *Investigations; Milestone RI010; January 31, 2001* (pp. 19–46). ERMS 516749. Carlsbad, NM:
36 Sandia National Laboratories.

- 1 Gillow, J.B., and A.J. Francis. 2001b. “Re-Evaluation of Microbial Gas Generation under
 2 Expected Waste Isolation Pilot Plant Conditions: Data Summary and Progress Report (February
 3 1–July 13, 2001), July 16, 2001, Rev. 0.” *Sandia National Laboratories Technical Baseline
 4 Reports; WBS 1.3.5.4, Repository Investigations; Milestone R1020; July 31, 2001* (pp. 3-
 5 1 through 3-21). ERMS 518970. Carlsbad, NM: Sandia National Laboratories.
- 6 Gillow, J.B., and A.J. Francis. 2002a. “Re-Evaluation of Microbial Gas Generation under
 7 Expected Waste Isolation Pilot Plant Conditions: Data Summary and Progress Report (July 14,
 8 2001–January 31, 2002), January 22, 2002.” *Sandia National Laboratories Technical Baseline
 9 Reports; WBS 1.3.5.3, Compliance Monitoring; WBS 1.3.5.4, Repository Investigations;
 10 Milestone R1110; January 31, 2002* (pp. 2.1-1 through 2.1-26). ERMS 520467. Carlsbad, NM:
 11 Sandia National Laboratories.
- 12 Gillow, J.B., and A.J. Francis. 2002b. “Re-Evaluation of Microbial Gas Generation under
 13 Expected Waste Isolation Pilot Plant Conditions: Data Summary and Progress Report (February
 14 1–July 15, 2002), July 18, 2002.” *Sandia National Laboratories Technical Baseline Reports;
 15 WBS 1.3.5.3, Compliance Monitoring; WBS 1.3.5.4, Repository Investigations; Milestone R1130;
 16 July 31, 2002* (pp. 3.1-1 through 3.1-A10). ERMS 523189. Carlsbad, NM: Sandia National
 17 Laboratories.
- 18 Gillow, J.B., and A.J. Francis. 2003. *Microbial Gas Generation under Expected Waste Isolation
 19 Pilot Plant Repository Conditions* (Rev. 0, October 6) ERMS 532877. Upton, NY: Brookhaven
 20 National Laboratory.
- 21 Gitlin, B.C. 2006. Letter to D.C. Moody. 28 April 2006. ERMS 543319. U.S. Environmental
 22 Protection Agency, Office of Radiation and Indoor Air, Washington, DC.
- 23 Gradstein, F.M., J.G. Ogg, and A.G. Smith, eds. 2005. *A Geologic Timescale 2004*.
 24 Cambridge: Cambridge UP.
- 25 Hansen, C.W., L.H. Brush, M.B. Gross, F.D. Hansen, B., Y. Park, J.S. Stein, and
 26 T.W. Thompson. 2004. *Effects of Supercompacted Waste and Heterogeneous Waste
 27 Emplacement on Repository Performance, Rev. 2* (January 19). ERMS 533551. Carlsbad, NM:
 28 Sandia National Laboratories.
- 29 Hansen, C.W., and C.D. Leigh. 2003. *A Reconciliation of the CCA and the PAVT Parameter
 30 Baselines* (Rev. 3, April 30). ERMS 528582. Carlsbad, NM: Sandia National Laboratories.
- 31 Hansen, F.D. 2005. Memorandum to D.S. Kessel (Subject: Magnesium Oxide Super Sack
 32 Rupture under WIPP Conditions). 11 May 2005. ERMS 539724. Sandia National Laboratories,
 33 Carlsbad, NM.
- 34 Hazen, R.M., and E. Roedder. 2001. “How Old Are Bacteria from the Permian Age?” *Nature*,
 35 vol. 411: 155.
- 36 Hunter, K.S., Y. Wang, and P. Van Cappellan. 1998. “Kinetic Modeling of Microbially Driven
 37 Redox Chemistry of Subsurface Environments: Coupling, Transport, Microbial Metabolism, and
 38 Geochemistry.” *Journal of Hydrology*, vol. 209: 53–80.

- 1 Institute for Regulatory Science (RSI). 2006. *Application of Magnesium Oxide as an*
2 *Engineered Barrier at [the] Waste Isolation Pilot Plant—Report of the Expert Panel* (February
3 21). RSI-06-01. Alexandria, VA: Institute for Regulatory Science.
- 4 Institute for Regulatory Science (RSI). 2008. “About Us—Functional Statement.”
5 <<http://www.nars.org/aboutfunc-frame.htm>> 19 April 2008.
- 6 Kanney, J.F., A.C. Snider, T.W. Thompson, and L.H. Brush. 2004. *Effect of Naturally*
7 *Occurring Sulfate on the MgO Safety Factor in the Presence of Supercompacted Waste and*
8 *Heterogeneous Waste Emplacement* (March 5). ERMS 534150. Carlsbad, NM: Sandia
9 National Laboratories.
- 10 Kanney, J.F., and E.D. Vugrin. 2006. Memorandum to D.S. Kessel (Subject: Updated Analysis
11 of Characteristic Time and Length Scales for Mixing Processes in the WIPP Repository to
12 Reflect the CRA-2004 PABC Technical Baseline and the Impact of Supercompacted Mixed
13 Waste and Heterogeneous Waste Emplacement). 31 August 2006. ERMS 544248. U.S.
14 Department of Energy, Sandia National Laboratories, Carlsbad, NM.
- 15 Kirchner, T.B., and E.D. Vugrin. 2006. Memorandum to D.S. Kessel (Subject: Uncertainty in
16 Cellulose, Plastic, and Rubber Measurements for the Waste Isolation Pilot Plant Inventory). 12
17 June 2006. ERMS 543848. U.S. Department of Energy, Sandia National Laboratories,
18 Carlsbad, NM.
- 19 Koper, O.B., J.S. Klabunde, G.L. Marchin, K.J. Klabunde, P. Stoimenov, and L. Bohra. 2002.
20 “Nanoscale Powders and Formulations with Biocidal Activity toward Species and Vegetative
21 Cells of *Bacillus* Species, Viruses, and Toxins.” *Current Microbiology*, vol. 44: 49-55.
- 22 Krumhansl, J.L., J.W. Kelly, H.W. Papenguth, and R.V. Bynum. 1997. Memorandum to E.J.
23 Nowak (Subject: MgO Acceptance Criteria). 10 December 1997. ERMS 248997. U.S.
24 Department of Energy, Sandia National Laboratories, Albuquerque, NM.
- 25 Krumhansl, J.L., K.M. Kimball, and C.L. Stein. 1991. *Intergranular Fluid Compositions from*
26 *the Waste Isolation Pilot Plant (WIPP), Southeastern New Mexico*. SAND90-0584.
27 Albuquerque: Sandia National Laboratories.
- 28 Lang, W.B. 1939. “Salado Formation of the Permian Basin.” *American Association of*
29 *Petroleum Geologists Bulletin*, vol. 23: 1569–72.
- 30 Langmuir, D. 2007. Memorandum to S.L. Ostrow (Subject: Letter Report Review of the
31 SC&A Draft Report “Review of MgO-Related Uncertainties in the Waste Isolation Pilot Plant”).
32 4 November 2007. Hydrochem Systems Corporation, Silverthorne, CO.
- 33 Leigh, C.D. 2003. *Estimate of Cellulosics, Plastics, and Rubbers in a Single Panel in the WIPP*
34 *Repository in Support of AP-107* (Supersedes ERMS 530959) (September 4). ERMS 531324.
35 Carlsbad, NM: Sandia National Laboratories.
- 36 Leigh, C.D. 2004a. Memorandum to Record (Subject: Waste Parameters for a Single Panel
37 Assuming a 50/50 Volume Split between INEEL Supercompacted Waste and Waste from Other

- 1 Sites, Rev. 1). 26 February 2004. ERMS 534016. U.S. Department of Energy, Sandia National
2 Laboratories, Carlsbad, NM.
- 3 Leigh, C.D. 2004b. Memorandum to Record (Subject: Waste Parameters for an Alternative
4 TDOP Loading Assumption in the AMW Analysis, Rev. 1). 26 February 2004. ERMS 534017.
5 U.S. Department of Energy, Sandia National Laboratories, Carlsbad, NM.
- 6 Leigh, C., J. Kanney, L. Brush, J. Garner, G. Kirkes, T. Lowry, M. Nemer, J. Stein, E. Vugrin, S.
7 Wagner, and T. Kirchner. 2005. *2004 Compliance Recertification Application Performance*
8 *Assessment Baseline Calculation* (Revision 0). ERMS 541521. Carlsbad, NM: Sandia National
9 Laboratories.
- 10 Leigh, C.D., and J.R. Trone. 2005. *Calculation of the Waste Unit Factor for the Performance*
11 *Assessment Baseline Calculation* (Rev. 0, May 3). ERMS 539613. Carlsbad, NM: Sandia
12 National Laboratories.
- 13 Li, Y.H., and S. Gregory. 1974. "Diffusion of Ions in Sea Water and in Deep Sea Sediments."
14 *Geochimica et Cosmochimica Acta*, vol. 33, no. 5: 703-14.
- 15 Lowenstein, T.K. 1983. "Deposition and Alteration of an Ancient Potash Evaporite: The
16 Permian Salado Formation of New Mexico and West Texas." Ph.D. Dissertation. Baltimore:
17 The Johns Hopkins University.
- 18 Lowenstein, T.K. 1988. "Origin of Depositional Cycles in a Permian 'Saline Giant': The
19 Salado (McNutt Zone) Evaporites of New Mexico and Texas." *Geological Society of America*
20 *Bulletin*, vol. 100: 592-608.
- 21 Marcinowski, F. 2001. Letter to I.R. Triay (1 Enclosure). 11 January 2001. ERMS 519362.
22 U.S. Environmental Protection Agency, Radiation Protection Division, Washington, DC.
- 23 Marcinowski, F. 2004. Letter to R.P. Detwiler (Subject: Approving the DOE's Request to
24 Dispose of Compressed (Supercompacted) Waste from the Advanced Mixed Waste Treatment
25 Program in the WIPP). 26 March 2004. ERMS 534327. U.S. Environmental Protection
26 Agency, Office of Air and Radiation, Washington, DC.
- 27 Martin Marietta Magnesia Specialties. 2006. "Everything You Ever Wanted to Know About
28 Magnesium Oxide." <<http://www.magspecialties.com/students.htm>> 14 November 2006.
29 ERMS 544711.
- 30 Meldrum, F.C., and S.T. Hyde. 2001. "Morphological Influence of Magnesium and Organic
31 Additives on the Precipitation of Calcite." *Journal of Crystal Growth*, vol. 231: 544-58.
- 32 Molecke, M.A. 1983. *A Comparison of Brines Relevant to Nuclear Waste Experimentation*.
33 SAND83-0516. Albuquerque: Sandia National Laboratories.
- 34 Moody, D.C. 2006. Letter to E.A. Cotsworth (Subject: Transmittal of Planned Change
35 Request; 1 Enclosure). 10 April 2006. ERMS 543262. U.S. Department of Energy, Carlsbad
36 Field Office, Carlsbad, NM.

- 1 Morse, J.W. 1983. "The Kinetics of Calcium Carbonate Dissolution and Precipitation."
2 *Carbonates: Mineralogy and Chemistry*. Ed. R.J. Reeder. Blacksburg, VA: Mineralogical
3 Society of America. *Reviews in Mineralogy*, vol. 11, 227-64.
- 4 Munson, D.E., R.L. Jones, D.L. Hoag, and J.R. Ball. 1987. *Heated Axisymmetric Pillar Test*
5 *(Room H): In Situ Data Report (February, 1985 - April, 1987), Waste Isolation Pilot Plant*
6 *(WIPP) Thermal/Structural Interactions Program*. SAND87-2488. Albuquerque: Sandia
7 National Laboratories.
- 8 National Research Council (NRC) Committee on the Waste Isolation Pilot Plant. 1996. *The*
9 *Waste Isolation Pilot Plant: A Potential Solution for the Disposal of Transuranic Waste*.
10 Washington, DC: National Academy Press.
- 11 National Research Council (NRC) Committee on the Waste Isolation Pilot Plant. 2001.
12 *Improving Operations and Long-Term Safety of the Waste Isolation Pilot Plant, Final Report*.
13 Washington, DC: National Academy Press.
- 14 Nemer, M.B. 2006. Memorandum to the SNL/WIPP Records Center (Subject: Expected Brine
15 volumes, Cumulative Brine Inflow, and MgO-to-Brine Solid-to-Liquid Ratio from PABC
16 BRAGFLO Results). 3 March 2006. ERMS 542612. Carlsbad, NM: Sandia National
17 Laboratories.
- 18 Nemer, M.B. and J.S. Stein. 2005. *Analysis Package for BRAGFLO: 2004 Compliance*
19 *Recertification Application Performance Assessment Baseline Calculation* (June 28). ERMS
20 540527. Carlsbad, NM: Sandia National Laboratories.
- 21 Nichols, M. 1996. Letter to A. Alm (1 Enclosure). 19 December 1996. U.S. Environmental
22 Protection Agency, Office of Radiation and Indoor Air, Washington, DC.
- 23 Novak, C.F. 1997. Memorandum to R.V. Bynum (Subject: Calculation of Actinide Solubilities
24 in WIPP SPC and ERDA-6 Brines under MgO Backfill Scenarios Containing either
25 Nesquehonite or Hydromagnesite as the Mg-CO₃ Solubility-Limiting Phase). 21 April 1997.
26 ERMS 246124. Albuquerque, NM: Sandia National Laboratories.
- 27 Novak, C.F., R.C. Moore, and R.V. Bynum. 1996. *Prediction of Dissolved Actinide*
28 *Concentrations in Concentrated Electrolyte Solutions: A Conceptual Model and Model Results*
29 *for the Waste Isolation Pilot Plant (WIPP)*. SAND96-2695C. ERMS 238628. Presentation at
30 the 1996 International Conference on Deep Geological Disposal of Radioactive Waste,
31 September 16–19, 1996, Winnipeg, Manitoba.
- 32 Oversby, V.M. 2000. *Plutonium Chemistry under Conditions Relevant for WIPP Performance*
33 *Assessment: Review of Experimental Results and Recommendations for Future Work*. EEG-77.
34 Albuquerque: Environmental Evaluation Group.
- 35 Papenguth, H.W. 1999. Memorandum to M.G. Marietta (Subject: Evaluation of Candidate
36 MgO Materials for Use as Backfill at WIPP). 12 November 1999. ERMS 520314. U.S.
37 Department of Energy, Sandia National Laboratories, Albuquerque, NM.

- 1 Parkes, R.J. 2000. "A Case of Bacterial Immortality?" *Nature*, vol. 407: 844–45.
- 2 Peterson, A.C. 1996. *Mass of MgO That Could Be Added as Backfill in the WIPP and the Mass*
3 *of MgO Required to Saturate the Brine and React with the CO₂ Generated by Microbial*
4 *Processes* (March 11). ERMS 236214. Albuquerque: Sandia National Laboratories.
- 5 PECOS Management Services, Inc. (PMS). 2007. *Review of the DOE Request for Magnesium*
6 *Oxide Requirement Reduction*. Albuquerque, NM: PMS.
- 7 Popielak, R.S., R.L. Beauheim, S.R. Black, W.E. Coons, C.T. Ellingson, and R.L. Olsen. 1983.
8 *Brine Reservoirs in the Castile Formation, Waste Isolation Pilot Plant Project, Southeastern*
9 *New Mexico*. TME 3153. Carlsbad, NM: U.S. Department of Energy, WIPP Project Office.
- 10 Powers, D.W., R.H. Vreeland, and W.D. Rosenzweig. 2001. "Reply to 'How Old Are Bacteria
- 11 from the Permian Age?'" *Nature*, vol. 411: 155.
- 12 Reyes, J. 2008. Letter to D.C. Moody (5 Enclosures). 11 February 2008. U.S. Environmental
- 13 Protection Agency, Office of Air and Radiation, Washington, DC.
- 14 S. Cohen and Associates (SCA). 2006. *Preliminary Review of the Degradation of Cellulosic,*
15 *Plastic, and Rubber Materials in the Waste Isolation Pilot Plant, and Possible Effects on*
16 *Magnesium Oxide Safety Factor Calculations* (September 11). Vienna, VA: SCA.
- 17 S. Cohen and Associates (SCA). 2007. *Response to Comments by Langmuir (2007)* (December
- 18 1). Vienna, VA: SCA.
- 19 S. Cohen and Associates (SCA). 2008. *Review of MgO-Related Uncertainties in the Waste*
20 *Isolation Pilot Plant* (January 24). Vienna, VA: SCA.
- 21 Sandia National Laboratories (SNL). 1996. *Conceptual Models Information for the Peer*
22 *Review Panel* (May 13). ERMS 542940. Albuquerque: Sandia National Laboratories.
- 23 Sandia National Laboratories (SNL). 1997. *Chemical Conditions Model: Results of the MgO*
24 *Backfill Efficacy Investigation* (April 23). Unpublished report. ERMS 419794. Albuquerque:
25 Sandia National Laboratories.
- 26 Satterfield, C.L., T.K. Lowenstein, R.H. Vreeland, W.D. Rosenzweig, and D.W. Powers. 2005.
27 "New Evidence for 250 Ma Age of Halotolerant Bacterium from a Permian Salt Crystal."
28 *Geology*, vol. 33, no. 4: 265–68.
- 29 Sawai, J. 2003. "Quantitative Evaluation of Antibacterial Activities of Metallic Oxide Powders
30 (ZnO, MgO, CaO) by Conductimetric Assay." *Journal of Microbiological Methods*, vol. 54:
31 177–82.
- 32 Sawai, J., H. Igarashi, A. Hashimoto, T. Kokugan, and M. Shimizu. 1995a. "Evaluation of
33 Growth Inhibitory Effect of Ceramics Powder Slurry on Bacteria by Conductance Method."
34 *Journal of Chemical Engineering of Japan*, vol. 28: 288–93.

- 1 Sawai, J., H. Kojima, I. Saito, F. Kanou, H. Igarashi, A. Hashimoto, T. Kokugan, and
2 M. Shimizu. 1995b. "Mutagenecity Test of Ceramic Powder[s] Which Have Growth Inhibitory
3 Effect on Bacteria." *Journal of Chemical Engineering of Japan*, vol. 28: 352–54.
- 4 Sawai, J., H. Igarashi, A. Hashimoto, T. Kokugan, and M. Shimizu. 1996. "Effect of Particle
5 Size and Heating Temperature of Ceramic Powders on Antibacterial Activity of Their Slurry."
6 *Journal of Chemical Engineering of Japan*, vol. 29: 288–93.
- 7 Sawai, J., H. Kojima, H. Igarashi, A. Hashimoto, S. Shoji, T. Sawaki, A. Hakoda, E. Kawada,
8 T. Kokugan, and M. Shimizu. 2000a. "Antibacterial Characteristics of Magnesium Oxide
9 Powder." *World Journal of Microbiology and Biotechnology*, vol. 16: 187–94.
- 10 Sawai, J., H. Kojima, H. Igarashi, A. Hashimoto, S. Shoji, A. Takehara, T. Sawaki, T. Kokugan,
11 and M. Shimizu. 2000b. "Escherichia coli Damage by Ceramic Powder Slurries." *Journal of*
12 *Chemical Engineering of Japan*, vol. 30: 1034–39.
- 13 Sayles, F.L., and W.S. Fyfe. 1973. "The Crystallization of Magnesite from Aqueous Solutions."
14 *Geochimica et Cosmochimica Acta*, vol. 37: 87-99.
- 15 Schlesinger, W.H. 1997. *Biogeochemistry: An Analysis of Global Change*. New York:
16 Academic.
- 17 Snider, A.C. 2002. "MgO Studies: Experimental Work Conducted at SNL/Carlsbad: Efficacy
18 of Premier Chemicals MgO as an Engineered Barrier." *Sandia National Laboratories Technical*
19 *Baseline Reports; WBS 1.3.5.3, Compliance Monitoring; WBS 1.3.5.4, Repository*
20 *Investigations; Milestone RI110; January 31, 2002* (pp. 3.1–1 through 3.1–18). ERMS 520467.
21 Carlsbad, NM: Sandia National Laboratories.
- 22 Snider, A.C. 2003a. *Calculation of the Quantities of MgO Required for Consumption of CO₂ for*
23 *the WIPP Compliance Recertification Application* (July 3). ERMS 530220. Carlsbad, NM:
24 Sandia National Laboratories.
- 25 Snider, A.C. 2003b. "Hydration of Magnesium Oxide in the Waste Isolation Pilot Plant."
26 *Sandia National Laboratories Technical Baseline Reports; WBS 1.3.5.3, Compliance*
27 *Monitoring; WBS 1.3.5.4, Repository Investigations; Milestone RI 03-210; January 31, 2003*
28 (pp. 4.2-1 through 4.2-6). ERMS 523189. Carlsbad, NM: Sandia National Laboratories.
- 29 Snider, A.C. 2003c. *Verification of the Definition of Generic Weep Brine and the Development*
30 *of a Recipe for This Brine*. ERMS 527505. Carlsbad, NM: Sandia National Laboratories.
- 31 Snider, A.C. 2003d. *Calculation of MgO Safety Factors for the WIPP Compliance*
32 *Recertification Application and for Evaluating Assumptions of Homogeneity in WIPP PA*
33 (September 11). ERMS 531508. Carlsbad, NM: Sandia National Laboratories.
- 34 Snider, A.C., and Y. Xiong. 2002a. "Carbonation of Magnesium Oxide." *Sandia National*
35 *Laboratories Technical Baseline Reports; WBS 1.3.5.3, Compliance Monitoring; WBS 1.3.5.4,*
36 *Repository Investigations; Milestone RI130; July 31, 2002* (pp. 4.1-1 through 4.1-28). ERMS
37 523189. Carlsbad, NM: Sandia National Laboratories.

- 1 Snider, A.C., and Y.-L. Xiong. 2002b. *Experimental Study of WIPP Engineered Barrier MgO*
2 *at Sandia National Laboratories Carlsbad Facility* (Rev. 2, October 2). TP 00-07. ERMS
3 523957. Carlsbad, NM: Sandia National Laboratories.
- 4 Snider, A.C., and Y.-L. Xiong. 2004. *Continuing Investigations of the Hydration and*
5 *Carbonation of Premier Chemical MgO* (October 12). ERMS 537188. Carlsbad, NM: Sandia
6 National Laboratories.
- 7 Snider, A.C., Y.-L. Xiong, and N.A. Wall. 2004. *Experimental Study of WIPP Engineered*
8 *Barrier MgO at Sandia National Laboratories Carlsbad Facility* (Rev. 3, August 26). TP 00-07.
9 ERMS 536591. Carlsbad, NM: Sandia National Laboratories.
- 10 Stamatakis, M.G. 1995. "Occurrence and Genesis of Huntite-Hydromagnesite Assemblages,
11 Kozani, Greece: Important New White Fillers and Extenders." *Transaction of the Institution of*
12 *Mining and Metallurgy, Section B: Applied Earth Science*, vol. 104: B179–B186.
- 13 Stein, C.L. 1985. *Mineralogy in the Waste Isolation Pilot Plant (WIPP) Facility Stratigraphic*
14 *Horizon*. SAND85-0321. Albuquerque: Sandia National Laboratories.
- 15 Stein, J.S., and W. Zelinski. 2003. *Analysis Package for BRAGFLO: Compliance*
16 *Recertification Application* (October 23). ERMS 530163. Carlsbad, NM: Sandia National
17 Laboratories.
- 18 Stoimenov, P.K., R.L. Klinger, G.L. Marchin, and K.J. Klabunde. 2002. "Metal Oxide
19 Nanoparticles as Bactericidal Agents." *Langmuir*, vol. 18: 6679–86.
- 20 Telander, M.R., and R.E. Westerman. 1993. *Hydrogen Generation by Metal Corrosion in*
21 *Simulated Waste Isolation Pilot Plant Environments*. SAND92-7347. Albuquerque: Sandia
22 National Laboratories.
- 23 Telander, M.R., and R.E. Westerman. 1997. *Hydrogen Generation by Metal Corrosion in*
24 *Simulated Waste Isolation Pilot Plant Environments*. SAND96-2538. ERMS 223456.
25 Albuquerque: Sandia National Laboratories.
- 26 Triay, I. 2000. Letter to F. Marcinowski (Subject: Requesting EPA Approval of the
27 Elimination of MgO Minisacks from the WIPP). 21 July 2001. ERMS 519362. U.S.
28 Department of Energy, Carlsbad Field Office, Carlsbad, NM.
- 29 Trinity Engineering Associates (TEA). 2004. *Review of Effects of Supercompacted Waste and*
30 *Heterogeneous Waste Emplacement on WIPP Repository Performance* (March 17). Cincinnati:
31 Trinity Engineering Associates.
- 32 Trovato, E.R. 1997a. Letter to G. Dials (2 Enclosures). 25 April 1997. ERMS 247206. U.S.
33 Environmental Protection Agency, Office of Air and Radiation, Washington, DC.
- 34 Trovato, E.R. 1997b. Letter to G. Dials (Enclosures: Parameters that Are no Longer of Concern
35 and Parameters that DOE must Use for the PAVT). 17 April ERMS 247196. U.S.
36 Environmental Protection Agency, Office of Air and Radiation, Washington, DC.

- 1 U.S. Department of Energy (DOE). 1996a. *Title 40 CFR Part 191 Compliance Certification*
2 *Application for the Waste Isolation Pilot Plant* (October). 21 vols. DOE/CAO-1994-2184.
3 Carlsbad, NM: Carlsbad Area Office.
- 4 U.S. Department of Energy (DOE). 1996b. *Transuranic Waste Baseline Inventory Report*
5 (Revision 3). DOE/CAO-95-1121. Carlsbad, NM: Carlsbad Area Office.
- 6 U.S. Department of Energy (DOE). 2000. *MgO Mini-Sack Elimination Proposal* (July 21).
7 ERMS 519362. Carlsbad, NM: Carlsbad Area Office.
- 8 U.S. Department of Energy (DOE). 2004. *Title 40 CFR Part 191 Compliance Recertification*
9 *Application for the Waste Isolation Pilot Plant* (March). 10 vols. DOE/WIPP 2004-3231.
10 Carlsbad, NM: Carlsbad Field Office.
- 11 U.S. Environmental Protection Agency (EPA). 1987. “40 CFR Parts 264 and 265 (FRL-3222-5)
12 Hazardous Waste Management System; Containerized Hazardous Liquids Requirements.”
13 *Federal Register*, vol. 52: 23695–697.
- 14 U.S. Environmental Protection Agency (EPA). 1992a. “40 CFR Part 264-Standards for Owners
15 and Operators of Hazardous Waste Treatment, Storage, and Disposal Facilities.” *Federal*
16 *Register*, vol. 57: 54452–460.
- 17 U.S. Environmental Protection Agency (EPA). 1992b. “40 CFR Part 265-Interim Status
18 Standards for Owners and Operators of Hazardous Waste Treatment, Storage, and Disposal
19 Facilities.” *Federal Register*, vol. 57: 54452–461.
- 20 U.S. Environmental Protection Agency (EPA). 1993. “40 CFR Part 191 Environmental
21 Radiation Protection Standards for the Management and Disposal of Spent Nuclear Fuel, High-
22 Level and Transuranic Radioactive Wastes; Final Rule.” *Federal Register*, vol. 58: 66398–416.
- 23 U.S. Environmental Protection Agency (EPA). 1995. “40 CFR Parts 264, 265, and 271
24 (FRL 5226–9) Hazardous Waste Management: Liquids in Landfills.” *Federal Register*, vol. 60:
25 35703–706.
- 26 U.S. Environmental Protection Agency (EPA). 1998a. “CARD No. 44: Engineered Barriers.”
27 *Compliance Application Review Documents for the Criteria for the Certification and*
28 *Recertification of the Waste Isolation Pilot Plant’s Compliance with the 40 CFR 191 Disposal*
29 *Regulations: Final Certification Decision* (May) (pp. 44-1 through 44-36). Washington, DC:
30 Office of Radiation and Indoor Air.
- 31 U.S. Environmental Protection Agency (EPA). 1998b. “40 CFR Part 194: Criteria for the
32 Certification and Recertification of the Waste Isolation Pilot Plant’s Compliance with the
33 Disposal Regulations: Certification Decision; Final Rule.” *Federal Register*, vol. 63 (May 18,
34 1998): 27353–406.
- 35 U.S. Environmental Protection Agency (EPA). 1998c. “CARD No. 23: Models and Computer
36 Codes.” *Compliance Application Review Documents for the Criteria for the Certification and*
37 *Recertification of the Waste Isolation Pilot Plant’s Compliance with the 40 CFR 191 Disposal*

- 1 *Regulations: Final Certification Decision* (May) (pp. 23-1 through 23-93). EPA 402-R-97-013.
2 Washington, DC: Office of Radiation and Indoor Air.
- 3 U.S. Environmental Protection Agency (EPA). 1998d. *Technical Support Document for*
4 *Section 194.23: Models and Computer Codes*. Washington, DC: Office of Radiation and
5 Indoor Air.
- 6 U.S. Environmental Protection Agency (EPA). 1998e. *Technical Support Document for*
7 *Section 194.23: Parameter Justification Report* (May). Washington, DC: Office of Radiation
8 and Indoor Air.
- 9 U.S. Environmental Protection Agency (EPA). 1998f. *Technical Support Document for*
10 *Section 194.24: EPA's Evaluation of DOE's Actinide Source Term*. Washington, DC: Office of
11 Radiation and Indoor Air.
- 12 U.S. Environmental Protection Agency (EPA). 2001. *Approval of Elimination of Minisacks*.
13 Washington, DC: Office of Radiation and Indoor Air.
- 14 U.S. Environmental Protection Agency (EPA). 2004. *Discussion of Major Issues Associated*
15 *with EPA's Compressed Waste Review*. ERMS 534327. Washington, DC: Office of Air and
16 Radiation.
- 17 U.S. Environmental Protection Agency (EPA). 2006. *Evaluation of the Compliance*
18 *Recertification Actinide Source Term and Culebra Dolomite Distribution Coefficient Values*.
19 Technical Support Document for Section 194.24. CRA-2004. Docket No. A-98-49.
- 20 U.S. Environmental Protection Agency (EPA). 2008. *Overview Summary of Planned Change*
21 *Request Decision*. Washington, DC: Office of Radiation and Indoor Air.
- 22 Usdowski, E. 1989. "Synthesis of Dolomite and Magnesite at 60 °C in the System Ca²⁺-Mg²⁺-
23 CO₃²⁻-Cl-H₂O." *Naturwissenschaften*, vol. 76, no. 8: 374–75.
- 24 Usdowski, E. 1994. "Synthesis of Dolomite and Geochemical Implications." *Dolomites: A*
25 *Volume in Honour of Dolomieu* (pp. 345–60) Eds. B. Purser, M. Tucker, and D. Zenger.
26 Oxford: Blackwell. Special Publication No. 21 of the International Association of
27 Sedimentologists.
- 28 Villarreal, R., J.M. Bergquist, and S.L. Leonard. 2001a. *The Actinide Source-Term Waste Test*
29 *Program (STTP) Final Report, Volume I*. LA-UR-01-6822. Los Alamos: Los Alamos National
30 Laboratory.
- 31 Villarreal, R., J.M. Bergquist, and S.L. Leonard. 2001b. *The Actinide Source-Term Waste Test*
32 *Program (STTP) Final Report, Volume II*. LA-UR-01-6912. Los Alamos: Los Alamos
33 National Laboratory.
- 34 Villarreal, R., M. King, and S.L. Leonard. 2001. *The Actinide Source-Term Waste Test*
35 *Program (STTP) Final Report, Volume IV*. LA-UR-01-6914. Los Alamos: Los Alamos
36 National Laboratory.

- 1 Villarreal, R., A.C. Morzinski, J.M. Bergquist, and S.L. Leonard. 2001. *The Actinide*
2 *Source-Term Waste Test Program (STTP) Final Report, Volume III*. LA-UR-01-6913. Los
3 Alamos: Los Alamos National Laboratory.
- 4 Vreeland, R.H., W.D. Rosenzweig, and D.W. Powers. 2000. "Isolation of a 250-Million-Year-
5 Old Halotolerant Bacterium from a Primary Salt Crystal." *Nature*, vol. 407: 897–900.
- 6 Vugrin, E.D., M.B. Nemer, and S.W. Wagner. 2006. *Uncertainties Affecting MgO Effectiveness*
7 *and Calculation of the MgO Effective Excess Factor* (Rev. 0, November 17). ERMS 544781.
8 Carlsbad, NM: Sandia National Laboratories.
- 9 Vugrin, E.D., M.B. Nemer, and S.W. Wagner. 2007. *Uncertainties Affecting MgO Effectiveness*
10 *and Calculation of the MgO Effective Excess Factor* (Rev. 1, June 26). ERMS 546377.
11 Carlsbad, NM: Sandia National Laboratories.
- 12 Wall, N.A. 2005. *Preliminary Results for the Evaluation of Potential New MgO* (January 27).
13 ERMS 538514. Carlsbad, NM: Sandia National Laboratories.
- 14 Wall, N.A., and S.A. Matthews. 2005. "Sustainability of Humic Acids in the Presence of
15 Magnesium Oxide." *Applied Geochemistry*, vol. 20: 1704–13.
- 16 Wang, Y. 1998. *WIPP PA Validation Document for FMT (Version 2.4), Document Version 2.4*.
17 ERMS 251587. Carlsbad, NM: Sandia National Laboratories.
- 18 Wang, Y. 2000a. Memorandum to B.A. Howard (Subject: Methanogenesis and Carbon
19 Dioxide Generation in the Waste Isolation Pilot Plant [WIPP]). 5 January 2000. ERMS 519362.
20 U.S. Department of Energy, Sandia National Laboratories, Carlsbad, NM.
- 21 Wang, Y. 2000b. Memorandum to B.A. Howard (Subject: Effectiveness of Mixing Processes
22 in the Waste Isolation Pilot Plant Repository). 21 June 2000. ERMS 512401. U.S. Department
23 of Energy, Sandia National Laboratories, Carlsbad, NM.
- 24 Wang, Y. and L.H. Brush. 1996a. Memorandum to M.S. Tierney (Subject: Estimates of Gas-
25 Generation Parameters for the Long-Term WIPP Performance Assessment). 26 January 1996.
26 ERMS 231943. U.S. Department of Energy, Sandia National Laboratories, Albuquerque, NM.
- 27 Wang, Y. and L.H. Brush. 1996b. Memorandum to M.S. Tierney (Subject: Modify the
28 Stoichiometric Factor γ in the BRAGFLO to Include the Effect of MgO Added to WIPP
29 Repository as a Backfill). 23 February 1996. ERMS 232286. U.S. Department of Energy,
30 Sandia National Laboratories, Albuquerque, NM.
- 31 Wang, Y., and L.H. Brush. 1996c. Memorandum to P. Vaughn (Subject: An Adjustment for
32 Using Steel Corrosion Rates in BRAGFLO to Reflect Repository Chemical Condition Changes
33 Due to Adding MgO as Backfill). 29 February 1996. ERMS 235181. U.S. Department of
34 Energy, Sandia National Laboratories, Albuquerque, NM.

- 1 Wang, Y., and C.R. Bryan. 2000. *Experimental Study of WIPP MgO Backfill at Sandia*
2 *National Laboratories Carlsbad Facility* (Rev. 0, July 11). TP 00-07. ERMS 512216.
3 Carlsbad, NM: Sandia National Laboratories.
- 4 Wang, Y., C.R. Bryan, and N.A. Wall. 2001. Experimental Study of WIPP MgO Backfill at
5 Sandia National Laboratories Carlsbad Facility (Rev. 1, June 22). TP 00-07. ERMS 518747.
6 Carlsbad, NM: Sandia National Laboratories.
- 7 Wang, Y., and P Van Cappellan. 1996. “A Multicomponent Reactive-Transport Model of Early
8 Diagenesis: Application of Redox Cycling in Coastal Marine Sediments.” *Geochimica et*
9 *Cosmochimica Acta*, vol. 60: 2993–3014.
- 10 Washington TRU Solutions (WTS). 2003. *Specification for Prepackaged MgO Backfill* (Rev.
11 5). D-0101. Carlsbad, NM: Washington TRU Solutions.
- 12 Washington TRU Solutions (WTS). 2005. *Specification for Prepackaged MgO Backfill* (Rev. 7,
13 May 12). Specification D-0101. Carlsbad, NM: Washington TRU Solutions.
- 14 Washington TRU Solutions (WTS). 2006. *CH Waste Processing* (Rev. 23, January). Technical
15 Procedure WP05-WH1011. Carlsbad, NM: Washington TRU Solutions.
- 16 Westinghouse Waste Isolation Division (WID). 1997. *Dose Assessment of Hand Emplacement*
17 *of MgO Sacks around CH Waste 7-Packs at the Waste Isolation Pilot Plant* (April). WIPP
18 Radiological Control Position Paper 97-05. Carlsbad, NM: Westinghouse WID.
- 19 Wolery, T.J. 1992a. *EQ3/6, A Software Package for Geochemical Modeling of Aqueous*
20 *Systems: Package Overview and Installation Guide* (Version 7.0). UCRL-MA-110662 PT I.
21 Livermore, CA: Lawrence Livermore National Laboratory.
- 22 Wolery, T.J. 1992b. *EQ3NR, A Computer Program for Geochemical Aqueous*
23 *Speciation-Solubility Calculations: Theoretical Manual, User’s Guide, and Related*
24 *Documentation* (Version 7.0). UCRL-MA-110662 PT III. Livermore, CA: Lawrence
25 Livermore National Laboratory.
- 26 Wolery, T.J., and S.A. Daveler. 1992. *EQ6, A Computer Program for Reaction-Path Modeling*
27 *of Aqueous Geochemical Systems: Theoretical Manual, User’s Guide, and Related*
28 *Documentation* (Version 7.0). UCRL-MA-110662 PT IV. Livermore, CA: Lawrence
29 Livermore National Laboratory.
- 30 Xiong, Y., and A.S. Lord. 2008. “HHHExperimental Investigations of the Reaction Path in the
31 MgO-CO₂-H₂O System in Solutions with Various Ionic Strengths, and Their Applications to
32 Nuclear Waste IsolationHHH.” *Applied Geochemistry*, vol. 23: 1634–59.
- 33 Xiong, Y., and A.C. Snider. 2003. “Carbonation Rates of the Magnesium Oxide Hydration
34 Product Brucite in Various Solutions.” *Sandia National Laboratories Technical Baseline*
35 *Reports; WBS 1.3.5.3, Compliance Monitoring; WBS 1.3.5.4, Repository Investigations;*
36 *Milestone RI 03-210; January 31, 2003* (pp. 4.3-1 through 4.3-11). ERMS 526049. Carlsbad,
37 NM: Sandia National Laboratories.

- 1 Yamamoto, O., J. Sawai, M. Hotta, H. Kojima, and T. Sasamoto. 1998. "Growth Inhibition of
2 Bacteria by MgO-ZnO Solid-Solution Powders." *Journal of the Ceramic Society of Japan*,
3 vol. 106: 1252–54.
- 4 Zhang, P.-C., H.L. Anderson, J.W. Kelly, J.L. Krumhansl, and H.W. Papenguth. 1999. *Kinetics
5 and Mechanisms of Formation of Magnesite from Hydromagnesite in Brine*. SAND99-1946J.
6 ERMS 514868. Albuquerque: Sandia National Laboratories.
- 7 Zhang, P.-C., J. Hardesty, and H.W. Papenguth. 2001. "MgO Hydration Experiments
8 Conducted at SNL-ABQ," Sandia National Laboratories Technical Baseline Reports;
9 WBS 1.3.5.4, Repository Investigations; Milestone RI010; January 31, 2001 (pp. 55–65).
10 ERMS 516749. Carlsbad, NM: Sandia National Laboratories.